



Fakultät Wissenschaftszentrum Weihenstephan für Ernährung,  
Landnutzung und Umwelt

# Characterisation of transgenic mice for cardiac fibroblast-specific transgenesis

**Megha Saraiya**

Vollständiger Abdruck der von der Fakultät Wissenschaftszentrum Weihenstephan für Ernährung, Landnutzung und Umwelt der Technischen Universität München zur Erlangung des akademischen Grades eines

**Doktors der Naturwissenschaften (Dr. rer. nat.)**

genehmigten Dissertation.

**Vorsitzender:** Univ-Prof. Dr. Hannelore Daniel

**Prüfer der Dissertation:**

1. Univ.-Prof. Angelika Schnieke, Ph.D
2. Univ.-Prof. Dr. Dr. Stefan Engelhardt

Die Dissertation wurde am 08.06.2016 bei der Technischen Universität München eingereicht und durch die Fakultät Wissenschaftszentrum Weihenstephan für Ernährung, Landnutzung und Umwelt am 07.11.2016 angenommen.

# ABBREVIATIONS

$\alpha$ -MHC	alpha-myosin heavy chain
ANOVA	analysis of variance
AMCF	adult mouse cardiac fibroblasts
AMCM	adult mouse cardiomyocytes
AU	arbitrary units
ATP	adenosine triphosphate
$\beta$ -AR	Adrenoceptor
BAC	bacterial artificial chromosome
BSA	bovine serum albumin
BW	body weight
Ccdc80	coiled-coil domain containing 80
CF (s)	cardiac Fibroblast / cardiac Fibroblasts
CM	cardiomyocytes
CMV	cytomegalovirus
Cre	cyclization recombination
DAG	diacylglycerol
ddH <sub>2</sub> O	double distilled water
DMSO	dimethylsulphoxide
DNA	deoxyribonucleic acid
dNTP	deoxyribonucleotidetriphosphate
DTT	dithiothreitol
ECL	enhanced chemiluminescence
<i>E.coli</i>	Escherichia coli
ECM	extra cellular matrix
EDTA	ethylenediaminetetraacetic acid
EMT	epithelial–mesenchymal-transition
EndMT	endothelial– mesenchymal-transition
ERT2	mutated form of human Estrogen Receptor1
FCS	fetal calf serum
Fsp1	fibroblast specific protein-1
GFP	green fluorescent protein
Gsn	gelsolin
GW	Gateway system
HF	heart failure
HW	heart weight
Kb	kilobases
IFs	intermediate filaments
loxP	locus of X-over P1
LV	left ventricle
LVID	left ventricular inner diameter
LVPW	left ventricular posterior wall thickness
M	molar
mA	milli ampere
mGFP	membrane targeted GFP

min	minute
MI	myocardial Infraction
mTom	membrane targeted tdTomato
NRCF	neonatal rat cardiac fibroblasts
NRCM	neonatal rat cardiomyocytes
PCR	polymerase chain reaction
pH	power of hydrogen
Postn	periostin
RNA	ribonucleic acid
RT	room temperature
Rabgap1l	RAB GTPase Activating Protein 1-Like
s	second
s.e.m.	Standard error mean
SD	standard deviation
TAC	transverse aortic constriction
TAE	tris-acetate EDTA
Tam	tamoxifen
Tg	transgenic
TL	tibia length
UV	ultraviolet
v/v	volume to volume
Vim	vimentin
VSMCs	vascular smooth muscle cells
w/v	weight to volume
°C	degree Celsius

# LIST OF FIGURES

Figure no.	Title	Page No.
1.1	Cardiac fibroblast in heart	3
1.2	Major functions of the fibroblast during cardiac development and wound healing	6
1.3	Cre and FLP recombinase systems	11
1.4	Inducible Cre system	13
1.5	Vimentin expression in healthy and failing myocardium	20
1.6	Fibroblast-specific protein-1 (FSP1) expressing cells in neonatal and adult Fsp1-GFP reporter mouse myocardium.	22
4.1	Screening of cardiac fibroblast specific genes using mouse microarray database	56
4.2	Validation of selected gene in cardiac tissues and isolated primary cells	58
4.3	BAC clone (bMQ193n13) having genomic region (upstream and downstream) of Ccdc80 gene	59
4.4	Analysis of amplified promoter sequences for transcriptional activity <i>in vitro</i>	61
4.5	Cloning strategy for generation of Promoter-Cre Constructs	62
4.6	Analytical digestion of Ccdc80 and periostin promoter Cre constructs	64
4.7	Verification of promoter vector for efficient expression of Cre recombination <i>in vitro</i> .	65
4.8	Genotyping of Ccdc80-Cre founders by PCR	66
4.9	Cre recombination in Ccdc80-Cre; Rosa26 <sup>lacZ</sup> bi-transgenic mice	67
4.10	Shown is the construct for generation of VimCreERT2 transgenic mice by BAC recombination	68
4.11	Validation of Vimentin promoter activity in frozen heart section after tamoxifen injection compared with described fibroblast –Cre mice	69
4.12	Characterization of VimCreER lineage tagged cells in heart sections by immunofluorescence	71
4.13	Cell-specific expression of Vimentin promoter compared to described fibroblast promoter	72
4.14	Cardiac Fibroblast-specific Cre recombination	73
4.15	Vimentin promoter activity in TAC operated heart. Comparison with described fibroblast promoter (Fsp1)	75
4.16	Immunofluorescence staining for endothelial cell marker (CD31) along with GFP in frozen heart section of TAC-operated bitransgenic mice	77
4.17	Cardiac phenotyping in VimCreER mice post TAC	78
4.18	Tamoxifen-independent Cre recombination in VimCreER;mT/mG bi-transgenic mice	79
4.19	Direct fluorescence for mTom-mGFP signals in different tissue sections of VimCreER;mT/mG mice	80
4.20	Administration of tamoxifen (TM) to lactating mT/mG <sup>fl/fl</sup> mouse mothers leads to efficient recombination in the nourished pups	81

4.21	Immunofluorescence for fibroblast cell markers at postnatal day 7 (P7).	82
4.22	Immunofluorescence staining for vascular smooth muscle cell marker in postnatal day 7 and 6 weeks old hearts	83
4.23	Cre mediated recombination in endothelial cells in postnatal day 7 and 6 weeks old hearts	85
5.1	Vimentin is expressed in the blood vessels in the heart	90

# CONTENTS

<b>1</b>	<b>INTRODUCTION</b>	<b>1</b>
<b>1.1</b>	<b>The cardiac fibroblasts</b>	<b>1</b>
1.1.1	Origin and organization of cardiac fibroblasts in the heart	2
1.1.2	Functions of cardiac fibroblasts	3
1.1.3	Dynamic interaction between cardiac fibroblast and cardiomyocytes	4
1.1.4	Cardiac fibroblasts in wound healing	5
1.1.5	Cardiac fibroblasts in regenerative processes	7
1.1.6	Current state of gene targeting in cardiac fibroblasts	7
<b>1.2</b>	<b>Gene targeting in mice using the cre/lox system</b>	<b>8</b>
1.2.1	Cre-loxP recombination system	9
1.2.2	Tamoxifen-inducible conditional gene targeting	12
1.2.3	Tetracycline-inducible Cre recombination	14
<b>1.3</b>	<b>Cardiac fibroblast-specific markers</b>	<b>17</b>
1.3.1	Vimentin	19
1.3.2	Fibroblast-specific protein-1	21
1.3.3	Periostin	22
<b>1.4</b>	<b>Aim of this study</b>	<b>23</b>
<b>2</b>	<b>MATERIALS AND METHODS</b>	<b>25</b>
<b>2.1</b>	<b>MATERIALS</b>	<b>25</b>
2.1.1	Chemicals	25
2.1.2	Kits	27
2.1.3	Enzymes	27
2.1.4	Bacterial strains:	27
2.1.5	Bacterial artificial chromosome (BAC) clones:	27
2.1.6	Plasmids	28
2.1.7	Oligonucleotide primers	28
2.1.8	Buffers and Media	31
2.1.9	Antibodies	35
<b>3</b>	<b>METHODS</b>	<b>35</b>
<b>3.1</b>	<b>Molecular biology methods</b>	<b>35</b>
3.1.1	Polymerase chain reaction (PCR)	35
3.1.2	Isolation and purification of PCR-amplified DNA	36
3.1.3	Agarose gel electrophoresis	37
3.1.4	Gel extraction	37
3.1.5	Precipitation of DNA with sodium acetate	37
3.1.6	Endonuclease digestion	37
3.1.7	Phosphatase treatment of DNA	38
3.1.8	Ligation of DNA fragments	38
3.1.9	Cre-expressing constructs adapted for gateway recombination reactions	38
3.1.10	Insertion of cDNA into plasmids by GatewayR™ recombination	39

3.1.11 Transformation	40
3.1.12 Mini culture and mini DNA purification	41
3.1.13 Maxi/midi culture and purification	41
3.1.14 Endofree maxi DNA purification	41
3.1.15 Sequencing of plasmid DNA	41
3.1.16 Software	42
<b>3.2 Cell culture methods</b>	<b>42</b>
3.2.1 Isolation of neonatal rat cardiomyocytes (NRCM) and fibroblast (NRCF)	42
3.2.2 Isolation of adult mouse cardiomyocytes (AMCM) and Fibroblast (AMCF)	42
3.2.3 Cultivation of NIH-3T3 mouse fibroblasts	43
3.2.4 Transfection of NIH-3T3 cells with promoter vectors	43
3.2.5 Generation of stable cell lines	44
<b>3.3 Methods for RNA analysis</b>	<b>44</b>
3.3.1 Isolation of RNA	44
3.3.2 Reverse transcription	45
3.3.3 Quantitative real time PCR	45
<b>3.4 Methods for protein analysis</b>	<b>47</b>
3.4.1 Preparation of protein lysates	47
3.4.2 BCA protein quantification	47
3.4.3 Western blot	47
<b>3.5 Immunofluorescence</b>	<b>48</b>
3.5.1 In tissues	48
3.5.2 In isolated cells	50
<b>3.6 Staining</b>	<b>50</b>
3.6.1 Detection of $\beta$ -Galactosidase activity (X-gal staining)	50
3.6.2 Fast green/Sirius red staining for cryosections	51
<b>3.7 Microscopy</b>	<b>51</b>
3.7.1 Confocal microscopy	51
3.7.2 Automated fluorescent microscopy	51
<b>3.8 Methods for animal experiments</b>	<b>51</b>
3.8.1 Generation of a Ccdc80-Cre mouse line	51
3.8.2 Isolation of genomic DNA	52
3.8.3 Genotyping PCR	52
3.8.4 Animal models	54
<b>3.9 Methods for cardiovascular phenotyping of mice</b>	<b>54</b>
3.9.1 Echocardiography	55
3.9.2 Transverse aortic constriction (TAC)	55
3.9.3 Statistics	55
<b>4 RESULTS</b>	<b>56</b>
<b>4.1 Generation and characterisation of a Ccdc80-Cre transgenic mouse line</b>	<b>56</b>
4.1.1 Identification of cardiac fibroblast specific gene and validation of candidates	56
4.1.2 Cloning and validation of candidate promoters <i>in vitro</i>	59
4.1.3 Generation of a mouse line that expresses Cre recombinase under the control of the Ccdc80 promoter	65
4.1.4 Efficacy of the Ccdc80-Cre transgene <i>in vivo</i>	66
<b>4.2 Characterization of VimCreERT2 transgenic mice expressing Cre recombinase in</b>	

<b>the heart</b>	<b>68</b>
4.2.1 Vimentin promoter activity in heart tissue in comparison to Fsp1 promoter activity	68
4.2.2 VimCreER marks non-myocytes in the heart.	70
4.2.3 Cardiac fibroblast specific Cre recombination in VimCreER bitransgenic mice	72
4.2.4 Vimentin promoter activity in the TAC model for chronic cardiac pressure overload	74
4.2.5 Tamoxifen-independent recombination in the Vim-CreER mouse heart	79
4.2.6 Recombination in the heart of VimCreER;mT/mG mice during postnatal development	80
<b>5 DISCUSSION</b>	<b>86</b>
5.1 Screening for cardiac fibroblast specific genes	86
5.2 Ccdc80 promoter activity in cardiomyocytes <i>in vivo</i>	87
5.3 Vimentin promoter activity in non-myocyte cells in heart tissue	88
5.4 Cardiac fibroblast-specific Cre recombination in VimCreER; mT/mG bitransgenic mice	91
5.5 Vimentin promoter activity in the pressure-overloaded myocardium	91
5.6 Vimentin promoter activity in endothelial cell of VimCreER; mT/mG bitransgenic mice during postnatal development	93
5.7 Challenges and limitations of study	94
5.8 Conclusions	95
<b>6 SUMMARY/ ZUSAMMENFASSUNG</b>	<b>97</b>
<b>7 REFERENCE</b>	<b>101</b>
<b>8 APPENDIX</b>	<b>120</b>
8.1 Tabular result of the Microarray analysis	120
8.2 Map of Ccdc80 and Periostin promoter constructs used for study	124
8.3 DNA sequence of Ccdc80-Cre targeting Vector	126
8.4 Acknowledgement	133
8.5 Curriculum vitae	134



# 1 INTRODUCTION

Cardiovascular diseases are one of the leading causes of death worldwide. Due to aging population, the estimated number of cardiovascular deaths will increase from 16.7 million in 2002 to 23.3 million in 2030<sup>1</sup>. Among the different cardiovascular diseases, heart failure (HF) is a primary health concern. Heart failure (HF) is a complex clinical syndrome, associated with impaired ability of the ventricles to fill with or to eject blood. Coronary artery disease and heart attack, High blood pressure (hypertension), faulty heart valves,, cardiomyopathy (damaged heart muscles), arrhythmias (abnormal heart rhythms) or inherited mutations in structural or contractile proteins are the underlying pathologies linked to HF <sup>2</sup>. At cellular level, it is associated with cardiomyocyte hypertrophy (characterized by an increment in the cardiomyocyte size, enhanced protein synthesis, and alteration in organization of the sarcomere structure), cardiomyocyte apoptosis, alteration in the expression of genes regulating energy metabolism, calcium handling, and genes that are normally expressed in the embryonic heart <sup>2</sup>.

Besides cardiomyocytes, also non-myocyte cell populations are increasingly appreciated for their contributions in the performance of the normal and failing heart. The cardiac fibroblast (CFs) that has been recognized as the major non-myocyte cell type in the heart, contributes to multiple aspects of myocardial function and pathophysiology. Cardiac fibroblasts produce a variety of growth factors along with extracellular matrix proteins (e.g., collagens), which are involved in the intercellular signaling with cardiomyocytes. Still, the exact function of cardiac fibroblasts during adaptive responses of the myocardium remains unclear <sup>3</sup>.

## 1.1 The cardiac fibroblasts

Cardiomyocytes, fibroblasts and vascular cells (smooth muscle, endothelium) are the major cellular components in the heart. Originally, fibroblasts were described in the late 19th century based solely on their location and on morphological criteria<sup>4,5</sup>. They are typically identified by their spindle-shaped flattened morphology, their ability to adhere to culture plates<sup>5</sup> and the absence of markers of epithelial, smooth muscle, endothelial, perineural, and histiocytic cells<sup>5</sup>. Their nuclei are large and euchromatic and possess prominent nucleoli. Fibroblast cells are phenotypically diverse and exhibit heterogeneity between fibroblasts from different tissues <sup>6</sup>.

### 1.1.1 Origin and organization of cardiac fibroblasts in the heart

Cardiac fibroblasts (CFs) are thought to be predominantly derived from the epicardium during heart development (Fig.1.1) <sup>7</sup>. Villous-like projections protrude from the venous pole of the developing heart to form the pro-epicardium <sup>8,9</sup>. Cells from the pro-epicardium detach and attach on the beating ventricular surface to form the epicardium<sup>10</sup>. Subsequently epithelial cells of the epicardium undergo epithelial–mesenchymal-transition (EMT) to form mesenchymal cells that invade the developing myocardium<sup>11</sup>. A subset of these mesenchymal cells after EMT acquire migratory properties and invade the developing myofascial planes to occupy interstitial positions in between cardiomyocytes to become resident cardiac fibroblasts <sup>12,13</sup>. In contrast to cardiac fibroblasts, valvular fibroblasts are thought to derive from the endothelium overlying the region of the cardiac cushions (site of atrio-ventricular valve formation) <sup>14-16</sup>. The endothelium overlying the valve leaflets undergoes the endothelial-mesenchymal transition (EndMT) to generate cardiac fibroblasts that invade the valvular mesenchyme and contribute to the collagenous structure of the valve (Figure 1.1).

At the cellular level, the normal adult human heart comprises 30% cardiomyocytes and 70% nonmyocytes, of which the majority is CFs. Although CFs are the predominant cell type in number, the cardiomyocytes actually occupy the greatest volume <sup>17,18</sup>. Unlike cardiomyocytes, endothelial cells, and vascular smooth muscle cells, CFs have no basal membrane and display multiple processes<sup>3</sup>. Thus, CFs can be distinguished from other non-myocyte lineages upon the use of laminin or collagen IV to test for the absence of a basal membrane in CF. CFs are found throughout the heart in a 3D network surrounding myocyte<sup>19</sup> and bridging the gaps between myocardial tissues <sup>17,20</sup>. Myocytes are arranged in laminae bounded by endomysial collagen, and the CFs lie within this endomysial network <sup>18,21</sup>.

In the developing murine heart, CFs are observed at stage E12.5, that is 12.5 days post fertilization (dpf). Their numbers progressively increase in postnatal life, comprising 27% of the total number of cells in the adult murine heart <sup>22</sup>, approximately 2/3 of the total numbers of cells in the rat heart <sup>23,22</sup> and in humans, the non-myocyte cells comprise approximately 70% of the total number of cardiac cell types <sup>19,24</sup>. The higher number of fibroblasts in rat and human hearts thus relates to a larger heart size, greater wall tension and consequently a need for greater production of extracellular matrix (ECM) <sup>22</sup>.

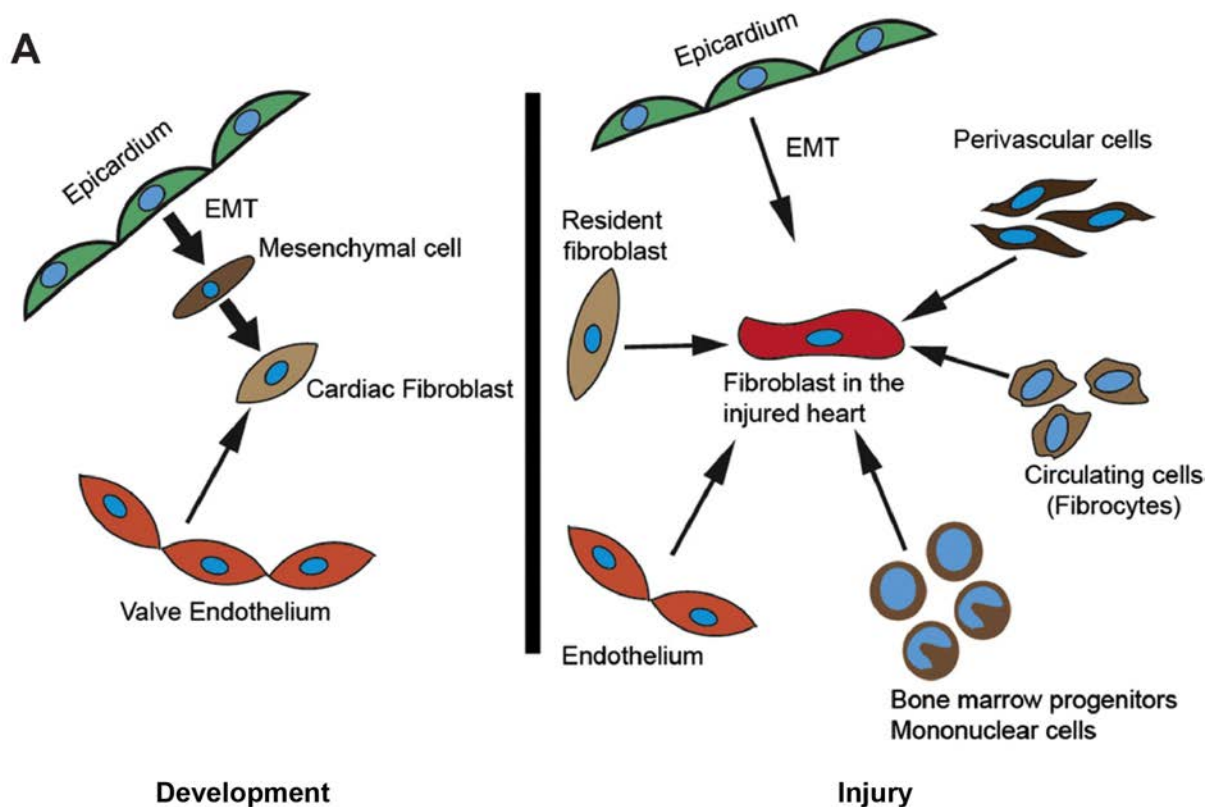


**Figure 1.1 Cardiac fibroblasts in heart. (A)** The origin of cardiac fibroblasts during cardiac development and following injury. The cardiac fibroblasts in the injured heart have diverse origins compared to a fibroblast in the developing heart (Ref: Deb A *et al.* 2014)<sup>27</sup>.

### 1.1.2 Functions of cardiac fibroblasts

CFs are crucial in maintaining normal cardiac function, biochemical and electrical features and structure of the heart, They are into many aspects of cardiac functions, such as homeostasis and remodeling of the extracellular matrix, cell–cell interaction with cardiomyocytes, and intercellular signaling with other CFs, endothelial or smooth muscle cells via production of growth factors and cytokines. Thus, influencing several cellular events in the heart such as angiogenesis, cell proliferation, cardiomyocytes hypertrophy or apoptosis (Figure 1.2). CFs are high membrane resistance conductors<sup>19</sup>. To ensure proper contraction of the heart, CFs electrically separate the atria and the ventricle, by casting the fibrotic annulus<sup>31</sup>. They are connected with cardiomyocytes via gap junctions, particularly connexins (Cx40, Cx43, and Cx45), which are essential to maintaining an optimal electrical conduction in the heart<sup>32,33</sup>. Fibroblasts also interact with endothelial cells by secreting growth factors like FGF and VEGF that act on endothelial cells and stimulate angiogenesis<sup>34</sup>. In the myocardial interstitium, CFs secretes a collection of bioactive molecules like

cytokines (TNF $\alpha$ , interleukins and TGF $\beta$ )<sup>35,36</sup> and active peptides (angiotensin II, endothelin 1), which function in autocrine and/or paracrine manners in the myocardium. CFs are the primary cell type responsible for ECM homeostasis in healthy and its remodeling in heart disease. The cardiac ECM consists of interstitial collagens (predominantly type 1 and type 3), proteoglycans, glycoproteins, cytokines, growth factors and proteases<sup>37</sup>. Cardiac fibroblasts not only synthesize new matrix proteins but also express various metalloproteinases (MMPs) that degrade extracellular matrix. In the healthy heart, synthesis and breakdown of extracellular matrix are tightly regulated, but in pathological states, increased MMP expression and activity can lead to excessive ECM degradation and turnover<sup>37,38</sup>. In pressure overload-induced cardiac hypertrophy in humans, MMP expression in the heart increases with the onset of left ventricular failure. In rodent models of pressure overload-induced cardiac hypertrophy increased expression of MMPs is associated with transition from compensation to heart failure<sup>39,40</sup>. However following acute myocardial infarction fibroblasts not only increase the synthesis of ECM proteins at the site of injury (replacement fibrosis) but also increase ECM protein synthesis in areas remote from the injury<sup>41,42</sup>.

### 1.1.3 Dynamic interaction between cardiac fibroblast and cardiomyocytes

Dynamic cross talk between cardiomyocytes and cardiac fibroblasts is a prominent feature of both development as well as injury-induced remodeling<sup>43,44</sup>. Throughout life, cardiac fibroblasts are responsible for controlling many aspects of the heart's microenvironments. During development, fibroblasts supports secretion of factors like platelet derived growth factor (PDGF)- $\beta$ , Sox9, thymosin  $\beta$  4, Ets factors, and fibroblast growth factors (FGFs). These factors are conducive to cardiomyocyte proliferation and establishment of a functionally competent ventricle. They also provide the structural stability required for transitioning from pre- to postnatal life, and directly coupling to cardiomyocytes via gap junctions<sup>17,32,45, 46, and 47</sup>. The paracrine, structural, and possibly electrical interactions between fibroblasts and cardiomyocytes that underlie normal development also modulate the pathological responses to injury in the adult heart. In the failing adult myocardium, fibroblasts secrete several proinflammatory cytokines that directly promote hypertrophy of cardiomyocytes including: IL-1 $\beta$ , IL-6, TNF- $\alpha$  and TGF $\beta$ <sup>43</sup>. Cardiomyocytes also secrete some of these same cytokines that induce fibroblast migration, stimulate transformation of fibroblasts into myofibroblasts (TGF $\beta$ 1 in particular), and increase synthesis of several ECM components<sup>48,43,45</sup>. Similarly, angiotensin II type-1 receptors on neighboring cardiomyocytes

play an important role in determining the action of cardiac fibroblasts in the early phase of cardiac remodeling<sup>49</sup>. This role of activated cardiomyocytes driving fibrosis is in agreement with transgenic overexpression studies using activated forms of calcineurin or calcium-dependent signal-transducing molecules<sup>50</sup>. Thus, intracellular signaling crosstalk creates an environment where cardiac fibroblasts and cardiomyocytes reciprocally influence each other's phenotype<sup>7</sup>. Fibroblasts have also been shown to have extensive electrical coupling to each other as well as to cardiomyocytes via gap junctions in vitro during both developmental stages as well as following injury<sup>32, 51</sup>; however, the functional significance of these interactions has yet to be established in vivo. Increasingly available information relating to the dynamic nature of the cardiac microenvironment further alludes to the possibility that cardiac fibroblasts may be a key regulatory cell capable of mediating in vivo communication to cardiomyocytes, which is critical for both normal heart development and facilitating pharmacological therapeutic approaches within the heart<sup>43</sup>.

### 1.1.4 Cardiac fibroblasts in wound healing

Fibroblasts in the injured heart are thought to have diverse origins (Fig. 1.1 A). Resident cardiac fibroblasts at the site of injury proliferate and are thought to be the predominant pool of cardiac fibroblasts contributing to cardiac fibrosis after injury, although rigorous fate mapping studies have not been done to confirm this<sup>7</sup>. Bone marrow-derived cells also contribute to cardiac fibrosis<sup>52</sup>. Several studies have demonstrated that between 3 and 24% of myofibroblasts in the injured region are of bone marrow origin<sup>53, 54</sup>. These circulating fibroblast precursors have been termed fibrocytes and express hematopoietic (CD45), monocytic (CD11b) and progenitor (CD34) markers. The ability of bone marrow-derived cells to contribute to cardiac fibrosis appears to be physiologically important as inhibition of fibrocyte recruitment diminished fibrosis and had salutary effects on remodeling<sup>53</sup>. In addition, after an acute cardiac injury a subset of epicardial cells undergoes EMT to generate cardiac fibroblasts, thus recapitulating a developmental program of epicardial EMT (Figure 1.1)<sup>55, 56</sup>. Following EMT, epicardial-derived cardiac fibroblasts reside in the sub-epicardial space, express collagen and contribute to a pro-fibrotic repair response. Endothelial cells undergo endothelial–mesenchymal transition (EndMT) and have been reported to contribute to 30% of the cardiac fibroblasts in a murine model of pressure overload injury<sup>20</sup>, but the degree to which endothelial cells contribute to fibrosis in the acutely injured heart is less certain. A small number of non-residing cells derived from other cell types (including monocytes and endothelial cells) that are functionally significant, also contributes to this CF fraction that infiltrate the heart in response to ischemia, MI or

pressure overload. Thus, it is apparent that resident cardiac fibroblasts are not the sole source of activated fibroblasts in cardiac remodeling.

The cardiac fibroblast plays a central role in wound healing after myocardial injury and affects various aspects of the wound healing response from deposition of extracellular matrix proteins to wound angiogenesis and scar maturation<sup>57</sup> (as shown in Figure 1.2).

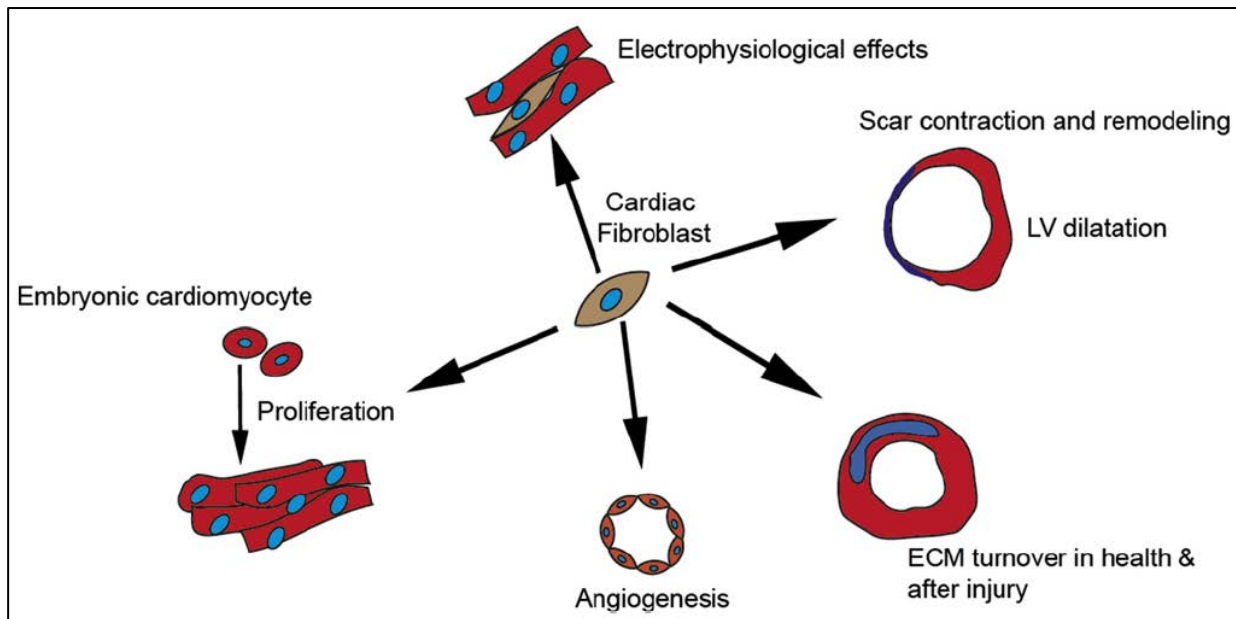


**Figure 1.2 Major functions of the fibroblast during cardiac development and wound healing.**

The fibroblast promotes proliferation of embryonic cardiomyocytes. It influences angiogenesis in the adult heart and regulates ECM turnover both in the adult uninjured heart and after acute injury. The fibroblast plays a pathophysiological role in scar contraction adverse remodeling and ventricular dilatation and exerts electrophysiological effects (Ref: Deb A *et al.* 2014)<sup>58</sup>.

Following acute myocardial infarction, cardiac fibroblasts in the heart become activated and rapidly proliferate. In rodent hearts, their peak number is achieved within 7–14 days after permanent ligation of the left anterior descending coronary artery<sup>59</sup> and within 3 days of ischemia–reperfusion injury<sup>60</sup>. Activated fibroblasts at the site of injury express contractile proteins such as smooth muscle actin (myofibroblasts) and secrete ECM proteins (mainly collagens). This early fibrotic repair response is critical for maintenance of cardiac structural integrity and performance after cardiac injury. Disruption of cardiac fibroblast activation early after injury leads to impaired wound healing and worsening cardiac performance<sup>55</sup>. In the later phases of wound healing (days to weeks), collagen fibers at the site of injury undergo cross-linking which increases the tensile strength of the scar<sup>57</sup>. The scar subsequently contracts undergoing a reduction in surface area and myofibroblasts expressing contractile proteins are thought to contribute to scar contraction (Figure 1.2).

Scar contraction and thinning lead to adverse changes in ventricular chamber geometry and compliance thereby causing congestive heart failure. Since fibroblasts exist in close interactions with endothelial cells; they also facilitate angiogenesis via expression of angiogenic cytokines (FGF, VEGF) and fibroblast-derived matrix proteins. Thus, activated fibroblasts play a pivotal role in the wound healing response by initiating a cascade of events in order to restore tissue integrity and homeostasis.

### 1.1.5 Cardiac fibroblasts in regenerative processes

Developmental biology research has opened important avenues for converting fully differentiated cells into various lineages via reprogramming technologies. As a crucial player in cardiac development, the cardiac fibroblast has recently been exploited as a key target to accomplish cardiac regeneration. Fibroblasts can also be reprogrammed into different cell types, such as pluripotent stem cells<sup>61</sup>, myoblasts<sup>62</sup>, neurons<sup>63</sup>. Expression of three transcription factors (Gata4, Mef2c, Tbx5, collectively referred to as GMT) mediated by retroviral gene transfer was shown to be sufficient to directly reprogram adult fibroblasts to become adult cardiomyocytes both *in vitro*<sup>64</sup>, and, most significantly, *in vivo*<sup>67</sup>. Identifying the derivatives of these reprogrammed cardiac fibroblasts was accomplished using the 3.9kb Periostin-Cre and Fsp1-Cre lineage reporters, in concert with various lacZ and fluorescent indicator mice<sup>67</sup>. Importantly, it has been demonstrated that in the absence of genetic reprogramming, no cardiomyocytes expressed any lacZ either before or after myocardial infarct; however, the retroviral-induced GMT cardiac fibroblasts were able to give rise to lacZ-positive cardiomyocyte-like cells, suggesting that these cells were derived from reprogrammed cardiac fibroblasts<sup>67</sup>. Not only did the reprogrammed fibroblasts differentiate into cardiomyocyte-like cells, but also these *in vivo* studies revealed that cellular reprogramming post-myocardial infarction resulted in improved cardiac function<sup>67</sup>. More recently, treatment with a combination of miRNAs (miRNAs 1, 133, 208 and 499) has been shown to facilitate the conversion of neonatal and adult cardiac fibroblasts into adult cardiomyocytes<sup>68</sup>. While both of these techniques show promise for increasing the regenerative capacity of the heart following ischemic injury, still they have low *in-vitro* efficiencies.

### 1.1.6 Current state of gene targeting in cardiac fibroblasts

Our knowledge regarding the functions of cardiac fibroblasts in the heart, their origins during cardiac development and in disease condition, the dynamic nature of their population, how that population may be in flux during time of injury or pressure overload is

derived from the genetic and cellular fate-mapping studies done so far. The Cre-loxP system is one of the most promising in vivo methods used to analyze the contribution of specific cell types in development and pathophysiological conditions in heart<sup>69</sup>. Unlike  $\alpha$ -myosin heavy chain promoter-Cre line (which enables cardiomyocyte-specific gene-knockout strategies in heart<sup>69</sup>), **there is no mouse line available that specifically expresses Cre recombinase in cardiac fibroblasts**. Though not organ specific, fibroblast-specific transgenic lines that express Cre under the control of a Postn promoter (Postn-Cre mice)<sup>48,67</sup>, a S100a4 [Fibroblast Specific Protein 1 (Fsp1)] promoter<sup>67, 70</sup>, and Transcription Factor 21 [Tcf21, also known as Podocyte-Expressed 1 (Pod1) combination, or a Capsulin or Class A Basic Helix-Loop-Helix 23 (bHLHa23)] promoter, have been reported<sup>71</sup>. The Postn-Cre mouse contains a 3.9 kb 5' upstream region of the mouse Periostin genomic DNA to promote the expression of an EGFP/Cre fusion expression vector<sup>66</sup>. Following intercrossing with the R26R indicator mice, lacZ expression (Indicative of earlier Cre expression) is present within all non-cardiomyocyte lineages of the fetal and neonatal heart<sup>72-73</sup>. Similar to endogenous Periostin<sup>48,74</sup>, Postn-Cre is also expressed within a few homeostatic CFs but is robustly expressed within the CFs and myocardial infarct sites following injury<sup>66, 75</sup>. FSP1 has been used as a fibroblast-specific marker in normal and fibrotic tissues<sup>75</sup>. However, a recent study documents the non-specific expression of Cre - recombinase in the heart tissue of Fsp1-Cre mice<sup>76</sup>. Specifically, in a myocardial infarction or pressure overload model, Fsp1-Cre-driven gene-deleted cells were not only cardiac fibroblasts, but also hematopoietic, endothelial, and vascular smooth muscle cells<sup>76</sup>. Using fate-mapping techniques, Acharya and co-workers have identified the transcription factor Tcf21 as a marker for cells that are committed to the cardiac fibroblast lineage and as an essential mediator in the development of cardiac fibroblasts<sup>77, 71</sup>. Very recently, genetic lineage tracing of CFs in pressure overload heart was done using a collagen1a1-GFP reporter line<sup>78</sup>. Studies done so far using these fibroblast-specific transgenic lines have yielded remarkable insights in identifying and mapping various cell lineages that initially give rise to the developing heart and deciphering many of the key morphological events that are required for both normal heart development and the underlying causes of congenital heart defects.

## 1.2 Gene targeting in mice using the cre/lox system

Genetically engineered mouse lines have emerged as powerful tools not only for understanding cardio-vasculogenesis but also for understanding the pathogenesis of cardiac disease through animal modeling<sup>79-81</sup>. The heart is composed of several cell types



that distinguish it from other organs<sup>82</sup>. Each has specific functions based on unique gene expression patterns that direct responses to its cellular, physiological, and stress environments<sup>83</sup>. Approaches are therefore required to identify these functions at the animal level because this complexity cannot be fully recapitulated *ex vivo*. Mice are a good choice for modeling the genetic basis of mammalian cardiovascular development and disease. Mice are mammals with a 4-chambered heart, their genes can be engineered in a highly specific manner and then expressed in both inducible and non-inducible manners<sup>84</sup>, the generation of genetically engineered mice is both cost and time effective relative to other mammals<sup>79</sup> and inbred strains of mice are available, which allow mutations to be introduced into defined genetic backgrounds<sup>85</sup>. Hereditary forms of cardiovascular disease can be modeled through germline mutations, and nonhereditary forms of the cardiovascular pathophysiology can be introduced in tissue-specific and inducible manners. Genes can be overexpressed or ablated in spatio-temporal fashion. Multiple gene defects can be combined or added in sequence through a combination of breeding and inducible systems. Polymorphisms can also be introduced in the germline or in tissue-specific and inducible manners. Similarly, the effects of microenvironment and stress can be functionally tested through gene alterations in specific cardiac cell types and through alteration of the animal's environment and application of stress conditions. Mouse strains with complex genetic combinations and highly controlled spatial and temporal regulation of genes now predominate the modeling of cardiac disease<sup>81</sup>. Advancement in molecular techniques allows the design of definite genetic modifications in the mouse. Now, along with defined nucleotide changes, also genetic switches designed to target expression or ablation of any gene (for which basic molecular information is available) to any tissue at any defined time can be engineered into the mouse genome. The most potential tool, both for the design of such genetic switches and for speeding the creation of gene-modified animals, is the Cre-LoxP recombination system.

### **1.2.1 Cre-loxP recombination system**

The Cre-LoxP recombination system is a special type of site-specific recombination system from bacteriophage P1, which is particularly simple and well characterized<sup>86</sup>. Cyclization recombination gene encodes a 38-kDa site-specific DNA recombinase, called **Cre**, which recognizes 34-bp loxP sites, and catalyzes both inter- and intramolecular recombination between two loxP sites (Fig. 1.6). The loxP (locus of X-over of P 1) is a site on bacteriophage P1 and consists of an 8-bp nonpalindromic core region flanked by two 13-bp inverted repeats. Cre-loxP mediated recombination between two directly repeated loxP sites

catalyze deletion of all DNA sequences located within the two sites. When the loxP sites are arranged in opposite directions, Cre catalyze inversion of the intervening DNA. In addition, intramolecular recombinations can be performed, also when the loxP sites are on different strands of DNA. Insertion of a DNA segment into a loxP site is also possible though the excision reaction is favored over the integration event. Since any DNA sequence introduced in between the loxP sequences (termed “floxed” DNA) is excised because of Cre-mediated recombination. Therefore, control of Cre expression in a transgenic animal, either with a tissue- or cell-specific promoter or with an inducible system, results in the spatial or temporal control of DNA excision between the two-loxP sites. In addition to conditional knockout and gene inactivation, this approach can be applied to protein over-expression. In that case, a floxed stop codon is inserted between the promoter sequence and the cDNA of interest and transgenic animals expressing Cre do not express the transgene, leading to excision of the floxed stop codon by Cre recombinase. This strategy has been successfully used to develop reporter mice that express LacZ<sup>87</sup> or different fluorescent proteins like green fluorescent protein (GFP)<sup>88</sup>, yellow fluorescent protein (YFP)<sup>89</sup>, cyan fluorescent protein (CFP)<sup>90</sup>, DsRed, a red fluorescent protein (RFP)<sup>91</sup> after Cre-mediated recombination. Since Cre is one of the few recombinases that do not require any additional cofactor or accessory molecules in eukaryotic cells, Cre is the first choice of investigators for introducing gene modifications into the mouse genome.

Currently, a large number of Cre transgenic mouse strains are available, allowing researchers to restrict conditional genetic modifications to particular cell types and to various other tissues of the mouse. Such Cre expressing mouse strains can be generated either by using conventional random transgenesis, by targeted insertion into a gene (knock-in), or by using a bacterial artificial chromosome (BAC) strategy. BACs are low-copy plasmids that stably maintain genomic DNA sequences, hundreds of kilobases (Kb) in length from mouse or human and can be obtained commercially. The use of BAC plasmids for transgenic gene expression is also gaining popularity over traditional proximal promoter-driven transgene expression. The main advantage of BAC is that they are most likely to contain all the important genomic regulatory elements required to recapitulate endogenous gene expression pattern<sup>92</sup>. Thus, BAC can also be used for expressing Cre recombinase along with endogenous genes, by the introduction of Cre gene into defined genes encoded by the BAC via homologous recombination in bacteria<sup>93</sup>. In addition to the Cre-loxP recombination system, FLP-FRT and Dre-rox systems are also available<sup>94,95</sup>. FLP-FRT recombination is analogous to Cre-lox recombination but involves the recombination of

sequences between short flippase recognition target (FRT) sites by the recombinase (Flp) derived from the 2 $\mu$ m plasmid of baker's yeast *Saccharomyces cerevisiae* (Figure 1.3).

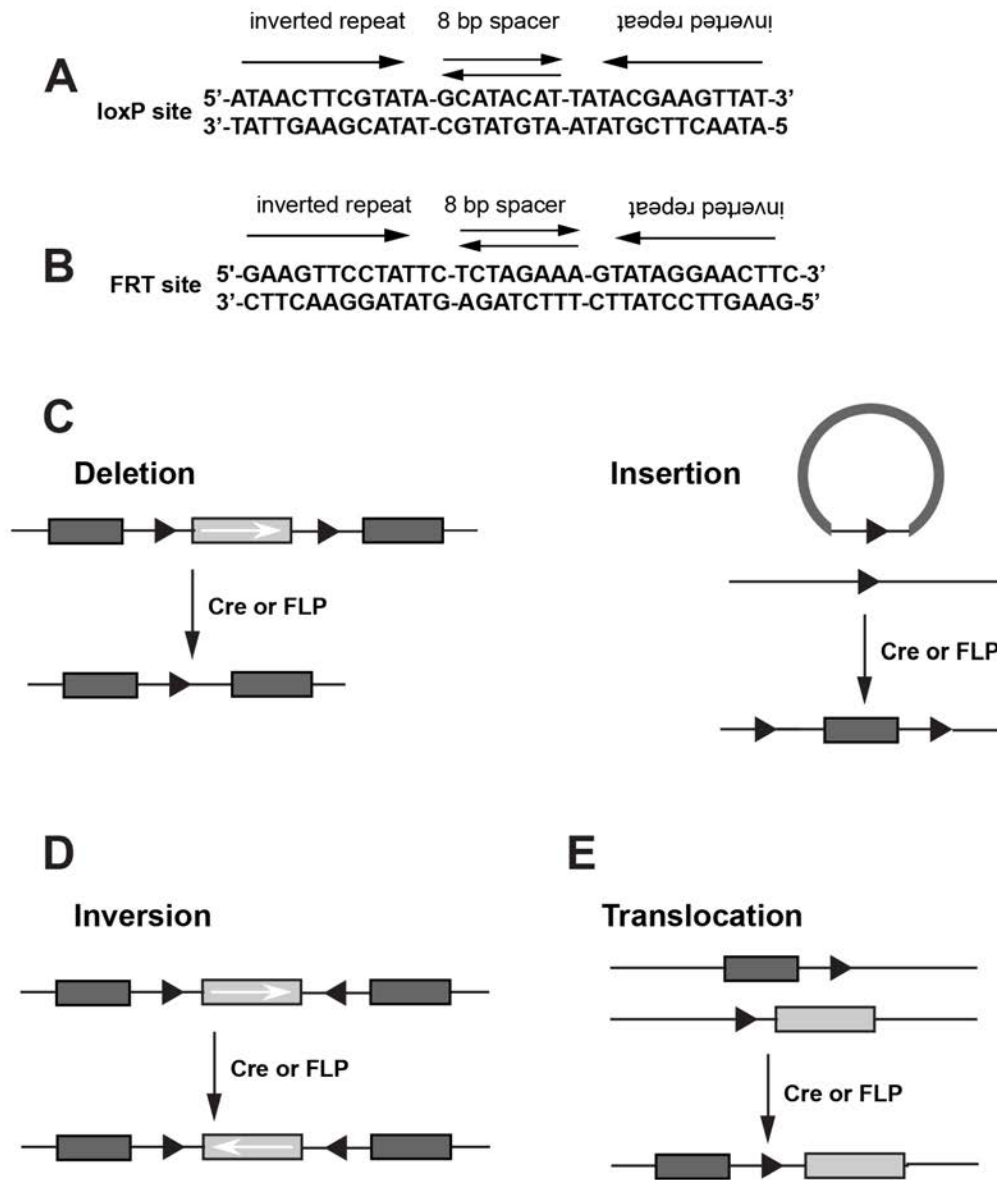


**Figure 1.3 Cre and FLP recombinase systems.**

Cre and FLP recombinases recognize loxP (A) and FRT (B) sequences, respectively. These 34-bp sequences contain 13-bp inverted repeats flanking 8 bp unique sequence motifs that have directionality. When 2 loxP or 2 FRT sites line up a recombination occurs at the 8 bp motif. Depending on whether the 8-bp motifs are in the same or opposite orientation a deletion or insertion (C), inversion (D) or translocation (E) can occur (Modified from Bockamp E *et al.* 2002)<sup>96</sup>.

### 1.2.2 Tamoxifen-inducible conditional gene targeting

In order to better understand the functioning of a given gene product in a given cell type at a given developmental stage, genetic techniques have been developed intentionally allowing the introduction of defined mutations into the mouse genome, in a specific cell type and at a chosen time. Use of the site-specific recombinase Cre is the basis of current conditional gene targeting system. Clearly, the key to successful conditional gene targeting is the availability of Cre transgenic mouse strains in which Cre activity is tightly controlled in space and time. To add inducibility to the Cre/lox system, ligand-dependent chimeric Cre recombinases, so-called CreER recombinases, have been developed. These consist of Cre fused to mutated hormone-binding domains of the estrogen receptor<sup>100, 101</sup>. Newer, more efficient versions of the ligand-dependent recombinase, termed Cre-ERT2 and ERT2-Cre-ERT2, have since then been developed<sup>102-104</sup>. Both, CreERT and CreERT2, do not bind to endogenous estradiol, but they bind to synthetic estrogen receptor ligand 4-hydroxytamoxifen or Tamoxifen (Tam) with high affinity (Figure 1.4). Generally, in the absence of hormone, estrogen receptors are largely located in the cytoplasm. Estrogen binding to the receptor translocates the receptor from the cytoplasm to the nucleus where it binds to DNA and regulates transcription of target genes<sup>105</sup>. However, the CreERT recombinase are inactive and remain in the cytoplasm but can be activated and translocated to the nucleus by Tam, thereby allowing for external temporal control of Cre activity<sup>100, 106</sup>.

A CreERT2 mouse can be a transgenic or a knockin of the CreERT2 coding region into an endogenous gene. A transgenic mouse is a biological model that has been genetically modified by the introduction of a foreign DNA sequence/fragment into the genome whereas knockin is a biological model that has a gene sequence inserted at a particular locus. ROSA26-CreERT2 mice were generated by targeting CreERT2 into the ROSA26 locus that have ubiquitous Tam-induced Cre recombination in adult mice<sup>107</sup>. In addition, cell-type-specific CreERT2 mice such as cardiac-specific  $\alpha$ MHC-CreERT2 (also called  $\alpha$ MHC-MerCreMer) mice have been effectively used in cell-type-specific Tam-inducible gene targeting<sup>108</sup>. In addition, Tam-inducible Cre recombination has been effectively used to modify gene function in mouse embryos in utero<sup>109, 107, 110</sup>. Tamoxifen can be administered via food (custom-made chow containing 0.4–1 g/kg Tam, Harlan), water intake (0.5–1 mg/mL), or either by intraperitoneal or IP injection (100  $\mu$ L of 10  $\mu$ g/mL Tam) or oral gavage (200 mg/kg) for 5 consecutive days.

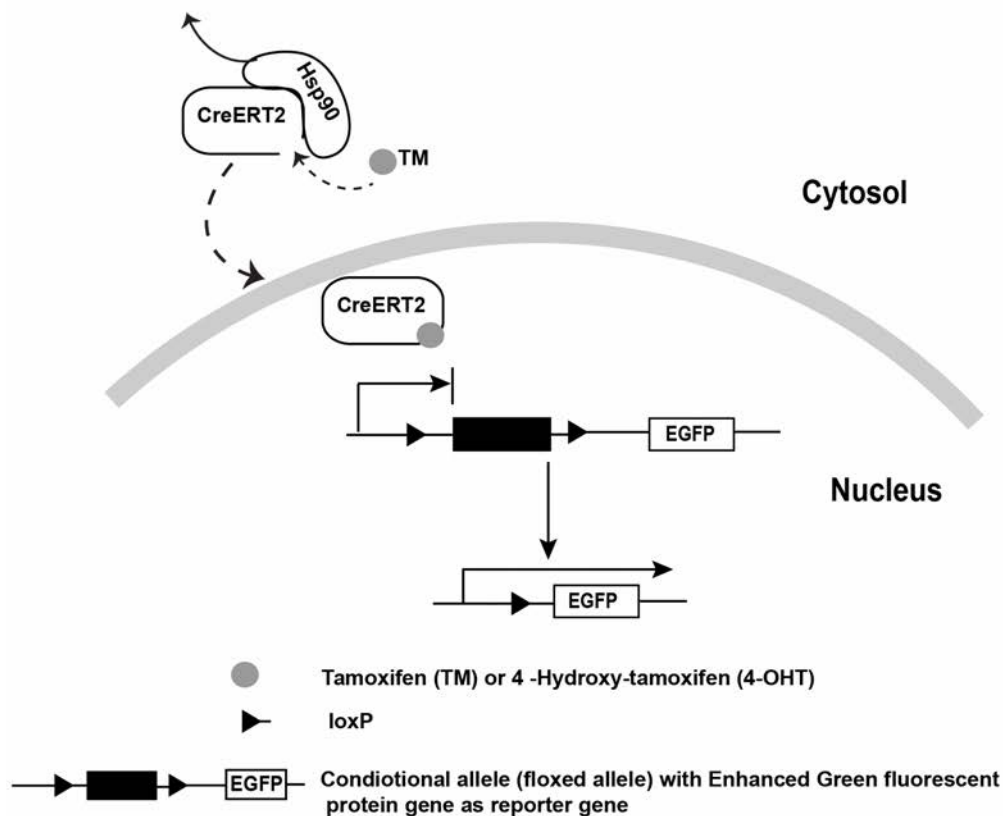


**Figure 1.4 Inducible-Cre system.**

Temporal restriction of Cre recombinase is achieved by fusing it to the tamoxifen-responsive ligand-binding domain of the estrogen receptor (Cre-ERT2). In the absence of appropriate ligand, the Cre recombinase fused estrogen receptor with mutated ligand binding domain is bound to the heat shock protein (Hsp90) and inhibited from entering the nucleus. Upon administration and binding of estrogen antagonist, tamoxifen (TM) or 4-hydroxytamoxifen (4-OHT) to the mutant estrogen receptor, Hsp90 dissociates from the CreERT2 and allows translocation of activated CreERT2 into the nucleus. In the nucleus, CreERT2 recognizes the loxP sites in the conditional allele of target genes and mediates recombination. Consequently, the reporter gene (EGFP) permanently marks the cells and appears green (Modified from Jung-Eun Kim, 2006) <sup>111</sup>.

The main advantage of inducible gene expression models is the temporal control of gene expression or deletion by the external application of a drug. It is an appropriate method to overcome problems such as prenatal lethality caused by conventional or tissue-specific inactivation of genes. It also allows the control of gene expression at specific time points. This is especially attractive for studying specific gene function at specific time points during development and homeostasis. Importantly, it allows investigators to turn genes on or off at different disease stages, enabling assessment of their importance during the progression of various diseases.

This inducible system also has several limitations. Besides the problem of choosing the right method for drug application, dose determination is another pitfall when using these systems.

Toxic side effects can result due to high dose or prolonged treatment and can ruin an experiment. Another side, low doses can result in the insufficient induction of the protein of interest (e.g., Cre), causing only a partial gene knockout. Another disadvantage of the tamoxifen approach to induce constitutive or cell-type-specific gene manipulation in utero is the risk of embryo abortion and death (can occur after 4 days of treatment), so it is useful only during those 4 days<sup>109, 107, 110</sup>. Intestinal problems from Tam administration have also been reported in homozygous ROSA26-CreERT2 mice<sup>107</sup>. There are also some concerns that Tam can cause behavioral alterations<sup>112</sup>. Despite these potential problems, numerous researchers have successfully used this approach to investigate cardiac-specific gene function in the physiology and pathophysiology of the heart<sup>81, 113</sup>.

### 1.2.3 Tetracycline-inducible Cre recombination

In the tetracycline-inducible system, expression of the target gene is dependent on the activity of an inducible transcriptional activator. The transcriptional activator is regulated reversibly by the inducing ligand tetracycline or tetracycline derivatives such as doxycycline (Dox). This system consists of the Tet-Off system (tetracycline-controlled transactivator protein (tTA) dependent) and the Tet-On system (reverse tetracycline-controlled transactivator protein (rtTA) dependent)<sup>114, 115</sup>. In each system, a recombinant tetracycline-controlled transcription factor (tTA or rtTA) interacts with a tTA/rtTA responsive promoter, Ptet, to drive expression of the gene of interest. In the Tet-Off system, target gene expression is turned off with the inducing ligand tetracycline or Dox. The Tet-Off system makes use of the tetracycline transactivator (tTA) protein, which is created by fusing one protein, TetR (tetracycline repressor), found in *Escherichia coli* bacteria, with the activation domain of another protein, VP16, found in the Herpes Simplex Virus. tTA binds to a tTA-responsive promoter (Ptet) to drive the expression of a gene in the absence of tetracycline or Dox. Addition of Dox, stops target gene expression due to formation of Dox-tTA complex with the transcription factor tTA, which cannot bind with Ptet. In contrast, in the Tet-On system, target gene expression is turned on by the inducing ligand. Addition of tetracycline or Dox, leads to binding of the transcription factor rtTA to Ptet through Dox-rtTA complex, thereby initiating the expression of gene under study. While the absence of Dox, inhibits the binding of rtTA with Ptet thus, inhibiting gene expression.

Several studies have indicated that the rtTA system is better suited for temporal control of rapid induction of gene expression<sup>116</sup>. Recently, many investigators have combined the Tet inducible system with the Tam-inducible Cre-loxP approach. This allows more flexibility producing more clinically relevant mouse models of human diseases<sup>116</sup>. Several laboratories

have integrated the Tet-inducible and Cre-loxP approaches and developed mice based on rtTA-dependent Dox-mediated gene induction following a Cre-mediated deletion to obtain a temporal and spatial or cell-, tissue-, and organ-specific gene targeting<sup>117, 118</sup>. Thus, gene targeting can be manipulated in specific cell types and lineages with a flexibility that is difficult to achieve with other methods. To make this system more sophisticated, a Tet-inducible CreERT2 has been targeted to the ROSA26 locus<sup>119</sup>. By introducing Tet induction, this Tam-inducible Cre driver line permits highly selective dual Tet and Tam regulation of loxP recombination, which could open new avenues for spatiotemporally controlled gene targeting in mice.

There are pitfalls inherent in Tet-inducible technology worth mentioning. The Tet system can be leaky<sup>120</sup>. This can occur either through weak binding of rtTA to Ptet even in the absence of Tet or Dox effectors, or through an unwanted basal activity of the Tet-responsive promoter even in the absence of rtTA. This leakiness can result in unexpected phenotypes when Tet is absent<sup>121</sup>. Although this leakiness can be tolerated in many experimental systems in which phenotypic outcomes are desired, it can be limiting when gene function is being investigated. Use of several Cre transgenic lines could obviate some of these difficulties. Another potential problem with the Tet system is that of tissue toxicity caused by overexpression of TetR proteins<sup>120</sup>. This can also be avoided by producing multiple transgenic lines expressing varying levels of Tet repressor. Taken together, it is very important that proper control animals are used in Tet-inducible gene targeting experiments to avoid misleading results due to these pitfalls. Overall, the ability to regulate gene activity in spatiotemporal and reversible fashions has made the Tet-inducible approach a favorite technology of numerous mouse geneticists.

Tamoxifen- and Tetracycline-inducible strategies have been applied to achieve this end<sup>122, 81,123</sup> and have been successful in demonstrating gene function in cardiac structure and function, cardiac physiology and pathophysiology, cardio-mechanics, cardiac calcium handling, and cardiac stress response<sup>113</sup>. The table given below summarizes the mice models validated for cardiac-specific inducible gene targeting.

**Table 1.** Validated mouse models for cardiac-specific inducible and/or conditional gene targeting

Cardiac-cell Type	Cre mice	Cre expression	Induction	Ref
Myocardium	$\alpha$ MHC-CreERT2	Myocardium	Tam	<sup>108</sup>

	$\alpha$ MHC-CrePR1		RU486	124
	$\alpha$ MHC-tTA, Tnnt2-rtTA/tetO		Doxy	120, 125
<b>Endothelium,</b>	Tie -CreERT, VE-cadherin-CreERT2	Cardiac & vascular endothelium,	Tam	126, 127
	Tie -(r)tT	ND	Doxy	<b>Tetmouse database</b>
<b>Cardiac and valvular fibroblasts</b>	Tcf 1-CreERT2	Epicardium, cardiac fibroblasts, valve interstitial cells,	Tam	71
	Col2-CreERT2	ND	Tam	128
	$\alpha$ SMA-CreERT2	ND	Tam	129
	$\alpha$ SM22a-(r)tTA	ND	Doxy	<b>Tetmouse database</b>
	Wnt1-CreERT2	ND	Tam	130
<b>Cardiac neural crest cells Epicardium</b>	Wt1-CreERT2	Epicardium, epicardium- derived cells	Tam	31
	Tcf21-CreERT2	Epicardium, cardiac fibroblasts, valve interstitial cells	Tam	71
	HCN4-CreERT2	SA node, AV	Tam	131
<b>Cardiac conduction system</b>	Cx40-CreERT2	node AV bundle, bundle branches, Purkinje fibers, atrial Cardiomyocytes,	Tam	132
	mink-CreERT	coronary vessels AV node, AV bundle, bundle branches	Tam	133

$\alpha$ MHC indicates  $\alpha$ -myosin heavy chain; CreER, Cre with the mutated progesterone receptor ligand-binding



domain; Tie2, tyrosine-protein kinase receptor TIE-2; Tcf21, transcription factor 21; Col2, collagen 2;  $\alpha$ SMA, alpha smooth muscle actin; SM22a, SM22alpha; Wnt1, wingless-related MMTV integration site 1; Wt1, Wilms tumor 1 homolog; HCN4, hyperpolarization-activated, cyclic nucleotide-gated K<sub>4</sub>; Cx40, connexin 40; ND, not determined; mink, Kcne1l potassium voltage-gated channel; tTA, tetracycline-controlled transactivator; Tnnt2, rat troponin T; rtTA, reverse tetracycline controlled transactivator; tetO, tetracycline operator; AV, atrioventricular, Tam, Tamoxifen ; Doxy, Doxycycline.

### 1.3 Cardiac fibroblast-specific markers

Although CFs are widely acknowledged as prime targets for treatments of cardiac disease, our limited understanding of the details of the various roles that these cell populations play as well as how those various roles are intertwined in vivo hinder the design and application of potential therapies. **The paucity of markers to faithfully identify cardiac fibroblasts at a single time point is one of the major issues challenging the cardiovascular field today.** There are several well-known indicators of fibroblast phenotype, but none of them is both exclusive to fibroblasts and present in all fibroblasts. A few of the commonly used CF markers include: Discoidin domain collagen receptor (DDR)-2, Fibroblast-specific protein (Fsp1), Collagen type I, Fibroblast activation protein, Platelet-derived growth factor receptor alpha (Pdgfr $\alpha$ ), Periostin, Thy1 cell surface antigen, and Vimentin. The variable expression of the most commonly used markers at different stages of development is described in Table 2. For example, Vimentin, an intermediate filament protein has been extensively used to label cardiac fibroblasts<sup>134</sup>. However, though antibodies to Vimentin label fibroblasts with great sensitivity (at this stage, it is safe to assume that all fibroblasts are Vimentin-positive), they also label various other cell types, including endothelial cells<sup>17,134,42</sup>. In fact, Vimentin had first been described as an endothelial cell marker<sup>135</sup>. Fibroblast-specific protein 1 (Fsp1) is another indicator of fibroblast phenotype, which was identified in a differential expression screening comparing kidney fibroblasts and kidney epithelial cells<sup>136</sup>. It is also known as S100A4 and is also expressed by metastatic cancer cells. Immediate evidence suggests that it is specific for cardiac fibroblasts in the heart<sup>20</sup>. However, Fsp1 antibodies detect only a subset of cardiac fibroblasts in heart<sup>20</sup>. Recently it has been shown that Fsp1 is also expressed within inflammatory leukocytes and vascular cells in murine infarction and pressure overload-induced fibrosis models convoluting the future use of this marker<sup>76</sup>. In the healthy adult heart, valvular fibroblasts (also called as valvular interstitial cells) express alpha-smooth muscle actin ( $\alpha$ -SMA), but not interstitial fibroblasts of the myocardium<sup>48</sup>. In cardiac fibrosis, myocardial fibroblasts start expressing  $\alpha$ -SMA (then called as myofibroblasts), which is considered a sign of fibroblast activation<sup>137</sup>. Though, there are other cell types like vascular

smooth muscle cells and pericytes, lying in close proximity to fibroblasts, which also, found to express  $\alpha$ -SMA. These cells can be falsely identified as fibroblasts when immunofluorescence techniques with insufficient resolution are used.

**Table 2.** Commonly utilized fibroblast makers are listed along with their relative expression levels at varying developmental and/or injury states.

	Developmentally expressed markers	Adult CF resting markers	Myofibroblast markers	References
Thymus cell antigen-1 (Thy1)	++	++	++	[147,148]
Vimentin	++	++	++	[149, 150]
Periostin	++	+/-	++	[151, 74]
Ddr2	++	+	++	[37,19,4]
Fibroblast-specific protein-1 (Fsp1)	++	+/-	+++	[136, 152]
$\alpha$ Smooth muscle actin	+/-	+/-	+++	[65,153]
Platelet-derived growth factor receptor- $\alpha$ (PDGFR $\alpha$ )	++	++	++	[154]
Fibroblast activation protein	++	++	++	[37,155]

Discoidin domain receptor-2 (DDR2), a collagen receptor, has been used to identify and sort cardiac fibroblasts<sup>19,17</sup>. However, DDR2 is also expressed by lymphocytic lineages and identifies only subsets of fibroblasts. Periostin, a matricellular protein is only expressed in a small subset of CFs in the quiescent adult heart but is robustly up-regulated in response to injury<sup>138-142,74,75</sup>, therefore making it a useful marker of activated injury-site fibroblasts.<sup>76</sup> Additionally, developmental studies suggest that endogenous Periostin is one of the most

reliable markers of CFs in utero and throughout the early postnatal period<sup>48,65-67</sup> making it well suited to developmental and neonatal investigations. Collagen type I is the major fibrillar component of the cardiac ECM and one of many ECM proteins produced by fibroblasts. The promoter region for the pro- $\alpha 1(I)$  chain of type I collagen has been well characterized and it has been shown that different regions of this promoter can be used to drive expression of genes in specific collagen producing cell types including fibroblasts, osteoblasts, odontoblasts and some mesenchymal cells<sup>78, 143, 144</sup>. A number of commercially available reporter mice (Cre, fluorescent protein expressing, inducible) have been generated using the type I collagen  $\alpha 1$  chain promoter. Type I collagen is also produced by smooth muscle cells in response to TGF $\beta$ , EGF, and angiotensin II stimulation<sup>145, 146</sup>, therefore the use of a fibroblast-specific regulatory region from the pro- $\alpha 1(I)$  chain promoter could provide a valuable tool for marking fibroblasts within the heart. Thy1.1 (or CD90) is a membrane glycoprotein expressed on the surface of CFs but is also detectable on some endothelial cells<sup>77</sup>.

Thus, the absence of comprehensive markers has inhibited our ability to study the complex interactions between CFs and the surrounding cells *in vivo*. It may be that there is no ideal way to identify CFs with a single marker; however, the more we are able to understand the limitations of the tools that we do have available, the more effectively we will wield them. Combining multiple markers to more conclusively identify CFs or understanding which markers are best in a particular context are footsteps that are currently being taken to improve the confidence in the interpretation of findings.

### 1.3.1 Vimentin

#### 1.3.1.1 Type III Intermediate filament protein Vimentin

Vimentin is one of the most familiar members of the large protein family of intermediate filaments (IFs). It is the major protein in mesenchymal cells and it is frequently used as a developmental marker of cells and tissues. Vimentin also present a very high degree of sequence homology between species, from fish and *Xenopus* to humans<sup>156, 157</sup>, suggesting some important and evolutionary conserved physiological roles of this IF protein. Vimentin, a 57-kDa protein, along with microtubules and actin microfilaments make up the dynamic cytoskeleton that maintains cell shape, enables intracellular transport, and supports cell division<sup>158-160</sup>. Studies using ras-transformed cells<sup>161</sup> and transgenic mouse models<sup>162</sup> have shown that vimentin regulates cell growth and differentiation. Recent studies using vimentin-deficient (Vim $^{-/-}$ ) mice have revealed that loss of vimentin leads to failures in vascular adaptation resulting in pathological conditions, such as reduction of renal mass<sup>163</sup>,

malformation of glia cells<sup>164</sup>, impairment of wound healing<sup>165</sup>, reduced resistance of arteries to shear stress<sup>166</sup>, and disturbance of leukocytes homing to lymph nodes<sup>167</sup>. Similar to other IF proteins, vimentin expression is often reported in a wide range of other cell types including pancreatic precursor cells, sertoli cells, neuronal precursor cells, trophoblastic giant cells, fibroblasts, endothelial cells lining blood vessels, renal tubular cells, macrophages, neutrophils, mesangial cells, leukocytes, and renal stromal cells<sup>25-30</sup>.

### 1.3.1.2 Vimentin expression in heart

Two intermediate filaments, desmin and vimentin, are found in human fetal heart tissue. Desmin, an early marker expressed during cardiac embryogenesis<sup>168</sup>, found to be expressed by cardiomyocytes and the intensity of cardiomyocytes staining for desmin increases progressively with age. On the other hand, vimentin appears during cell differentiation and is expressed by all connective tissue cells, including fibroblasts<sup>169</sup>.

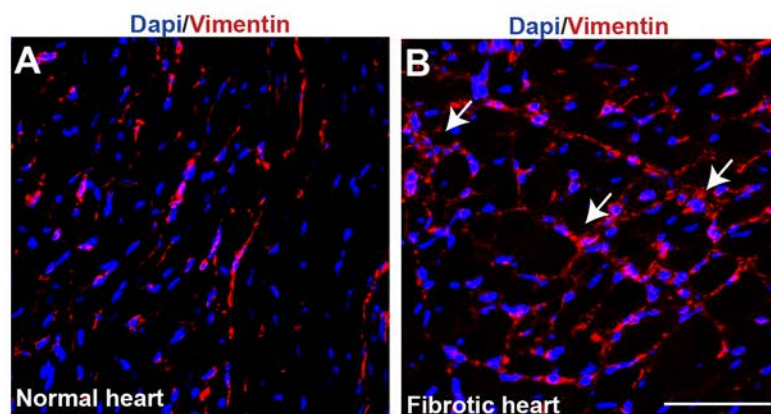


**Figure 1.5 Vimentin expressions in healthy and failing myocardium.**

Confocal images of immunofluorescence for fibroblast marker vimentin (red), with cell nuclei counterstained with dapi. **(A)** Normal myocardium with few fibroblasts and **(B)** In failing myocardium, increased expression of vimentin (red) in the fibrotic areas of failing heart. Scale bar represents 50 $\mu$ m.

During cardiac muscle cell differentiation, vimentin is replaced especially by desmin; however, some authors consider that vimentin is expressed in adults during post-ischemic regenerative processes<sup>170</sup>. During mouse development, vimentin expression begins on embryonic day 7.5 (E7.5)<sup>171</sup> and becomes predominant in the primitive streak stage<sup>172, 173</sup>, while in adult mice, vimentin expression was reported to be limited to connective tissue mesenchymal cells in the central nervous system and muscle<sup>174</sup>. Alterations of the cytoskeleton have been described in many excellent studies, by Tsutsui et al<sup>175</sup> and Tagawa et al,<sup>177</sup> in hypertrophied and failing right ventricles of feline<sup>175</sup> and canine<sup>180</sup> myocardium. The activation of cardiac fibroblasts and their differentiation into myofibroblasts is of

considerable clinical interest because of their contribution to cardiac fibrosis and hypertrophy. Vimentin, the intermediate filament of fibroblasts was used as an indicator of the cellularity of the interstitium in the myocardium. Increased expression of vimentin has been demonstrated in the interstitial spaces in fibrotic heart tissues<sup>176-179</sup> (Figure 1.5). However, an increased expression of vimentin has also been reported in various tumor cell lines and tissues including prostate cancer, breast cancer, endometrial cancer, tumors of the central nervous system, malignant melanoma, and gastrointestinal tract tumors etc.

### 1.3.2 Fibroblast-specific protein-1

#### 1.3.2.1 Fsp1/S100A4: a candidate marker for cardiac fibroblasts?

Fibroblast specific protein-1 (Fsp1) (also known as S100A4) is a member of the calmodulin S100 troponin C superfamily, and can be expressed by different cell types of mesenchymal origin. In fibrotic tissues, it is expressed by fibroblasts and has been suggested as a fibroblast-specific marker. Fsp1 has been involved in the regulation of a wide range of biological effects including cell motility<sup>181, 182</sup>, differentiation<sup>183</sup>, survival<sup>184, 183</sup> and contractility. It has both intracellular and extracellular effects. Differential hybridization studies identified Fsp1 as a filament-associated protein that is not expressed in epithelial cells, mesangial cells or embryonic endoderm, but only in fibroblast<sup>136</sup>. Antibody against Fsp1 identified fibroblasts both *in vitro* and *in vivo*. Furthermore, *in vitro* studies also demonstrated its role in mediating epithelial to mesenchymal transition<sup>185</sup>. In experimental models of pulmonary<sup>186</sup> and renal fibrosis<sup>136</sup> and in biopsied samples from patients with fibrotic disorders<sup>186</sup>, Fsp1 identified interstitial fibroblasts. Based on these observations, transgenic mice with GFP expression driven by the Fsp1 promoter (Fsp1.GFP mice) have been generated and used to map cell fate in fibroblast populations<sup>20</sup>. Though, Fsp1-Cre transgenic mouse models have served as a tool to study the effects of fibroblast-specific gene deletion in fibrotic and neoplastic conditions<sup>20, 187</sup>. However, growing evidence in recent years challenged the specificity of Fsp1 as a fibroblast marker, suggesting that other cell types infiltrating injured tissues, such as inflammatory macrophages<sup>188</sup>, dendritic cells<sup>189</sup>, lymphocytes<sup>190</sup> and vascular smooth muscle cells<sup>191</sup> may also express Fsp1.

#### 1.3.2.2 Fsp1/ S100A4 expression in heart

Originally described as a cytoplasmic protein in mesenchymal cells, Fsp1 was found to express after embryonic day 8.5 (E8.5) in developing tissues<sup>136</sup>. The heart of Fsp1-GFP transgenic mice displays no Fsp1-positive cells in the neonatal state, whereas only a few FSP positive cells are found in the adult heart (predominantly endothelial and perivascular cells) (Figure 1.6)<sup>76</sup>. Increased S100A4 mRNA and protein expression in hypertrophic left

ventricles of rats, mouse and human patients is reported, apparently regardless of the underlying experimental cause of hypertrophy<sup>183,76</sup>. Additionally S100A4 localizes to several activated, motile cell types of the injured hearts, including fibroblast-like cells, inflammatory cells, and endothelial cells, but not cardiomyocytes<sup>183, 192,76</sup>.

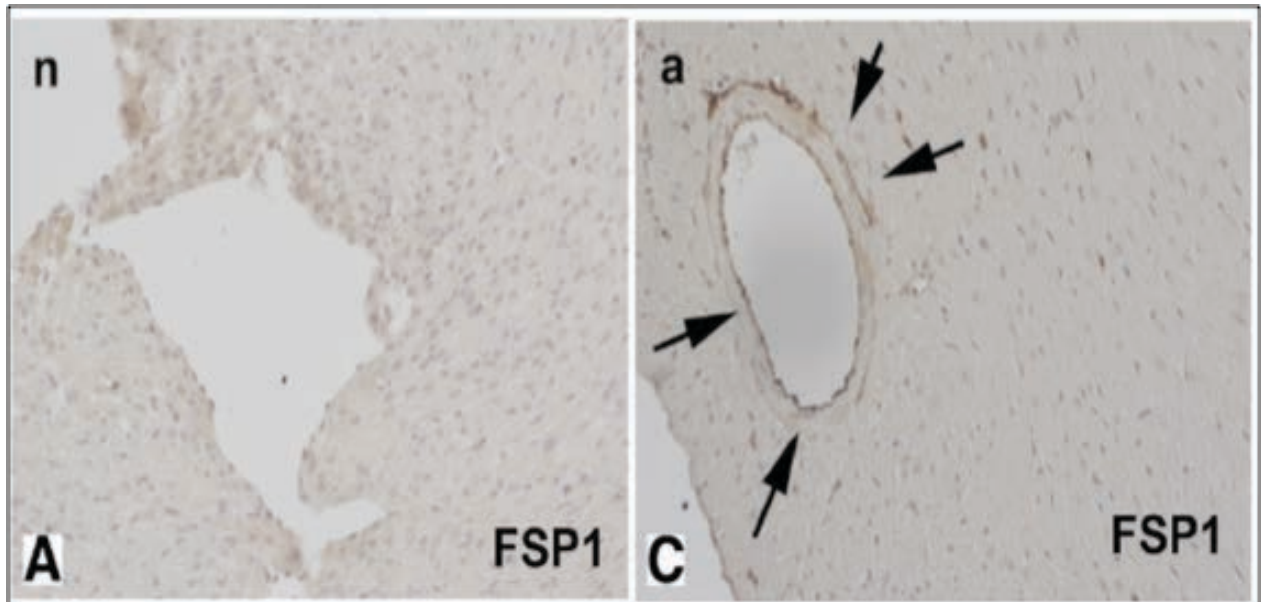


**Figure 1.6 Fibroblast-specific protein-1 (FSP1) expressing cells in neonatal (n:2 wk of age) and adult (a:3–4 month of age) Fsp1-GFP reporter mouse myocardium.** Neonatal hearts exhibit no FSP1 expression (A) while In adult mouse hearts, rare FSP1 cells are identified; these cells are either perivascular or endothelial (C, arrows) (Ref: Kong P *et al.* 2013<sup>76</sup>).

A recent study on the Fsp1-GFP mice in two models of cardiac remodeling (in the infarcted and pressure-overloaded myocardium) identified a large number of FSP1+ cells as endothelial cells, inflammatory leukocytes, and arteriolar smooth muscle cells<sup>76</sup>. This raises questions regarding the use of FSP1 as a cardiac fibroblasts marker and also raises concern regarding the use of FSP1-Cre animals as a tool for fibroblast-specific gene targeting *in vivo*.

### **1.3.3 Periostin**

Periostin, also termed osteoblast-specific factor 2, is a 93.3 kDa-secreted, vitamin K-dependent glutamate-containing matricellular protein, originally isolated from a mouse osteoblast cell line<sup>193,194</sup>. Periostin is assigned to the family of fasciclins based on its homology to fasciclin 1 (FAS1), initially identified in insects and is encoded by the Postn gene (genebank D13664) in humans. It is expressed in, vascular smooth muscle cells, cancer cells, periosteum and periodontal ligament, fibroblasts, and wound-site blood

vessels. On cell surface, periostin interacts with several integrin molecules ( $\alpha$ v $\beta$ 1,  $\alpha$ v $\beta$ 3, and  $\alpha$ v $\beta$ 5), thus, providing signals for tissue development and remodeling. In addition, periostin also participates in tumor angiogenesis, metastasis, and cell migration<sup>195-198</sup>. Analysis of Periostin deficient mice (Postn-deficient mice) has demonstrated the importance of periostin in the development of bone, tooth, and heart valves<sup>65,199</sup>. Periostin has also shown to have another physiological role in cutaneous wound repair<sup>200-202</sup>. Furthermore, periostin is involved in the development of various tumors via the integrin/PI3K/Akt pathway<sup>203</sup>. Expression of periostin during Th2-type immune responses, in lung fibroblasts and in fibrosis of bronchial asthma<sup>204,205</sup>, displays its role in allergic inflammation. In the heart, periostin is physiologically expressed in embryonic cardiac valves, while it is re-expressed abundantly in adult heart after pressure overload or myocardial infarction<sup>142,73, 206-209</sup>. During neonatal heart remodeling, peak expression of periostin induces collagen production; thereby mediating increased ventricular wall stiffness and valve functional maturation. However, periostin is downregulated in the postnatal cardiac fibroblast lineage and remains at a low level of expression. Abolishing periostin or TGF- $\beta$  reduces both proliferation and fibrosis and improved heart function<sup>210</sup>. Therefore, Postn-deficient mice are more prone to ventricular rupture within the first 10 days after myocardial infarction<sup>209</sup>, yet survivors showed less fibrosis and better ventricular performance. Furthermore, inducible periostin overexpression not only protected mice from ventricular rupture after myocardial infarction but also induced spontaneous hypertrophy with aging<sup>207</sup>. Accumulation of periostin has been demonstrated to be involved in repair after vascular injury<sup>197</sup> while, periostin insufficiency may contribute to valvular heart disease<sup>211, 212</sup>, heart failure<sup>75,213</sup>, and atherosclerosis<sup>214</sup>. Increased expression of periostin in both normal and pathologic hearts is confined to the cardiac fibroblast (non-cardiomyocyte) lineages, with TGF- $\beta$ 2 being required for periostin expression<sup>48</sup>. Thus, Postn is currently being discussed as a potential target for the prevention of heart failure<sup>75, 213</sup>.

### 1.4 Aim of this study

Over the years, research into the processes that control cardiac remodeling has focused on the cardiomyocyte as this cell type makes up the active beating part and also the biggest volume in the myocardial tissue. Only recently, more attention has been given to the fibroblast and a better understanding of its role in cardiac function. Though they have been recognized as active participants in the heart both in normal and disease condition; still, their exact physiological and pathological roles remain elusive, mainly due to the lack of specific markers. However, promising new techniques such as utilizing the Periostin-Cre

and Fsp1-Cre lines for lineage mapping and genetic modification of in utero and adult cardiac fibroblasts, as well as an increasing number of fibroblast markers are emerging to help address these challenges. Harnessing these new tools to examine the developmental origins of these cardiac fibroblast and their interactions with cardiomyocytes and other cell types and how they influence injury response may uncover methods of shifting pharmacologic interventions to a more proactive approach aimed at regeneration and undoing the damage caused by injury.

**The overall aim of this study was to identify a cardiac fibroblast specific gene whose promoter can then be used for studying fibroblast targeted genetic interventions.** This study was conducted in two parts. The first part included screening of genes enriched in CFs using microarray gene expression data. Validation of these candidate gene using qPCR-based gene expression profiling of cardiac fibroblasts and cardiomyocytes in order to identify genes enriched in cardiac fibroblasts in both neonatal as well as adult rodent hearts. Vectors enabling Cre-recombinase expression driven by selected candidate promoters were generated for validating promoter activity *in vitro* and *in vivo*. A transgenic mouse line that expresses Cre recombinase under Ccdc80 promoter was then generated to analyze promoter efficiency *in vivo*. Upon successful recombination after crossing with reporter mice, hearts and other tissues were studied for the promoter activity. Furthermore, another transgenic line, VimCreERT2, along with known fibroblast promoter-Cre mouse line (Fsp1-Cre) was characterised for cardiac fibroblast specific expression of Cre recombinase in both normal and disease condition in adult mouse heart and also during postnatal development.



## 2 MATERIALS AND METHODS

### 2.1 MATERIALS

#### 2.1.1 Chemicals

<b>Chemical</b>	<b>Manufacturer</b>
Acetic acid	J.T. Baker (Phillipsburg, USA)
Agar	Applichem (Darmstadt)
Agarose	Peqlab (Erlangen)
Ampicillin	Roth (Karlsruhe)
Ammonium peroxodisulphate (APS)	Sigma-Aldrich (Deisenhofen)
5-bromodeoxyuridine (BrDU)	Sigma-Aldrich (Deisenhofen)
Bovine Serum Albumin (BSA)	Applichem (Darmstadt)
Bromophenol blue	Merck (Darmstadt)
BDM	Sigma-Aldrich (Deisenhofen)
Chloroform	Roth (Karlsruhe)
Complete Mini (Protease inhibitor)	Roche (Mannheim)
Calcium Chloride (CaCl <sub>2</sub> )	Sigma-Aldrich (Deisenhofen)
Deoxynucleotide triphosphate (dNTP)	Invitrogen (Karlsruhe)
4,6-diamidino- phenylindole (DAPI)	Sigma-Aldrich (Deisenhofen)
DNase/RNase-free water	Gibco (Karlsruhe)
Dulbecco's modified eagle medium (DMEM)	Gibco (Karlsruhe)
Dimethylsulphoxide (DMSO)	Roth (Karlsruhe)
Ethylenediaminetetraacetate (EDTA)	Applichem (Darmstadt)
Ethanol	J.T. Baker (Phillipsburg, USA)
Ethidium bromide	Sigma-Aldrich (Deisenhofen)
Fetal bovine serum (FBS)	PAN (Aidenbach)
Fetal Calf serum (FCS)	PAN (Aidenbach)
D-Glucose	Merck (Darmstadt)
Fura- AM	Invitrogen (Karlsruhe)
Glycerol	Merck (Darmstadt)
Glycine	Applichem (Darmstadt)
Goat serum	Gibco (Karlsruhe)
50% Glutaraldehyde	Applichem (Darmstadt)
Haematoxylin	Roth (Karlsruhe)
HEPES Applichem (Darmstadt)	Applichem (Darmstadt)
Hydrochloric acid 37% (HCl)	Merck (Darmstadt)
Isofluran	Abbott (Wiesbaden)

## Materials and Methods

Isopropanol	Merck (Darmstadt)
Kanamycin	Fluka (Seelze)
Lipofectamine™ 2000	Invitrogen (Karlsruhe)
L-Glutamine	PAN Biotech (Aidenbach, D)
Milk powder	Applichem (Darmstadt)
Magnesium chloride (MgCl)	Merck (Darmstadt)
Magnesium sulphate (MgSO <sub>4</sub> ·7H <sub>2</sub> O)	Merck (Darmstadt)
Minimum essential medium (MEM)	Sigma-Aldrich (Deisenhofen)
β-mercaptoethanol	Applichem (Darmstadt)
Methanol	Sigma-Aldrich (Deisenhofen)
Opti-MEM I	Gibco (Karlsruhe)
Paraffin (Paraplast)	Sigma-Aldrich (Deisenhofen)
Paraformaldehyde (PFA)	Sigma-Aldrich (Deisenhofen)
Peanut Oil	Sigma Aldrich (Deisenhofen)
Peptone	Applichem (Darmstadt)
Penicillin/Streptomycin	Gibco (Karlsruhe)
Phenol/chloroform	Roth (Karlsruhe)
Phenylephrine (PE)	Sigma-Aldrich (Deisenhofen)
Phosphate buffered saline (PBS)	Gibco (Karlsruhe)
Potassium chloride (KCl)	Applichem (Darmstadt)
Potassium bicarbonate (KHCO <sub>3</sub> )	Sigma Aldrich (Deisenhofen)
Potassium di-hydrogen phosphate (KHPO <sub>4</sub> )	Roth (Karlsruhe)
Potassium Ferricyanide (K <sub>3</sub> [Fe(CN) <sub>6</sub> ])	Merck (Darmstadt)
Potassium Ferrocyanide (K <sub>4</sub> [Fe(CN) <sub>6</sub> ])	Applichem (Darmstadt)
Prestained protein ladder	Fermentas (St. Leon-Rot)
PVDF membrane	Millipore (Billerica USA)
6 ROX	
Sodium acetate (NaCH <sub>3</sub> COO)	Merck (Darmstadt)
Sodium chloride (NaCl)	Applichem (Darmstadt)
Sodium bicarbonate (NaHCO <sub>3</sub> )	Sigma Aldrich (Deisenhofen)
Sodiumdihydrogen phosphate dihydrate (NaH <sub>2</sub> PO <sub>4</sub> ·2H <sub>2</sub> O)	Applichem (Darmstadt)
Sodium dodecyl sulphate (SDS)	Roth (Karlsruhe)
Sodium hydrogen phosphate dibasic (Na <sub>2</sub> HPO <sub>4</sub> )	Sigma Aldrich (Deisenhofen)
Sodium hydroxide (NaOH)	Roth (Karlsruhe)
Sodium ortho vanadate (Na <sub>3</sub> VO <sub>4</sub> )	Sigma Aldrich (Deisenhofen)
SYBR green	
Tetramethylethylenediamine (TEMED)	Sigma Aldrich (Deisenhofen)
Taurine	Sigma Aldrich (Deisenhofen)
Tamoxifen	Sigma Aldrich (Deisenhofen)
X gal	Roth (Karlsruhe)

**2.1.2 Kits**

Plasmid DNA Maxi kit	Qiagen (Hilden)
Plasmid DNA Midi kit	Qiagen (Hilden)
QIAquick Gel extraction kit	Qiagen (Hilden)
QIAquick PCR purification kit	Qiagen (Hilden)

**2.1.3 Enzymes**

<b>Enzyme</b>	<b>Manufacturer</b>
Accuprime Pfx DNA Polymerase	Invitrogen (Karlsruhe)
Benzonase	Merck (Darmstadt)
Collagenase Typ2 II Worthington	(Lakewood, USA)
Difco Trypsin 250	BD (Heidelberg)
DNase	Sigma-Aldrich (Deisenhofen)
Gateway BP Clonase II enzyme mix	Invitrogen (Karlsruhe)
Gateway LR Clonase II enzyme mix	Invitrogen (Karlsruhe)
Platinum Taq DNA Polymerase	Invitrogen (Karlsruhe)
Proteinase K	Fermentas (St. Leon-Rot)
Restriction endonucleases	New England Biolabs (Frankfurt am Main)
Superscript II Reverse transcriptase	Invitrogen (Karlsruhe)
T4 DNA Ligase	New England Biolabs (Frankfurt am Main)
Taq DNA Polymerase	Fermentas (St. Leon-Rot)
Trypsin	Gibco (Karlsruhe)

**2.1.4 Bacterial strains:**

Strain Genotype Manufacturer

<i>E.coli</i> DH10B (electrocompetent)	Invitrogen (Karlsruhe)
<i>E.coli</i> TOP10 (chemically competent)	Invitrogen (Karlsruhe)

**2.1.5 Bacterial artificial chromosome (BAC) clones:**

BAC clones were used for PCR amplification of the promoter sequence used for generating the constructs for studying promoter activity.

<b>Gene name</b>	<b>Clone #</b>	<b>BAC library</b>	<b>Manufacturer</b>
Ccdc80 promoter	bMQ193n13	bMQ Mouse BAC library	Gene Service

Periostin promoter	bMQ304b19	bMQ Mouse BAC library	Gene Service
Gelsolin promoter	bMQ185d13	bMQ Mouse BAC library	Gene Service
Col2alpha1 promoter	CH-295P10	bMQ Mouse BAC library	Gene Service

### 2.1.6 Plasmids

The following plasmids were available in the laboratory and were used for the experiments.

Donor vector	Reference
pDONR-221	Invitrogen (Karlsruhe)
pT-Rex DEST30	Invitrogen (Karlsruhe)
pMIR-Report <sup>™</sup> β-gal control plasmid	Ambion
pCAG-Cre	Addgene
pLacZ-basic	Clontech Laboratories, Inc.
pCALNL-GFP	Addgene
pCAG-ERT2CreERT2	Addgene

The following plasmids were constructed using *Gateway® Recombination Cloning Technology* (Invitrogen, Life Technology) and were used for the experiments.

Constructs	Insert
pLacZ-Ccdc-80 pCcdc80-Cre pCcdc-80- ERT2CreERT2	Ccdc80 promoter (~4Kb)
pLacZ-Postn pPostn-Cre pPostn- ERT2CreERT2	Periostin promoter (3.9Kb)
pGsn-Cre pGsn- ERT2CreERT2	Gelsolin promoter (3kb)

### 2.1.7 Oligonucleotide primers

The oligonucleotides were purchased in HPSF-purified lyophilized powder from MWG Eurofins (Ebersberg) and Sigma-Aldrich. The primers were dissolved in double-distilled autoclaved water (ddH<sub>2</sub>O). 20 μM working solutions were used for PCR.

**Oligonucleotides for amplification of promoter fragments**

Promoter sequences were PCR amplified from the respective BAC clones. The Gateway® sequences are in small letters in the primer sequences used for generating promoter constructs using Gateway recombination technology. In case of LacZ constructs restriction sites (underlined) were added before promoter primer sequence for cloning.

Insert	BAC clone #	Constructs	Primer sequences (5'----3')
Ccdc80 promoter (~4Kb)	bMQ193n13	pCcdc80-Cre  pCcdc-80-ERT2CreERT2  pDONR-Ccdc80	FP:5'ggggacaagtttgtaaaaaagcaggcttcAT G AGT TCC AGG ATA CCC AGG RP: 5'ggggaccactttgtacaagaaagctgggtc CAT TGT ATT ATC CAC TTG GGG
		pCcdc-80-LacZ	FP: 5'AAC GCC <u>CCCGGG</u> GAG TTC CAG GAT ACC CAG GGC T (XmaI) RP: 5'AAC GCC <u>GCTAGC</u> TGT ATT ATC CAC TTG GGG A (NheI)
Periostin promoter (3.9Kb)	bMQ304b19	pPostn-Cre  pPostn-ERT2CreERT2  pDONR-Postn	FP: 5'ggggacaagtttgtaaaaaagcaggcttc CTA AGG TGG ACA GTG CGG AAG AC RP: 5'ggggaccactttgtacaagaaagctgggtc CCT TCA GCC CTG AGC TCC GTC C
		pPostn-LacZ	FP: 5' CCC <u>CCCGGG</u> CTA AGG TGG ACA GTG CGG AAG AC (XmaI) RP: 5'AAC G <u>CTCGAG</u> CCT TCA GCC CTG AGC TCC (XhoI)
Gelsolin promoter (3kb)	bMQ185d13	pGsn-Cre  pGsn-ERT2CreERT2  pDONR-Gsn	FP:5'ggggacaagtttgtaaaaaagcaggcttcG CA TCA CAG ACC CTG CCT TCT RP: 5'ggggaccactttgtacaagaaagctgggtcCAT GGC GAC GGT GAG GAC CCA
		pGsn-LacZ	FP: 5' AAC GCC <u>CCCGGG</u> GCA TCA CAG ACC CTG CCT TCT (XmaI) RP: 5' AAC GCC <u>CTCGAG</u> GGC GAC GGT GAG GAC CCA (XhoI)
attR1-Cm <sup>R</sup> -	pT-Rex DEST30	pCre-GW (adapted for	

<i>ccdB-attR2</i>		Gateway)	
<i>attR1-Cm<sup>R</sup>-ccdB-attR2</i>	pT-Rex DEST30	pERT2CreERT2-GW (adapted for Gateway	ACTAGT ATC AAC AAG TTTG TAC AAA AAA (SpeI) TTT CTT GTA CAA AGT GGT TGA T CAATTG (EcoRI)

Oligonucleotides for sequencing of the constructs

Plasmid	Forward primer (5'---> 3')	Reverse primer (5'---> 3')
pLacZ-basic	CGA TTT CGG CCT ATT GGT TA	CCGCCACATATCCTGATCTT
pCre-GW (adapted for gateway cloning)	AAA AAG GGA ATA AGG GCG AC (sits on Ampicillin gene)	TCA GTA AAT TGG CCA TGG TG (sits on Cre gene)
pERT2CreERT2-GW	ACT TTC ACC AGC GTT TCT GG (sits on Ampicillin gene)	GGT TCC TGT CCA AGA GCA AG (sits on ERT2CreERT2 gene)
pDONR-221 /pEntry	GTA AAA CGA CGG CCA G M13 For (-20)	CAG GAA ACA GCT ATG AC (M13 Rev)

Oligonucleotides for genotyping of Cre-transgenic mice

Mouse line	Allele	Sequence (5'---> 3')	Size (bp)
R26R (Rosa26-LacZ reporter)	Wild type Mutant	<b>R126</b> - AAA GTC GCT CTG AGT TGT TAT <b>R127</b> - GCG AAG AGT TTG TCC TCA ACC <b>R128</b> - GGA GCG GGA GAA AT	WT- 500bp Mut- 250bp
Ccdc80-Cre	Cre	<b>Cre 800</b> -GCT GCC ACG ACC AAG TGA CAG CAA TG <b>Cre1200</b> -GTA GTT ATT CGG ATC ATC AGC TAC AC	500bp
VimCreERT2	Cre	<b>Sense Cre</b> -CCT GGA AAA TGC TTC TGT CCG <b>Antisense Cre</b> - CAG GGT GTT ATA AGC AAT CCC	400bp
Fsp1-Cre	Cre	<b>Sense Cre</b> -CCT GGA AAA TGC TTC TGT CCG-3' <b>Antisense Cre</b> -CAG GGT GTT ATA AGC AAT CCC	400bp
R26-mTom-mGFP <sup>fl/fl</sup>	Wild type	<b>Common</b> -CTC TGC TGC CTC CTG GCT TCT <b>WT</b> -CGA GGC GGA TCA CAA GCA ATA	WT: 330bp

	Mutant	<b>Common</b> -CTC TGC TGC CTC CTG GCT TCT <b>Mut</b> -TCA ATG GGC GGG GGT CGT T	Mut: 250bp
--	--------	---	------------

**Real Time PCR (for mouse)**

Gene	Forward primer (5'--->3')	Reverse primer (5'--->3')	Size (bp)
Gapdh	TGG CAA AGT GGA GAT TGT TG	CATTATCGGCCTTGA CTGTG	140
RPL32	GCC CAA GAT CGT CAA AAA GA	GTC AAT GCC TCT GGG TTT	100
18s	ACC GCA GCT AGG AAT AAT GGA	GCC TCA GTT CCG AAA ACC A	63
Vim	CGG AAA GTG GAA TCC TTG CA	CAC ATC GAT CTG GAC ATG CTG T	111
Gsn	GCT TTG AGT CGT CCA CCT TC	TTG GGT ACC ACG TGT TTG AA	97
Ccdc80	CCA GGA GGA TCT CTG TGG TC	ACA CGC ATG GGT TTC TCA TT	100
Col8a1	CAA GGA CTT TGG TCC TCG AT	TGA TGA ACA GTA TTC CCA GCA	99
Postn	AAC CAA GGA CCT GAA ACA CG	GTG TCA GGA CAC GGT CAA TG	170
Myh6	GCC CAG TAC CTC CGA AAG TC	GCC TTA ACA TAC TCC TCC TTG TC	110
Rabgap1l	GGG CGT CTG ACA GAG TTG TT	CGA AGC TCT GAC CTC CAT TT	110

**2.1.8 Buffers and Media**

DNA loading buffer (5X)

Xylen-Cyanol	0,025g
EDTA (0.5M)	1.4ml
Glycerol	3.6ml
H <sub>2</sub> O	7.0ml

DNA lysis buffer (for genotyping)

Tris	12.1 g
EDTA	1.87 g
NaCl	11.7 g
SDS	0.2 g
ddH <sub>2</sub> O	adjust to 1 l

Lamelli buffer 2X

Tris-HCl (1M) pH 6.8	12.5 ml
SDS (10%)	40 ml
Glycerol	30 ml
β-mercaptoethanol	1 ml
Bromophenol blue	traces

## Materials and Methods

---

### Lower buffer 4X (for Western blot)

Tris	182 g
SDS (10%)	40 ml
ddH <sub>2</sub> O	adjust to 1 l
Adjust pH to 8.8 with HCl 37%	

### PBS (10X)

NaCl	80 g
KCl	2 g
Na <sub>2</sub> HPO <sub>4</sub> ·7H <sub>2</sub> O	11.5 g
KH <sub>2</sub> PO <sub>4</sub>	2 g
ddH <sub>2</sub> O	adjust to 1 l

### PBST

PBS 10X	100 ml
Tween® 20	1 ml
ddH <sub>2</sub> O	adjust to 1 l

### Protein lysis buffer

Tris (1M pH 6.7)	50 mM
SDS	2%
Na <sub>3</sub> VO <sub>4</sub>	1mM
Complete mini protease inhibitor	1 tablet per 10 ml

### Western running buffer (10X)

Tris-HCl	30 g
Glycine	144 g
SDS	15 g
ddH <sub>2</sub> O	adjust to 1 l

### TAE buffer (50X)

Tris	242 g
Acetic acid	57.1 ml
Na <sub>2</sub> EDTA·2H <sub>2</sub> O	37.2 g
ddH <sub>2</sub> O	adjust to 1 l

### Transfer buffer (for Western blot)

Tris (1M pH 8.3)	25 ml
Glycine	11.26 g
Methanol	100 ml
ddH <sub>2</sub> O	adjust to 1 l



## **Materials and Methods**

---

### Tris-EDTA (TE) buffer

Tris	10 mM
EDTA	1 mM

### Upper buffer 4X (for Western blot)

Tris	61 g
SDS (10%)	40 ml
ddH <sub>2</sub> O	adjust to 1 l
Adjust pH to 6.7 with HCl 37%	

### Tamoxifen (20mg/ml)

Tamoxifen	20mg
Peanut oil	1ml

### Perfusion Buffer (1X)

NaCl	6.6g
KCl	0.35g
KH <sub>2</sub> PO <sub>4</sub>	0.082g
Na <sub>2</sub> HPO <sub>4</sub>	0.085g
MgSO <sub>4</sub> ·7H <sub>2</sub> O	0.3g
Phenol Red	0.012g
NaHCO <sub>3</sub>	1.01g
KHCO <sub>3</sub>	1.01g
Herpes Buffer (1M)	10ml
Taurine	3.75g
ddH <sub>2</sub> O	adjust to 1 l
Sterile filtered the solution	

### Digestion Buffer

Collagenase Typ2 II	107mg
CaCl <sub>2</sub> (100mM)	15µl
Perfusion Buffer	50ml

### P1 Buffer

Perfusion buffer	9ml
FCS	1ml

## Materials and Methods

---

CaCl<sub>2</sub> (10mM) 12.5µl

### P2 Buffer

Perfusion buffer 47.5ml

FCS 2.5ml

CaCl<sub>2</sub> (10mM) 62.5µl

### DMEM +++ (HEK293-Cells)

DMEM 500ml

FBS 50ml

L-Glutamin 5ml

Penicillin/Streptomycin 5ml

### LB-Agar

Pepton 10g

Yeast -extract 5g

NaCl 5g

Agar 15g

NaOH (1M) 1ml

ddH<sub>2</sub>O adjust to 1 l

### LB-Medium

Pepton 10g

Yeast -extract 5g

NaCl 5g

NaOH (1M) 1ml

ddH<sub>2</sub>O adjust to 1 l

### NRCM incomplete medium

MEM 10.7 g

NaHCO<sub>3</sub> 0.35 g

Vitamin B12 67% (w/v) 1 ml

ddH<sub>2</sub>O adjust to 1 l

Adjust pH to 7.3 and sterile filtered the solution.

### AMCM preplating medium

Penicillin/Streptomycin 1 ml

FCS 5 ml

BDM (500mM) 2ml

L-Glutamine (200mM) 1ml

MEM 91 ml

10% AMCF preplating medium

Penicillin/Streptomycin	1 ml
FCS	5 ml
NRCM incomplete medium	89 ml

**2.1.9 Antibodies**

**Primary antibodies**

<b>Epitope</b>	<b>Host</b>	<b>Monoclonal /Polyclonal</b>	<b>Manufacturer</b>
β-actinin	mouse	Monoclonal	Sigma-Aldrich (# A7811)
PECAM-1/CD31	Rat	Polyclonal	BD pharmingen (#550274)
Fsp1/S100A4	Rabbit	Polyclonal	Millipore (#07-2274)
GFP	Chicken	Polyclonal	Abcam (#ab13970)
GFP	Rabbit	Polyclonal	Life technologies (#A-11122)
P4HB/PDIA4	Rabbit	Polyclonal	Protein Tech (#11245-1-AP)
SM22alpha	Goat	Polyclonal	Abcam (#ab10135)
Vimentin	Chicken	Polyclonal	Abcam (#ab24525)

**Secondary antibodies**

<b>Epitope</b>	<b>Host</b>	<b>Manufacturer</b>
Alexa Fluor® 647 Anti-chicken IgG	Goat	Life technologies (#A21449)
Alexa Fluor® 647 Anti –Rabbit	Goat	Life technologies (#A21244)
Alexa Fluor® 647 Anti –Rat	Goat	Life technologies (#A21247)
Alexa Fluor® 488 anti-rabbit IgG	Goat	Life technologies (#A11008)
Alexa Fluor® 488 anti-chicken	Goat	Life technologies (#A11039)
Biotinylated Anti-Goat IgG	Goat	Vector laboratories (#VC-BA 9500)
Anti-mouse IgG, F(ab') <sub>2</sub> -B	Goat	Santa Cruz (#sc-3795)

**3 METHODS**

**3.1 Molecular biology methods**

**3.1.1 Polymerase chain reaction (PCR)**

**Amplification of promoter fragment**

For amplification of promoter sequences from the BAC clone, Accuprime Pfx polymerase was used.

**Reaction mixture**

10X Accuprime Pfx buffer	5µl
Forward primer	20 pmol
Reverse primer	20 pmol
Template DNA	100 ng
Accuprime Pfx polymerase	2.5 Units
ddH <sub>2</sub> O	upto 50µl

**PCR conditions:** A 3-step PCR cycle was used for amplification.

95°C 2min

95°C 15sec (Denaturation)

55 – 66°C 30sec (Annealing)

68°C 60 sec per kb (Extension)

68°C 5min

16°C ∞

} x 30 cycles

Promoter	Sequence size (Kb)	Annealing temperature
For Ccdc80 promoter seq with attb site in primers	Approx. 4.2	66°C
For Ccdc80 promoter seq with RE sites (Xmal (FP) & NheI (RP)) in primers	Approx 4.2	66°C
For Postn promoter seq with attb site in primers	3.9	58°C
For Periostin (Postn) promoter seq with RE site (Xmal (FP) & XhoI (RP)) in primers	3.9	54°C
For Gelsolin (Gsn) promoter seq with Gsn_attb site in primers	Approx 6	66°C
For Gelsolin (Gsn) promoter seq with RE site (Xmal (FP) & XhoI (RP)) in primers	Approx 2.8	55°C

**3.1.2 Isolation and purification of PCR-amplified DNA**

PCR amplified products are purified using the QIAquick PCR purification kit (Qiagen, Hilden). 5 volumes of Buffer QG were added to 1 volume of PCR product. If the color of the sample turns violet or orange, 10µl of 3M-ammonium acetate solution was added (the sample turns yellow). The samples were then applied to QIAquick column and centrifuged at 13000 rpm for 1 min. In the presence of high concentration of salts, the DNA binds to the silica membrane of the column. The flow-through was discarded and the columns were washed

with 750µl of Buffer PE and centrifuged at 13000 rpm for 1 min. The flow-through was discarded and the empty columns were centrifuged to remove any residual solution from the column. The DNA was then eluted using 20µl of ddH<sub>2</sub>O into a fresh 1.5 ml microfuge tube.

### **3.1.3 Agarose gel electrophoresis**

PCR amplified products were separated by gel electrophoresis in a 0,8 % agarose gel. The agarose was heated and dissolved in the appropriate amount of TAE buffer. After cooling the solution to 60°C, 10µl of ethidium bromide solution (1mg/ml) was added. This substance intercalates into DNA and illuminated under UV light of 312nm wavelength. The DNA samples were mixed with DNA loading buffer and were subjected to 120-140 volts (DC Voltage) for 30-40min for separation. As size standards, 1 kb or 100bp DNA ladders were used (New England Biolabs).

### **3.1.4 Gel extraction**

The DNA fragments of the respective size were excised from the agarose gel using a sterile scalpel into a 2 ml microfuge tube and QIAquick gel extraction kit (Invitrogen, Karlsruhe) was used to extract the DNA. The DNA was eluted using 20 µl of autoclaved ddH<sub>2</sub>O.

### **3.1.5 Precipitation of DNA with sodium acetate**

The samples were mixed with the 1/10<sup>th</sup> volume of 3M sodium acetate and 2.5 volumes of 100% ethanol. The samples were incubated at -80°C for 20 min, centrifuged at 14000 rpm and were then incubated at 4°C for 30 min. The pellet was washed with 1 ml of 75% ethanol, centrifuged at 14000 rpm and then kept at 4°C for 15 min. The pellet was dried at room temperature and was resuspended in 15 µl ddH<sub>2</sub>O.

### **3.1.6 Endonuclease digestion**

Restriction endonuclease digestion was performed either to test the clones for insertion of the genes or for cloning. The restriction endonucleases were purchased from New England Biolabs and the digestion was performed in the buffers as per the manufacturers recommendations. 1 µg of DNA was digested with 1 unit of the enzyme for 1 hour at recommended temperatures. The restriction endonucleases were then inactivated by incubating the tubes at 65°C for 20 min.

### **3.1.7 Phosphatase treatment of DNA**

After linearization of the vector with a restriction endonuclease were the only 5' phosphate groups removed by treatment with Antarctic phosphatase to its to prevent re-ligation. For this

Digested Vector	2µg
Antarctic Phosphatase Reaction Buffer (10x)	5µl
Antarctic Phosphatase	5Units
ddH <sub>2</sub> O	adjust to 50µl

The mixture was initially 30 minutes at 37°C. and then for a further 30 min at 50°C incubated. By heat deactivation of the enzyme for 5min at 65°C, the dephosphorylated vector used directly for ligation.

### **3.1.8 Ligation of DNA fragments**

Ligation was done using the T4 DNA ligase New England Biolabs (Frankfurt am Main). The enzyme catalyzes the linkage of the 3'-hydroxy end of the 5 'phosphate end of the DNA fragments by forming a phosphodiester bond. The amount of insert was calculated using the following formula:

$$\text{Insert mass [ng]} = \frac{5 \times \text{Vector mass [ng]} \times \text{Insert length [bp]}}{\text{Vector length [bp]}}$$

For a reaction mixture in a final volume of 15 ul following were used:

Vector	10-50 ng
Insert	100-300 ng
Ligase buffer (5x)	1.5 ul
T4 DNA ligase	1 ul

The ligation was carried out overnight at 16 ° C (or available via 30 min to 1 h at room temperature).

### **3.1.9 Cre-expressing constructs adapted for gateway recombination reactions**

For cloning promoter sequences in different Cre vectors, the vectors were modified and adapted for Gateway recombination system, where the already existing promoters sequence from these constructs (for example, CAG promoter in case of pCAG-Cre & pCAG-ERT2CreERT2 plasmids) were removed using restriction enzymes (NEB). The GatewayR adaptation cassette i.e. attR1&R2 recombination site, Chloramphenicol resistant gene and ccdB gene (attR1-Cm<sup>R</sup>-ccdB-attR2) was PCR amplified using primers as

mentioned in section 2.1.7 from the pTREX-Dest30 vector. The amplified PCR product was then inserted in above linearized promoterless plasmids, which then became Destination Vector for LR reaction of Gateway recombination technology (**Fig 4.5 Results section**)

### **3.1.10 Insertion of cDNA into plasmids by GatewayR™ recombination**

For the cloning of the promoter fragments in front of Cre gene, the GatewayR system (Invitrogen) was used. This system ensures a higher cloning efficiency than conventional cloning and is based on a two-step homogeneous recombination strategy for creating different reporter and expression plasmids from a so-called Entry plasmid containing the relevant PCR product. To generate the homologue sequence, the characteristic attb-sites are added to the 5' end of each primer, which is homologue to the sequence at the integration site in the Gateway DONR vector. The sequence of the two attb-sites is not identical, ensuring integration in only one direction

The sequences of the attb-sites are shown below:

Forward primer: 5' GGGGACAAGTTTGTACAAAAAAGCAGGCT  
Reverse primer: 5' GGGGACCACTTTGTACAAGAAAGCTGGGT

#### **3.1.10.1 Gateway BP reaction**

The promoter fragments were amplified and purified as described above. The attb-site was added by the supplier (Invitrogen) to 5' end of each primer. The PCR product was cloned into an Entry clone by BP recombination. For the BP recombination the following protocol was applied, as suggested by the supplier:

pDONR221 (150 ng/μl)	1 μl
PCR Product	100 fmol
BP Clonase II	2 μl
TE-buffer	adjust 10 μl

The reaction was incubated overnight at 25°C. The recombination was stopped by adding 2 μl Proteinase K (Gateway-Kit®) for 10 min at 37°C.

The BP clonase catalyzes the recombination of the PCR Product with the attb-sites of the DONR vector. In between the attb-sites the ccdB Gene is expressed, encoding a toxic protein for most *E.coli* strains. Thus, after transformation only those *E.coli* will survive, which contain a plasmid comprising a successful recombination. The resulting plasmid is called Entry plasmid. It contains only the PCR fragment flanked by attb-sites and a kanamycin resistance.

The plasmids were transformed into DH10b cells and spread on a kanamycin agar plate. The Entry plasmids containing the promoter fragment were amplified and purified as described above. Before the following cloning steps, the plasmids were sequenced to assure a correct integration. Sequencing was ordered at Eurofins MWG Operon.

### 3.1.10.2 Gateway LR reaction

In the next step destination vectors (adapted for Gateway) was used where the promoter fragment was transferred from the pEntry plasmid to the destination vector by the LR-recombination

150 ng pENTRY  
150 ng Destination vectors (pCre-GW /pERT2CreERT2-GW)  
2µl LR-Clonase II  
ad 10 µl TE buffer

The reaction and transformation was performed as described for the BP reaction. To discriminate between insert carrying entry and destination vectors, the pCre-GW /pERT2CreERT2-GW vectors had an ampicillin resistance, whereas the entry vectors a kanamycin resistance. The recombination of the Entry clone with the destination vector is catalyzed by the LR clonase II. Successfully recombined plasmids are identified by antibiotic selection.

### 3.1.11 Transformation

#### 3.1.11.1 Electroporation of *E.coli* DH10B

An aliquot of ice-thawed electrocompetent *E.coli* DH10B cells (50 µl) and 2µl ligation reaction or 1 µl LR or BP reaction were mixed gently and transferred to Gene Pulser 0.1 cm cuvettes (Bio-rad). A short electromagnetic pulse (1.8 kV) was applied using the Bio-rad micropulser and the electroporated cell suspension was immediately mixed with 450 µl of LB medium and transferred into a 1.5 ml tube which was incubated at 37°C and 350 rpm in a thermomixer (Eppendorf) for 1 hour. 40 –100 µl of the cell suspension was then plated on LB agar plates containing the corresponding antibiotic (33 µg/µl Kanamycin or 100 µg/µl Ampicillin). The plates were incubated overnight at 37°C bacterial incubator.

#### 3.1.11.2 Heat shock-transformation

Chemically competent *E.coli* One Shot TOP10 cells (50µl) were mixed with 2 µl of LR or BP reaction or 10 µl of the ligation reaction and incubated on ice for 45 min. Heat-shock was applied by placing the samples at 42°C for 90 s and immediately transferring the tubes to ice. The cells were resuspended with 950 µl LB medium, incubated at 37°C in a thermomixer for 1 hour and were plated on LB agar plates containing corresponding antibiotic.



### **3.1.12 Mini culture and mini DNA purification**

A single bacterial colony was picked from an agar plate into 4 ml of LB medium containing appropriate antibiotic. The culture was grown overnight in a shaker at 180rpm in 37°C. To analyze the clones, a buffer of " Plasmid Maxi Kit" (Qiagen, Hilden) was used. 2ml of culture was centrifuged for 30sec at 13200 rpm. The pellet was dissolved in 250 ul of resuspension buffer (P1). RNase contained in P1 buffer degraded the bacterial RNA. After addition of 250 ul of lysis buffer (P2), the samples mixed and incubated for 5 min at room temperature, which led to the lysis of the cells in this alkaline solution. To neutralize the pH then 300ul neutralization buffer (P3) was added and incubated for 5 min on ice. The sample were centrifuged at 13200 rpm for 10 min at 4°C, the DNA contained in the supernatant was transferred to a new tube and precipitated with 750 ul of isopropanol for 5 minutes at room temperature. The pellet was again washed with 75% ethanol, air-dried and the DNA was resuspended in 20µl ddH<sub>2</sub>O.

### **3.1.13 Maxi/midi culture and purification**

100µl of the Mini-culture was incubated in 100 ml or 200 ml LB medium containing the corresponding antibiotics at 37°C and 180 rpm for 12 –16 hours for Midi- and Maxi-cultures, respectively. Maxi- and Midi- DNA purification kits were purchased from Qiagen (Hilden). The DNA pellets were resuspended in 50µl and 150µl ddH<sub>2</sub>O for Midi- and Maxi- DNA preparations, respectively.

### **3.1.14 Endofree maxi DNA purification**

Endotoxins, also known as lipopolysaccharides (LPS), are cell-membrane components of Gram-negative bacteria such as *E.coli*. Upon lysis of the bacterial culture, the endotoxins are released from the outer membrane into the lysate. The presence of endotoxin can influence the uptake of plasmid DNA in transfection experiments and can also induce non-specific activation of immune cells such as macrophages and B-cells in animal experiments. Endofree Maxi-DNA purification kit (Qiagen, Hilden) was used to produce endotoxin-free plasmids.

### **3.1.15 Sequencing of plasmid DNA**

2 µg of plasmid DNA was diluted in TE buffer to a final volume of 20 µl and the primers at a concentration of 10 pmol/µl in a volume of 10µl was sent to MWG Eurofins Operon (Ebersberg) for sequencing. The sequencing results were analyzed using the SDSC Biology workbench software (<http://workbench.sdsc.edu>) which is available online.

### **3.1.16 Software**

Insilico handling of DNA sequences for the cloning experiments were performed using the softwares - Gene Construction Kit (Textco, New Hampshire, USA) and MacVector 12.0.6 (Cambridge, UK).

## **3.2 Cell culture methods**

### **3.2.1 Isolation of neonatal rat cardiomyocytes (NRCM) and fibroblast (NRCF)**

Neonatal rat cardiomyocytes (NRCM) were obtained from 1-2 day old Sprague-Dawley rats isolated by enzymatic digestion. Whole hearts were excised and were transferred into Ca<sub>2+</sub> and bicarbonate-free HEPES-buffered Hanks' medium (HBSS). After removing the atria, the hearts were cut into pieces and digested with an enzyme solution containing trypsin (#215240, Becton Dickinson and PAN), and DNase under constant stirring. The suspension was collected over fixed intervals of time into tubes containing 9 ml FBS. The primary cells that were collected after passing through a 40µm cell strainer were seeded in uncoated plastic dishes for 1 hour at 37°C / 1% CO<sub>2</sub>. During the preplating time, the more rapidly adherent fibroblasts attach to the surface. The supernatant containing the cardiomyocytes was collected and either centrifuged at 900rpm for 1min to freeze the pellet at -80°C for RNA isolation or cultured in MEM containing vitamin B12, NaHCO<sub>3</sub>, BrdU and 1% FCS. The plastic dishes containing the attached cardiac fibroblasts (NRCF) were washed with PBS gently and cells were either frozen at 80°C for RNA isolation or cultured in MEM containing vitamin B12, NaHCO<sub>3</sub> and 1% FCS. A trained staff carried out the cardiomyocytes isolation from neonatal rats in a sterile condition.

### **3.2.2 Isolation of adult mouse cardiomyocytes (AMCM) and Fibroblast (AMCF)**

Isolation of adult mouse cardiomyocytes and cardiac fibroblast was performed using a Langendorff perfusion apparatus as previously described (O'Connell TD et. al). Briefly, mice were anesthetized and the heart was rapidly excised from the thoracic cavity, cannulated via the aorta, and perfused in the Langendorff mode with calcium-free perfusion buffer for 3 minutes at a rate of 4 mL/min, followed by digestion buffer (perfusion buffer plus 25µmol/L CaCl<sub>2</sub> and Collagenase (Worthington Biochemical) at a concentration of 280 units/mg) for 10 to 11 minutes. Following digestion, atria is removed and the heart were cut into small pieces with curved fine tip forceps in 2.5 mL of digestion buffer and 2.5ml of Stop 1 buffer (10%

fetal bovine serum (FBS) in perfusion buffer plus 25µmol/L CaCl<sub>2</sub>) in a small beaker. The suspension was filtered with 100µm nylon mesh filter into a 15 mL falcon tube (Pellet 1) and allowed to settle by gravity for 10 min at 37°C. The supernatant was transferred into another 15mL tube and marked as Cardiac fibroblast (AMCF) whereas the settled pellet (i.e. AMCM) was mixed in 10 mL of Stop 2 buffer (5% FBS in perfusion buffer plus 50µmol/L CaCl<sub>2</sub>) and transferred to a small conical flask. A final calcium level of 1mmol/L was reintroduced through a series of resuspensions containing increasing concentrations of CaCl<sub>2</sub>. Cardiomyocytes were either centrifuged at 900rpm for 1min to freeze the pellet at -80°C for RNA isolation or plated on laminin coated (10 µg/mL) coverslips in CM plating media for 1 h at 37°C, 5% CO<sub>2</sub> for immunofluorescence.

For cardiac fibroblast isolation the tube containing supernatant (labeled as AMCF above) was centrifuged at 1200rpm for 5mi and pellet was resuspended in AMCF plating medium with 5%FCS for 2h at 37°C, 1% CO<sub>2</sub>. Plated AMCF were then washed with 1x PBS and either frozen at -80°C for RNA isolation or cultured in medium containing 10%FCS for immunofluorescence experiments.

### **3.2.3 Cultivation of NIH-3T3 mouse fibroblasts**

NIH-3T3 mouse cells were cultured in DMEM medium containing 10% fetal bovine serum, 1% L-Glutamine and 1% Penicillin (10000U/ml)/Streptomycin (100mg/ml) in a humidified 37°C/5% CO<sub>2</sub> incubator. The cells grew as an adherent monolayer in culture dishes (Nunc, Langensfeld) and have a doubling time of about 24 hours. The cells were passaged to a maximal 30 times, after which new aliquots are thawed from the liquid nitrogen storage. The cells were split every 4 days. For splitting, the culture medium was aspirated from the culture dishes and the cells were washed once with DPBS (Dulbecco's phosphate buffered saline). The cells were trypsinized using trypsin-EDTA solution (0.5 g/l trypsin, 0.2 g/l EDTA) and centrifuged for 5 minutes (1000 rpm). The supernatant was discarded and the cell pellet was re-suspended in an appropriate volume of fresh culture media for cell counting by Trypan Blue. The cells were then seeded in new culture dishes or 96 well plates.

### **3.2.4 Transfection of NIH-3T3 cells with promoter vectors**

Transfection was carried out with Lipofectamine™2000 (Invitrogen, Karlsruhe) as per the manufacturer's guidelines. These are specially designed cationic lipids which complexes with negatively charged nucleic acids to form liposomes in aqueous conditions. The liposomes carrying a positive charge on its surface can then fuse with the negatively charged plasma membrane thereby facilitating delivery of the nucleic acids into the cell.

### **3.2.5 Generation of stable cell lines**

NIH-3T3 cells were grown in 10cm dishes and were transfected with pCALNL-GFP plasmids DNA using Lipofectamine (3.2.4). The expression plasmid pCALNL-GFP containing the neomycin resistance gene allows selection of cells expressing the introduced plasmid DNA stably integrated into its genome, using geneticin (G-418, Invitrogen, Karlsruhe, Germany). For this purpose, starting from 48h after transfection daily fresh medium with 0.8g/l geneticin added to the cell for two weeks. The further cultivation was carried out in medium containing 0.2-0.4 g/l geneticin.

pCALNL-GFP is a Cre recombinase-dependent expression of GFP, i.e. GFP is only expressed in the presence of Cre due to a transcriptional stop in between the loxP sites.

## **3.3 Methods for RNA analysis**

### **3.3.1 Isolation of RNA**

#### **3.3.1.1 peqGOLD Trifast™**

RNA from tissues was isolated exclusively with TriFast (Peqlab, Erlangen, Germany). Tissues (50-100 mg) were homogenized in 1 ml of peqGOLD Trifast™ using a turrax. The samples were then incubated at RT for 5 min. 200µl of chloroform was added to each sample, vortexed for 50 sec, and were incubated at RT for 10 min. After centrifugation at 12000 x g for 10 min at 4°C, the mixtures separated into three phases –upper aqueous phase (RNA), Interphase (DNA) and lower organic phase (protein). The upper phase containing the RNA was then transferred into a fresh 1.5 ml tube. 500 µl of isopropanol was added to the samples to precipitate the RNA. The samples were kept on ice for 10 min and then centrifuged at 12000 x g for 10 min at 4°C. The supernatant was discarded carefully and the RNA pellet was washed twice with 1 ml of 75% ethanol by vortexing gently and subsequent centrifugation at 12000 x g for 10 min at 4°C. After discarding the supernatant, the RNA pellet was air-dried to remove excess isopropanol.

#### **3.3.1.2 MirVana Kit**

RNA from cardiac cells was isolated for the mirVana kit (Applied Biosystems, (Darmstadt)) according to the manufacturer. It is a column-based technique to extract total RNA (including small RNAs). In both above isolation protocol the air-dried RNA pellet was taken up ultimately in 20µl of pre-warmed (55°C) nuclease-free water. The purity and concentration of the isolated RNA were determined using the NanoDrop spectrophotometer ND 1000 (Peqlab, Erlangen, Germany).

### 3.3.2 Reverse transcription

In the production of complementary strand (cDNA), the fact that makes use of the pre-mRNAs is polyadenylated on its 3' end. After binding of the oligo (dT) primers (MWG Biotech, Ebersberg, Germany), in this so-called poly (A) tail, the reverse transcriptase synthesizes the complementary strand (cDNA) complementary to the mRNA sequence. The cDNA can be used for gene expression studies using quantitative real-time PCR (qRT-PCR) as a template then. To ensure detection of genomic DNA in the subsequent qRT-PCR, an approach with pooled RNA (four RNA samples from isolation) without reverse transcriptase (as a negative control for reverse transcription reaction) was always treated in parallel with the rest of the samples according to the protocol.

#### Reaction mix

Reagents	Volume
RNA	0,5 µg
Oligo (dT) Primer (10 mM)	2 µl
RNAse free H <sub>2</sub> O	ad 11,9 µl
----- Incubation for 10 min at 70°C -----	
	4 µl
5x First Strand Buffer	
DTT (0,1 M)	2 µl
dNTPs (1 mM)	1 µl
RNAse Out/RNA Inhibitor	0,1 µl
SuperscriptIIReverse Transcriptase	1 µl

The entire mixture was incubated for 1 h min at 42 ° C and then heat inactivated (10 min, 70 °C). At the end for a final volume of 50 ul for 30 ul of water were added.

### 3.3.3 Quantitative real time PCR

The quantitative real-time PCR based on the conventional polymerase chain reaction, PCR that allows quantification of amplification. This is enabled by the detection of fluorescence signals (using SYBR green), which increase in proportion to the amount of PCR product. SYBR green is a non-specific fluorescent dye, which intercalates into the double-stranded DNA. The dye only fluoresces when bound with DNA. With each cycle of amplification, the emitted fluorescence intensity of the SYBR green increases as compared to the reference

## Materials and Methods

fluorophore 8-ROX (8-carboxy-X-rhodamine). The number of cycles at which the fluorescence intensity exceeds the threshold is called the cycle threshold (Ct). To quantify the gene expression for RNA of interest, it is normally normalized to the gene expression of a housekeeping gene such as GAPDH ( $\Delta\Delta C_t$ -method). This normalizes the variation in the amount and the quality of RNA between different samples. However, the expression of the reference gene needs to be similar between the samples.

The real-time PCR was carried out in StepOne Plus instrument (Applied Biosystems, New Jersey) and the reagents used were from Invitrogen (Karlsruhe).

### Reaction mix

Reagents	Volume
10X PCR buffer	1.25 $\mu$ l
50 mM MgCl <sub>2</sub>	0.375 $\mu$ l
Forward primer	0.25 $\mu$ l
Reverse primer	0.25 $\mu$ l
dNTP	0.2 $\mu$ l
1X ROX	0.5 $\mu$ l
5X SYBR Green	0.5 $\mu$ l
'Platinum' Taq polymerase	0.05 $\mu$ l
ddH <sub>2</sub> O	6.625 $\mu$ l
cDNA (2.5 ng/ $\mu$ l)	2.5 $\mu$ l

Temperature program (StepOne Plus, Applied Biosystems, New Jersey, USA.)

Steps	Temperature	Time	Number of Cycles
Pre-denaturation	94 °C	120 sec	X 40 Cycle
Denaturation	94 °C	20 sec	
Annealing	56 °C	20 sec	
Elongation	65 °C	35 sec	
Final Elongation	65 °C	1min 30 sec	
Dissociation	16 °C	$\infty$	

### **3.4 Methods for protein analysis**

#### **3.4.1 Preparation of protein lysates**

Tissues (50-100 mg) were homogenized in 800 µl of protein lysis buffer using a turrax. In the case of adherent cells such as NRCM and NRCF, the stimulated cells were washed with PBS and 250 µl of cold protein lysis buffer was added to the plates. The cells were scraped using a cell scraper and the lysates were transferred into a 1.5 ml tube. The cell lysates were then sonicated. The lysates were then incubated with 1/10<sup>th</sup> volume of 5% (v/v) Benzonase at RT for 10 min. Benzonase is a genetically engineered endonuclease which degrades all forms of nucleic acids (DNA, RNA). The tubes were then placed in an ultrasonic bath at 4°C for 5 min. The samples were then centrifuged at 12000 rpm for 20 min at 4°C to clear the lysates and were stored at -80°C until use.

#### **3.4.2 BCA protein quantification**

The concentration of the protein lysates was determined by the Bicinchoninic acid colorimetric assay using the BCA protein assay kit (Thermo Scientific, Rockford USA). The peptide bonds in the protein reduce the divalent copper ions to monovalent ions, which then chelates with the bicinchoninic acid to form a purple coloured complex with maximum absorption at 562 nm. The absorbance of the samples at 562 nm was measured using an Infinite 200 spectrophotometer (Tecan, Männedorf). The protein concentration was then evaluated with reference to internal calibration standards such as bovine serum albumin.

#### **3.4.3 Western blot**

Depending on the size of the detected proteins, 8 – 12% polyacrylamide gels were used.

	Stacking gel	Running gel		
Acrylamide/Bisacrylamide 30%/0.8% (v/v)	0.5 ml	4ml	4.5ml	5ml
Lower buffer (4X)	-	3.8ml	3.8ml	3.8ml
Upper buffer (4X)	1.25ml	-	-	-
H2O	3.2	4.7 ml	4.2 ml	3.7 ml
Glycerol (80%)	-	2.5 ml	2.5 ml	2.5 ml
TEMED	6 µl	12 µl	12 µl	12 µl
APS (10%)	48 µl	72 µl	72 µl	72 µl

The gels were casted on Mini-PROTEAN casting stand (Biorad, München). The samples were prepared by boiling at 95°C for 5 min. The gel electrophoresis chamber was filled with 1X running buffer, samples were loaded into the wells and 30 mA current per gel was applied at maximum voltage. Under denaturing conditions, the proteins are separated based on their molecular weight. The proteins were then transferred onto a PVDF membrane (Millipore, Billerica USA) using wet transfer (Mini-PROTEAN transfer system, Biorad, München). The PVDF membrane was cut to the size of the mini-gel and was activated using methanol. The membrane was placed on the cassette facing the anode and the gel was placed facing the cathode side. The membrane and the gel were sandwiched between 1-2 layers of filter paper. The transfer was carried out at 350 mA current at the maximum voltage for 90 min. The membrane was blocked with 10% non-fat milk for 1 hour at RT on a horizontal shaker and then incubated with the primary antibody for overnight at 4°C. The following antibodies diluted in 5% milk block buffer were used: anti-Cre (Millipore, 1:1000), anti-Beta-gal (Abcam, # ab616), anti-HSP90. The membrane was washed thrice with 1X PBST for 10 min at RT. The membranes were then incubated with the appropriate peroxidase-conjugated secondary antibodies (1:10000) at RT for 90 min. The membranes were again washed with the PBST buffer. The proteins were detected by chemiluminescence. ECL Plus (GE Healthcare, München) was applied to the membrane according to the manufacturer's instructions. The signal was visualized using a Fujifilm LASmini4000 instrument (Fujifilm, Düsseldorf). The blots were then analysed using the Multigauge software (Fujifilm, Düsseldorf).

### **3.5 Immunofluorescence**

#### **3.5.1 In tissues**

Heart tissues were processed in two ways:

- (A) **4% PFA perfused hearts tissues for visualizing mTomato and mGFP direct fluorescence**- Hearts tissue was isolated from anesthetized mice perfused with 4% paraformaldehyde (PFA) in 0.1M phosphate buffer saline (PBS), fixed for 2 hours in 4% PFA at 4°C, followed by overnight incubation in 30% sucrose, and embedded in OCT (Tissue Tek). 5mm sections were cut. The slides were shortly rinsed with PBS and mount with Vectashield fluorescence mounting medium containing DAPI and imaged at a confocal microscope for mTomato and mGFP direct fluorescence.

The PFA perfused heart sections of 7 days old and 6 weeks old mice were also used



## Materials and Methods

for single staining with a different antibody (mentioned below) in case of vimentin promoter study after maternal injection.

(B) **Sucrose section for immunostaining-** Heart tissues was dissected and cryoprotected in 30% sucrose overnight at 4 degrees, followed by embedding in OCT. The cryosections (5mm) were fixed either with 4% PFA or cold methanol, followed by permeabilization (only in case of PFA fixation) with 0.2% Triton X-100 or 0.05% PBST and blocking with 10% Goat serum or BSA for 1 h at room temperature. The sections were then incubated with either with primary antibody against GFP (Abcam 1:1000) alone or with cocktail of antibody against vimentin (Abcam, 1:200), CD31 (1:200, Pharmingen, San Diego, CA), SM22 $\alpha$  (Abcam 1:200), P4HB (1:50, Proteintech) and ACTN ( $\alpha$ -Actinin) (Sigma, 1:600) for overnight at 4 °C followed by secondary Alexa Fluor 647 goat anti-rabbit, goat anti-rat, goat anti-mouse, donkey anti-goat or Alexa Fluor 488 goat anti-chicken (Invitrogen, Carlsbad, CA). (1:200) for 1h at RT. Confocal microscopy (a Zeiss LSM 510 system and Leica SP5) was performed using a 40X oil immersion lens.

Brief information about the double antibody staining (co-staining) protocol used for the study is given in below in tabular format

Co-staining	Fixation	Blocking	Primary antibody	Secondary antibody
Vimentin and GFP	4% PFA for 10min at RT, 5-10min permeabilization with 0.2% triton X100 in PBS for at RT	10%goat serum	Cocktail o/n at 4°C of vimentin (1:200) and GFP (1:1000)	Cocktail for 1h at RT Alexa Fluor® 647 Goat Anti-chicken IgG (H+L) (1:200) Alexa Fluor® 488 Goat Anti-rabbit IgG (H+L) (1:500)
P4HB and GFP	Methanol (cold) for 10min at -20°C. Washing with 0.05% PBST reduces the background	10% goat serum	Cocktail o/n at 4°C P4HB (1:50) GFP (1:1000)	Cocktail for 1h at RT Alexa 647 Anti –Rabbit (1:200) & Alexa 488 anti-chicken (1:500)
CD31 and GFP	4% PFA for 10min at RT, 5-10min permeabilization with 0.2% triton X100 in PBS at RT	10% goat serum	Cocktail o/n at 4°C CD31 (1:100) GFP (1:1000)	Cocktail for 1 h at RT of Alexa 647 Anti–Rat (1:200) & Alexa 488 anti-chicken (1:500)
SM22a and GFP	4% PFA for 10min at RT, 5-10min	10% BSA	1step: SM22alpha (goat) (1:100)	Cocktail for 1h at RT Biotinylated IgG (anti-goat) (1:200) & Alexa 488 anti-

	permeabilization with 0.2% triton X100 in PBS at RT		o/n at 4°C 2step: GFP Rabbit (1:600) at 37 for 2hrs	chicken (1:500) Followed by additional incubation (30min) with Streptavidin Alexa-647 conjugate (1:300) for SM22a at 37 °C.
--	---	--	---	---

### 3.5.2 In isolated cells

For visualizing mTomato and mGFP signals the isolated cardiomyocytes (CM) were plated on laminin coated coverslip for 1hrs and the cardiac fibroblasts (CF) for 48hrs on normal coverslips were fixed with 4% paraformaldehyde for 10 min, washed shortly with PBS and mount with 50% glycerol containing DAPI. However, for co-staining the CF were fixed with 4%PFA, permeabilized with 0.2% Triton X-100 for 5 min and then incubated with primary antibodies as used above against GFP, Vimentin, P4HB, CD31 and  $\alpha$ -actinin for 1 h at 37°C incubator. Following three washes in PBS, coverslips were incubated with secondary antibodies conjugated to Alexa Fluor dyes as above (Invitrogen; 1:200) for 35 min at 37°C. The coverslips were then washed three times in PBS, mounted onto glass slides using mounting medium containing Dapi and subjected to automated fluorescent microscopy (20X or 10X).

## 3.6 Staining

### 3.6.1 Detection of $\beta$ -Galactosidase activity (X-gal staining)

For Xgal staining of cryosections, whole hearts were harvested, cryoprotected in 30% sucrose overnight at 4°C and were embedded in Tissue-Tek OCT. Cryosections (5mm) were prepared and stained for  $\beta$ -galactosidase activity. Prior to staining, sections were fixed in cold PBS containing 0.2% glutaraldehyde, 5mM EGTA (pH 7.3) for 10 min. Sections were washed three times for 5 min in X-gal wash buffer (2mM MgCl<sub>2</sub>, 0.01% sodium deoxycholate, 0.02% Nonidet-P40 (NP-40) in PBS) and then stained in Xgal staining solution (1 mg/ml Xgal, 5mM potassium ferrocyanide, and 5mM potassium ferricyanide in washing buffer) at 37°C for 3-4hours. Sections were rinsed in PBS, counterstained with eosin, moved through a graded ethanol series for dehydration, incubated in toluene for 3min and then mounted with DePEX. X-gal staining was used to check whether a cell expresses the  $\beta$ -galactosidase enzyme, which is encoded by the lacZ gene.  $\beta$ -galactosidase cleaved X-gal by yielding galactose and 5-bromo-4-chloro-3-hydroxyindole. The latter is then oxidized into 5,5'-dibromo-4,4'-dichloro-indigo, which is an insoluble blue product. X-gal itself is colorless, the presence of blue-colored product therefore used as a test for the

presence of an active  $\beta$ -galactosidase (or LacZ gene).

### **3.6.2 Fast green/Sirius red staining for cryosections**

This method was used for measurement of collagen contents in heart tissues. The total amount of collagen and non-collagenous proteins in tissue sections is determined by differential staining with two dyes, sirius red and fast green. Sirius Red binds to all types of collagen, whereas fast green stains non-collagenous proteins. For this, the sections were incubated in preheated Bouin's Solution at 58°C for 1 hour, washed in running tap water and stained with fast green dye for 20min and Sirius red solution for 30 min, RT and then washed briefly in ddH<sub>2</sub>O (10 sec). The sections were subjected to an ascending ethanol series (70%: 1 min, 100%: 1 min), incubated in toluene (3 min), covered with DEPEX and dried overnight at RT. The quantification was performed using the MetaMorph Basic Imaging software package (Molecular Devices, Downingtown, USA).

## **3.7 Microscopy**

### **3.7.1 Confocal microscopy**

Confocal images were taken using two confocal Microscope- **(A)** Zeiss LSM 510 META where, Alexa-488, mTomato, Alexa 647 and DAPI were excited at 488nm, 543nm, 633nm and 364nm laser lines, respectively and 40X oil immersion objective was used. **(B)** Leica SP5 confocal microscope where, mGFP/Alexa 488, mTomato, Alexa 647 and DAPI were excited at 488nm, 561nm, 633nm and 405nm laser lines and 63X glycerin objective was used. The images were processed using Adobe Photoshop software.

### **3.7.2 Automated fluorescent microscopy**

Images were acquired automatically using a 10X or 20X objective on an AxioObserver.Z1 (Zeiss, Jena), a motorized scanning stage (Märzhäuser, Wetzlar), Lumen200 fluorescence illumination system (Prior, Cambridge UK) and Retiga4000 CCD fluorescence camera (QImaging, Surrey Canada). Metamorph imaging software (Molecular Devices, Downingtown USA) was used to drive the microscope automatically and also for subsequent analysis of the acquired images.

## **3.8 Methods for animal experiments**

### **3.8.1 Generation of a Ccdc80-Cre mouse line**

The Ccdc80-Cre targeting vector was prepared amplifying promoter sequence (4.2kb) from BAC clone (Gene Service) that was cloned in Cre expressing Vector through Gateway

Recombination Technique (Invitrogen). Ccdc80-Cre vector was first amplified in bacteria and purified with the Endotoxin free Maxi Kit (Qiagen) according to the manufacturer's instructions. 50-100 ug of the vector were then linearized with the Aval restriction enzyme (NEB) incubation (Section 3.1.6). Linearized vector was sent to the Institute of Laboratory Animal Science, the University of Zurich for generation of transgenic mice through pronuclear injection.

**Establishing Ccdc80-Cre founder lines:** The transgenic technology facility returned forty pups' ear punches from eleven foster mothers for screening of transgene. 13 of 40 pups were positive for the Cre gene. Genotype diagnostics were carried out using PCR amplification followed by gel electrophoresis with DNA isolated from ear punches.

Four chosen founders were returned from the transgenic technology facility that was then crossed with the R26R-lacZ reporter line to histologically determine the expression of promoter activity. One out of those four founders was able to show active promoter activity driving cre expression through LacZ staining in heart and other tissues.

### 3.8.2 Isolation of genomic DNA

Genomic DNA was isolated from tail biopsies incubated overnight at 55°C and 1100 rpm in 500 µl of DNA lysis buffer (for genotyping) containing 2.5µl of 'Fermentas' Proteinase K (20mg/ml). To the tubes, 500 µl of 'Roth' phenol-chloroform was added and were centrifuged at 14000 rpm for 10 min. The upper phase of the cleared lysates was then transferred into fresh 1.5 ml microfuge tubes. The DNA was precipitated by addition of 200 µl of isopropanol and subsequent centrifugation at 14000 rpm at 4°C for 10 min. The supernatant was discarded and the pellet was washed with 500 µl of 70% ethanol. After centrifugation at 14000 rpm at 4°C for 5 min, the pellets were air-dried and resuspended in 20 µl ddH<sub>2</sub>O.

### 3.8.3 Genotyping PCR

The PCR reaction was set up as follows:

#### 1. Rosa (R26R) PCR

Substance	Volume
Genescript Taq Buffer (10X)	2µl
RF126 (25pmol/µl)	0.3µl
RF127 (25pmol/µl)	0.3µl
RF128 (25pmol/µl)	0.3µl
dNTPs (10mM)	0.4µl

Taq Polymerase	0.1 $\mu$ l
H <sub>2</sub> O	15.6 $\mu$ l
gDNA	1 $\mu$ l

**2. Cre Gene**

Substance	Volume
Genescript Taq Buffer (10X)	2 $\mu$ l
Sense Cre (20pmol/ $\mu$ l)	0.3 $\mu$ l
Antisense Cre (20pmol/ $\mu$ l)	0.3 $\mu$ l
dNTPs (10mM)	0.4 $\mu$ l
Taq Polymerase	0.2 $\mu$ l
H <sub>2</sub> O	15.5 $\mu$ l
gDNA (50ng/ $\mu$ l)	1 $\mu$ l

**3. mTom-mGFP Gene**

Substance	Volume
Taq Buffer (5X) Go taq Promega	4 $\mu$ l
oIMR 7318 (20pmol/ $\mu$ l)	0.5 $\mu$ l
oIMR 7319 (20pmol/ $\mu$ l)	0.5 $\mu$ l
oIMR 7320 (20pmol/ $\mu$ l)	0.5 $\mu$ l
dNTPs (10mM)	0.4 $\mu$ l
Taq Polymerase	0.1 $\mu$ l
H <sub>2</sub> O	11 $\mu$ l
gDNA (50ng/ $\mu$ l)	1 $\mu$ l

The subsequent amplification reaction was performed in a thermocycler (Mastercycler pro, Eppendorf, Hamburg, Germany) with the following temperature program

	Step	Temperature	Time	Number of cycles
<b>Stage 1</b>	Before denaturation	94°C	120-300s	1x
<b>Stage 2</b>	Denaturation	94°C	30 s	30-35x
<b>Stage 3</b>	Hybridization	Depending on primer sequences		

<b>Stage 4</b>	Elongation	Depending on the template length (1 min / 1000 nucleotide)		
<b>Stage 5</b>	Final elongation	72°C	180-300 s	1x

### **3.8.4 Animal models**

#### **3.8.4.1 Reporter Mice used for study**

Two reporter mouse models are used for the study.

**(A) Rosa26-lacZ reporter mice (Soriano, 1999):** The R26R mouse strain should be of wide use for monitoring Cre expression, as well as for analysing cell lineages during development, and is available from the Induced Mutant Resource of the Jackson Laboratory (stock numbers 003309 and 003310). Rosa transgenic mice contain a lacZ reporter gene that is transcriptionally silenced by a floxed stop sequence immediately upstream. Upon expression of Cre-recombinase in target tissues, the stop sequence is cleaved, and the beta-galactosidase reporter is transcribed.

**(B) mTomato-mGFP (mT/mG) dual fluorescent reporter mice (Muzumdar, 2007)<sup>234</sup>:** ROSA mT/mG is a cell membrane-targeted, two-color fluorescent Cre reporter allele; expressing cell membrane-localized red fluorescence in widespread cells/tissues prior to Cre recombinase exposure, and cell membrane-localized green fluorescence in Cre recombinase expressing cells (and future cell lineages derived from these cells). It is also available at Jackson Laboratory (stock number 007576).

#### **3.8.4.2 VimCreERT2 transgenic mice**

VimCreERT2 transgenic mice were generated using BAC recombination in Dr Robert F. Schwabe Laboratory, New York. These transgenic mice express tamoxifen inducible Cre recombinase under the control of mouse vimentin promoter. The mice received as a gift from Dr Schwabe and Dr Micheal Quante (Technical University in Munich) for the study.

#### **3.8.4.3 Fsp1-Cre (or S100A4-Cre)**

These transgenic mice express Cre recombinase under the control of the mouse S100 calcium binding protein A4 (S100A4) promoter. Cre recombinase expression is detected specifically in stromal fibroblasts of tissues such as the prostate, forestomach and mammary gland. Mice that are homozygous for the transgene are viable, normal in size and do not display any gross physical or behavioral abnormalities.

## **3.9 Methods for cardiovascular phenotyping of mice**

The following methods were carried out by trained personal.

### 3.9.1 Echocardiography

To be tested, mice were anesthetized by inhalation anesthesia (a mixture of 2 % isoflurane and 98 % oxygen) and were fixed on a hot plate (40 ° C). For ultrasound examination of the Vevo 700 (Visual Sonics, Ontario, CAN) was used. After shaving off the chest, the ultrasound probe was parasternal placed on them and the left ventricle in the long axis (B-mode) optimally aligned for measurement. For the recording of the echocardiogram in the short axis (M-mode) of the transducer was rotated 90°C. Following parameters in diastole (d) and systole (s) were read from the echocardiogram: interventricular septum thickness (IVS), left ventricular internal diameter (LVID) and left ventricular posterior wall (LVPW). Other parameters (fractional shortening (FS), ejection fraction (EF)) were quantified with the corresponding formulas.

### 3.9.2 Transverse aortic constriction (TAC)

TAC was performed as described previously (Rockman HA, et al). Briefly, mice (8 weeks old) were sedated by 2% isoflurane and 600 mL/min O<sub>2</sub>. The animals were then placed in a supine position, an endotracheal tube was inserted and the chest cavity was exposed by cutting open the proximal portion of the sternum. After the aortic arch between the innominate and left common carotid arteries was isolated, it was constricted with a 6-0 silk suture tied firmly 2 times against a 27-gauge blunted needle. Sham-operated mice underwent the identical surgical procedure, including isolation of the aorta, but without placement of the suture. Animals were anesthetized and euthanized 21 days after TAC for histological studies.

In case of vimentin promoter study six weeks old Vim-CreER;mTom/mGFP<sup>fl/+</sup> mice were treated with vehicle and tamoxifen (2mg/mouse/day) i.p. for 6 consecutive days prior to TAC.

### 3.9.3 Statistics

Average data are presented as mean±SEM. Statistical analysis was performed using the Prism software package (Graph Pad, San Diego, U.S.A.). To compare two groups, unpaired student t-test was performed. Statistical significance was evaluated using one-way ANOVA followed by Bonferroni test or 2-way ANOVA/ Bonferroni posttest. Differences were considered significant if P< 0.05 and were represented P<0.001 (\*\*\*), P<0.01 (\*\*) or P<0.05 (\*).

## 4 RESULTS

### 4.1 Generation and characterisation of a *Ccdc80*-Cre transgenic mouse line

#### 4.1.1 Identification of cardiac fibroblast specific gene and validation of candidates

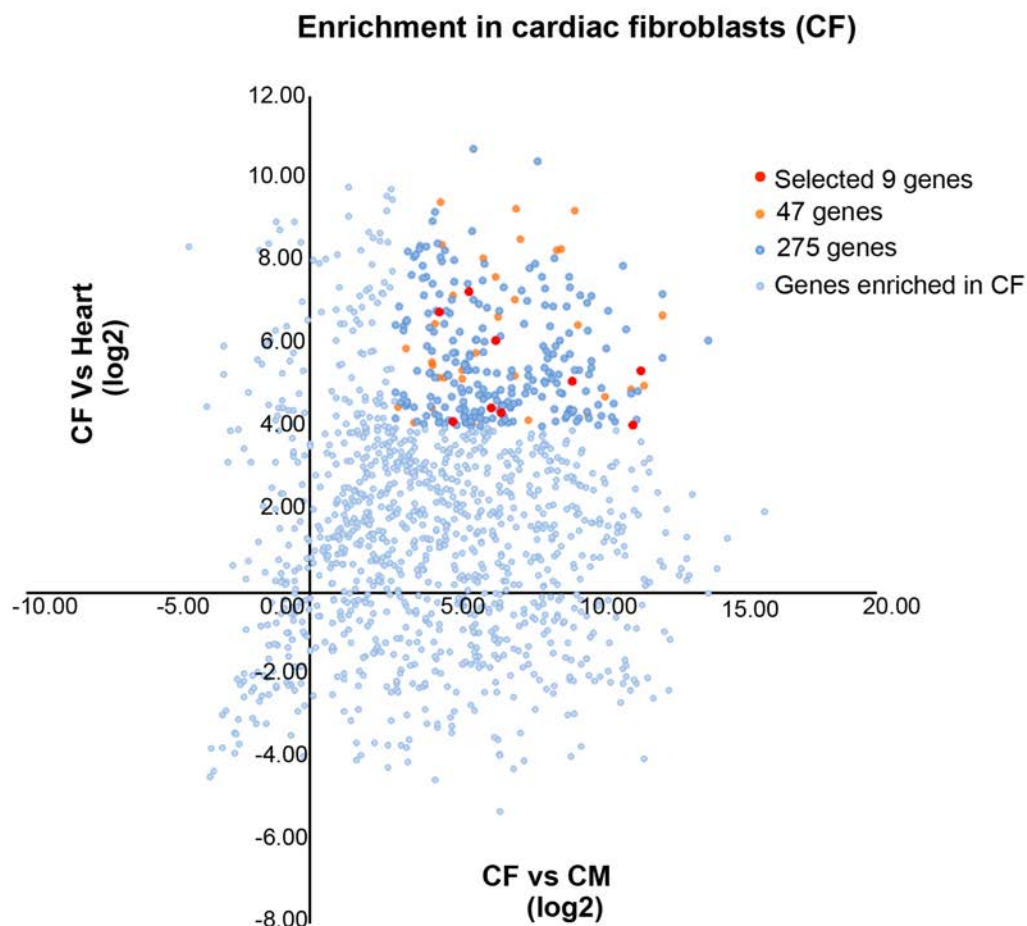


**Figure 4.1 Screening of cardiac fibroblast-specific genes using mouse microarray database.** Scatter plot illustrating the expression of 1371 genes enriched in CFs as compared to heart (>6 fold) and CM (>16 fold). The selected 9 candidate genes (marked in red) were then used for further validation.

In order to search for cardiac fibroblast-specific genes, a microarray database was generated, which includes gene expression data from CFs & CM of adult mouse and neonatal rat, CFs of  $\beta$ 1-AR transgenic mice and fibroblast from lung, liver, skin, kidney of neonatal rats.  $\beta$ 1-transgenic mice were generated by overexpression of  $\beta$ 1-adrenergic receptor under the control of heart-specific  $\alpha$ -MHC promoter<sup>99</sup>, and was used as the heart



failure models in the study. From this database, 1371 genes that are strongly expressed in mouse CFs were pre-selected. Then the expression of these pre-selected genes in CFs were compared to their expression in the whole heart (>6 fold) & in CM (>16 fold) where 275 genes were left out (Figure 4.1).

To further assess the expression of these 275 genes in different tissues, another published microarray mouse data of Henrichsen *et al.* (2009)<sup>215</sup> was included in the microarray database. The microarray data of Henrichsen *et al.* analyzed the transcriptome in different tissues of the mouse. To constrain the search for the gene, the 275 genes were related to the Henrichsen *et al.*, mouse data where genes with a preferential cardiac expression as compared to other tissues were searched out. This analysis resulted in 47 genes (as mentioned in 8.1 in appendix section). Finally the cardiac expression of these 47 genes was confirmed using publically available databases GENECARD that results in leaving only nine candidate genes (as shown in Figure 4.1)

In order to determine the expression of nine candidate genes in different tissues, total RNA was isolated from six different tissues (lung, liver, kidney, heart, brain, skeletal muscle) of 3 months old FVB/N mice. Reverse transcription (using Invitrogen RT-Kit) and real-time PCR analysis were carried out. Here only four out of nine genes showed a high level of expression in the heart as compared to other tissues as shown in Figure 4.2 A.

Several scientific groups reported increased expression of periostin and gelsolin<sup>216</sup> in a diseased heart. Further investigation was done for the expression of these four genes in disease condition in the heart. For this total RNA was isolated from non-failing hearts, (here a wild-type mouse is a model for a non-failing heart) and failing hearts ( $\beta$  1-adrenergic receptor transgenic mice as a heart failure model). Reverse transcription and real-time PCR was carried out. **Ccdc80 gene showed a significant up-regulation (around two-fold) in failing heart as compared to non-failing heart** while Rabgap1l showed a slight increase in failing heart that was non-significant (Figure 4.2 B). Similar to previous findings, periostin and gelsolin expression levels were up-regulated in failing heart (Figure 4.2 B). In order to further validate the cell-specific expression of these candidate genes, real-time PCR was performed on RNAs isolated from CM and CFs of neonatal rat (NR) and of an adult mouse(AM). **In the neonatal rat, Ccdc80 had two-fold expression and periostin three-fold expression in CFs compared to CM while gelsolin was found to be expressed in CM.** There was no expression detected for Rabgap1l gene in any of the two cell type (Figure 4.2C).

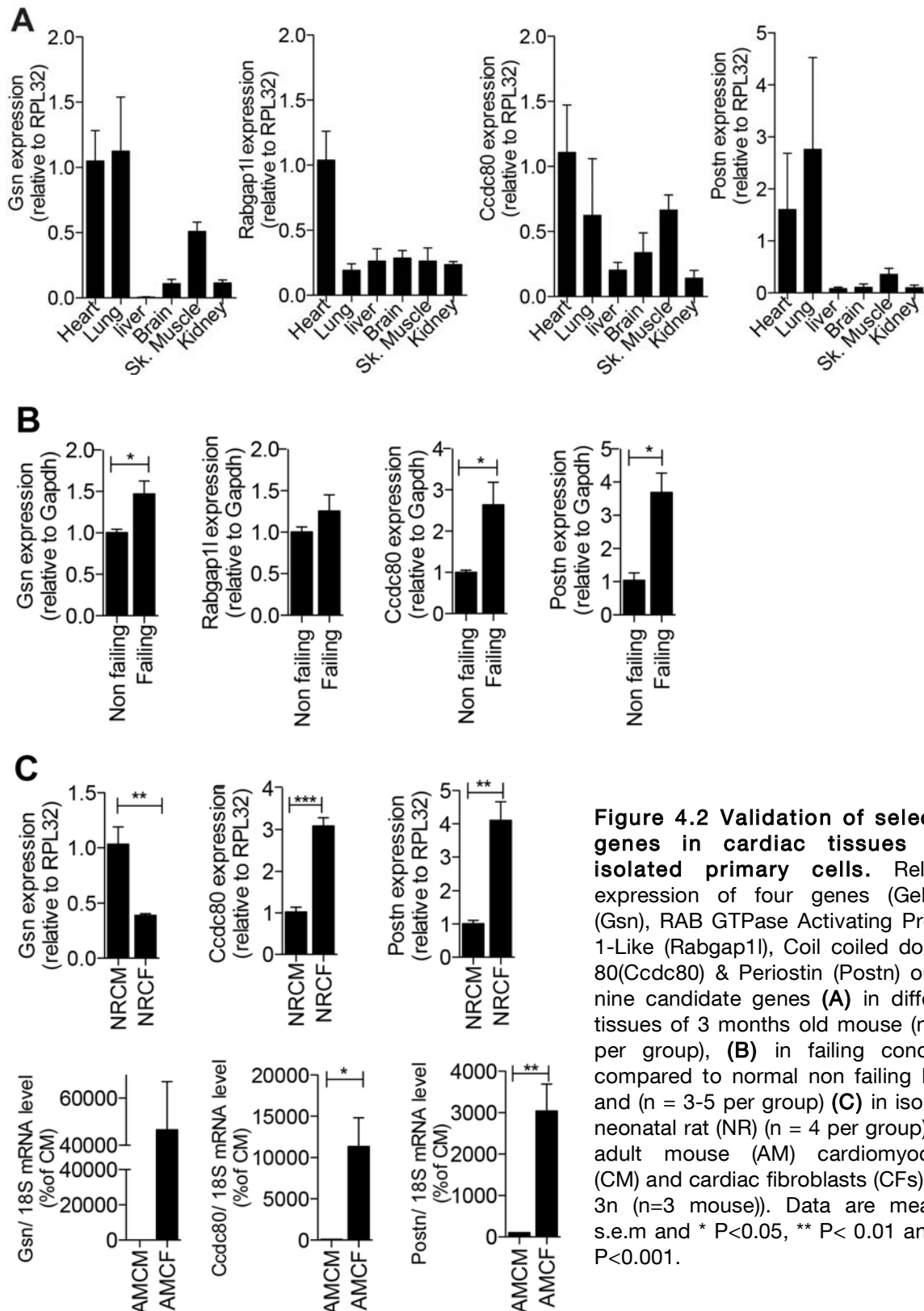


**Figure 4.2 Validation of selected genes in cardiac tissues and isolated primary cells.** Relative expression of four genes (Gelsolin (Gsn), RAB GTPase Activating Protein 1-Like (Rabgap11), Coil coiled domain 80(Ccdc80) & Periostin (Postn) out of nine candidate genes (A) in different tissues of 3 months old mouse (n = 3 per group), (B) in failing condition compared to normal non failing heart and (n = 3-5 per group) (C) in isolated neonatal rat (NR) (n = 4 per group) and adult mouse (AM) cardiomyocytes (CM) and cardiac fibroblasts (CFs) (N = 3n (n=3 mouse)). Data are mean ± s.e.m and \* P<0.05, \*\* P< 0.01 and \*\*\* P<0.001.

Similarly significantly increased expression of Ccdc80 and periostin gene was observed in AMCF compared to AMCM. However, we also observed an increased

expression of gelsolin this time in AMCF instead of AMCM but this increase was not significant (Figure 4.2 C).

#### 4.1.2 Cloning and validation of candidate promoters *in vitro*

Putative promoter sequences (5-7Kb upstream) of two respective candidates genes *Ccdc80* (4.2Kb) and *Periostin* (3.9Kb) were amplified from BAC clones (mentioned in Materials section) using PCR.

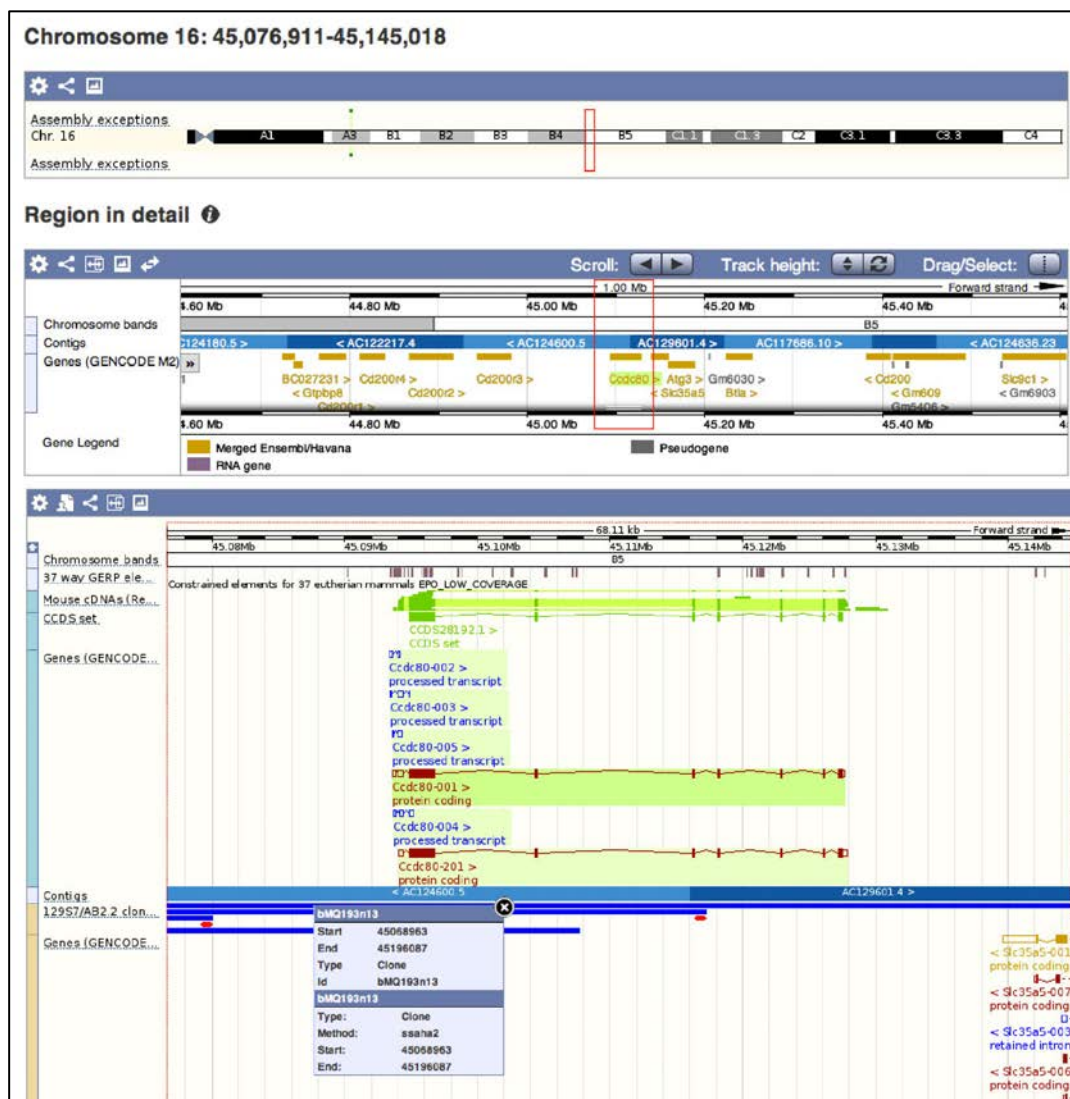


Figure 4.3 BAC clone (bMQ193n13) having genomic region (upstream and downstream) of *Ccdc80* gene at Chromosome16: 45,076,911-45,145,018 (as represented by blue line), was used for amplifying *Ccdc80* promoter sequence (5000bases upstream) (Ref. [www.ensembl.org](http://www.ensembl.org).)

The BAC clones used for amplification of promoter sequences were ordered from Mouse bMQ BAC library as displayed on the Ensembl genome browser within a DAS (Distributed

Annotation Server) for desired genomic region. Figure 4.3 showed a snapshot of ensemble browser showing the BAC clone for Ccdc80.

In order to verify that these promoters have indeed a CFs-specific expression, we used a **LacZ reporter** approach first. Moreover, as our main goal was to be able to specifically target genes in the cardiac fibroblast *in vivo*, promoter constructs to drive **Cre-recombinase** were also generated.

### 4.1.2.1 Cloning and analysis of candidate promoter activity using a LacZ reporter vector

The well-characterized bacterial *E.coli lacZ* gene, which encodes  $\beta$ -galactosidase ( $\beta$ -gal), has become a standard tool for following localized transgene expression in many organisms, including mammalian cells and transgenic animals. Detection of the encoded  $\beta$ -galactosidase activity is achieved either by direct enzymatic assay using fluorogenic or chromogenic substrates or by visualization *in situ* using the chromogenic substrate 5-bromo-4-chloro-3-indolyl- $\beta$ -D-galactopyranoside (X-gal). Because X-gal forms an insoluble blue precipitate upon hydrolysis by  $\beta$ -galactosidase, it allows *in situ* detection of lacZ transgene expressing cells *in vitro* and facilitates spatial determination of reporter gene expression in transgenic animals *in vivo*.

In order to analyze the amplified promoter sequences for its transcriptional activity *in vitro*, the respective promoter sequences (Ccdc80 (4.2Kb) & Periostin (3.9Kb)) were cloned into the promoterless-LacZ vector (Clontech, GenBank Accession No.U13184) (Figure 4.4 A&B). To assess the expression of LacZ reporter gene under the control of these respective promoters, standardization of  $\beta$ -Galactosidase ( $\beta$ -Gal) staining protocol was done using a  $\beta$ -Gal control vector (Ambion) as a positive control. This vector consists of CMV promoter that drives the LacZ gene expression. The promoter activities were then analyzed *in vitro* by transfecting fibroblast cell line (NIH-3T3 cells) and by performing a  $\beta$ -Gal staining 24 hours post-transfection. As shown in Figure 4.4 C, cells stained in blue were observed after transfection with the CMV-LacZ control vector ( $\beta$ -Gal control vector), and also with Ccdc80-LacZ and Periostin-LacZ (Postn-LacZ) construct. Thereby, demonstrating the efficient activity of both promoter sequences *in vitro*. However, low transfection efficiency was observed with both the promoter-LacZ reporter constructs, but this may be due to their larger sequence sizes.

Similarly, electroporation of neonatal rat cardiomyocytes (CM) and cardiac fibroblast (CFs) with these promoter-LacZ reporter constructs (Ccdc80-LacZ & Postn-LacZ) was done in order to analyze the preferential CFs specificity *in vitro*. There also very low transfection

efficiency observed (data not shown).

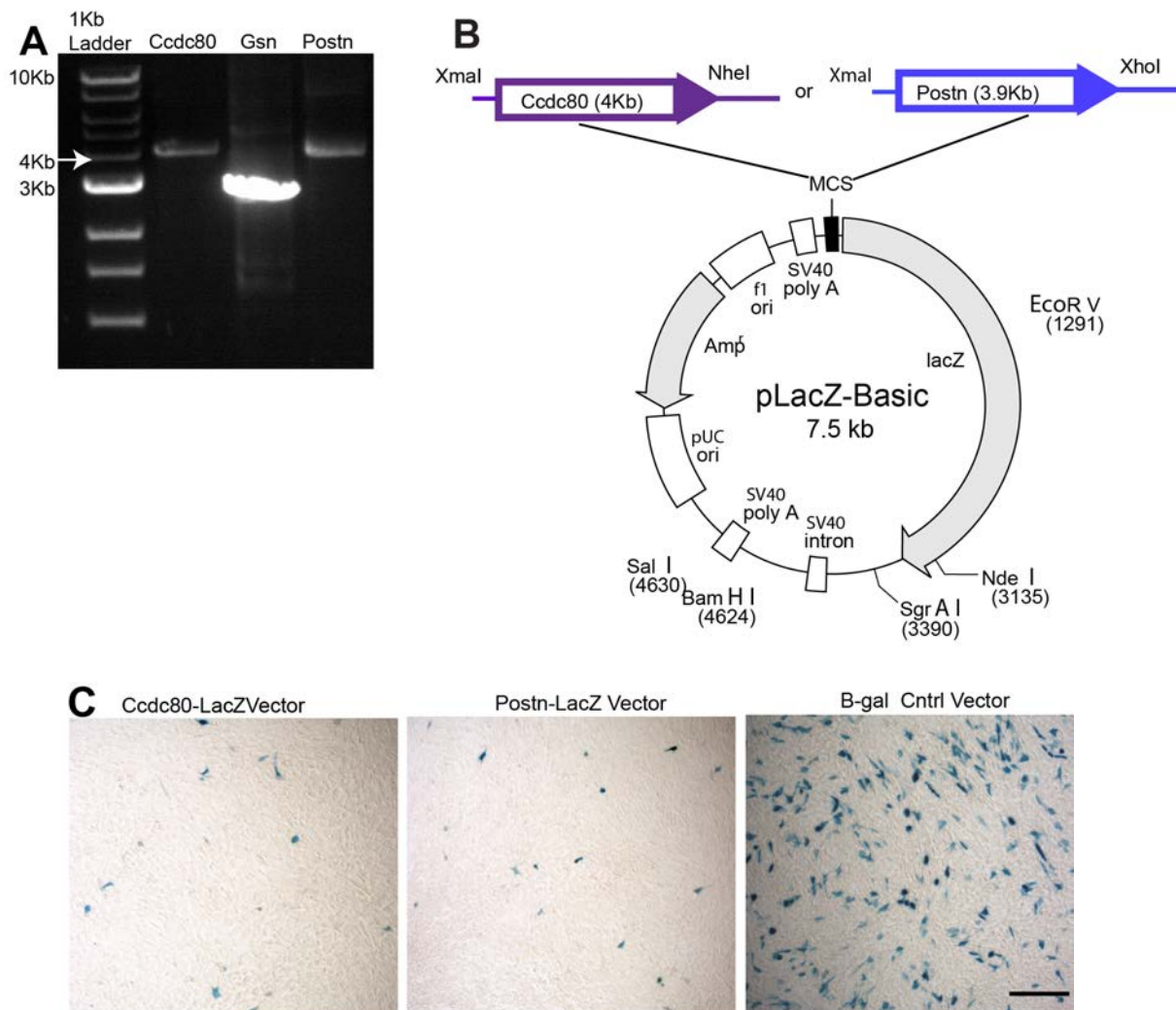


**Figure 4.4 Analysis of amplified promoter sequences for transcriptional activity *in vitro*.** (A) PCR Amplified Ccdc80 (4.2Kb), Gelsolin (Gsn) and perisiotin (3.9Kb) promoter sequence on 0.7% agarose gel. (B) Schematic diagram showing cloning of amplified Ccdc80 promoter sequence having restriction site (Xmal & NheI) and periostin promoter sequence (Xmal & XhoI) into the multiple cloning sites (MCS) of promoterless pLacZ –basic vector (Ref. MacGregor GR *et al.* 1987). (C)  $\beta$ -Gal staining of transfected fibroblast cell line with Promoter-LacZ constructs. Scale bar represents 100 $\mu$ m.

#### 4.1.2.2 Generation of vectors enabling cre-recombinase expression driven by the candidate promoters

Mouse strains expressing the site-specific Cre recombinase facilitate conditional ablation of genes when loxP sites flanked one or several exons of the gene of interest. In order to genetically modulate gene expression specifically in cardiac fibroblasts *in vivo*, several constructs were generated allowing the expression of the Cre driven by the candidate promoters.

#### Cloning of the promoter sequence in Cre recombinase expression vectors

Due to the non-availability of a promoterless-Cre construct, the pCAG-CRE construct (Addgene) was first adapted as a destination vector (pCre-GW) for gateway cloning. The

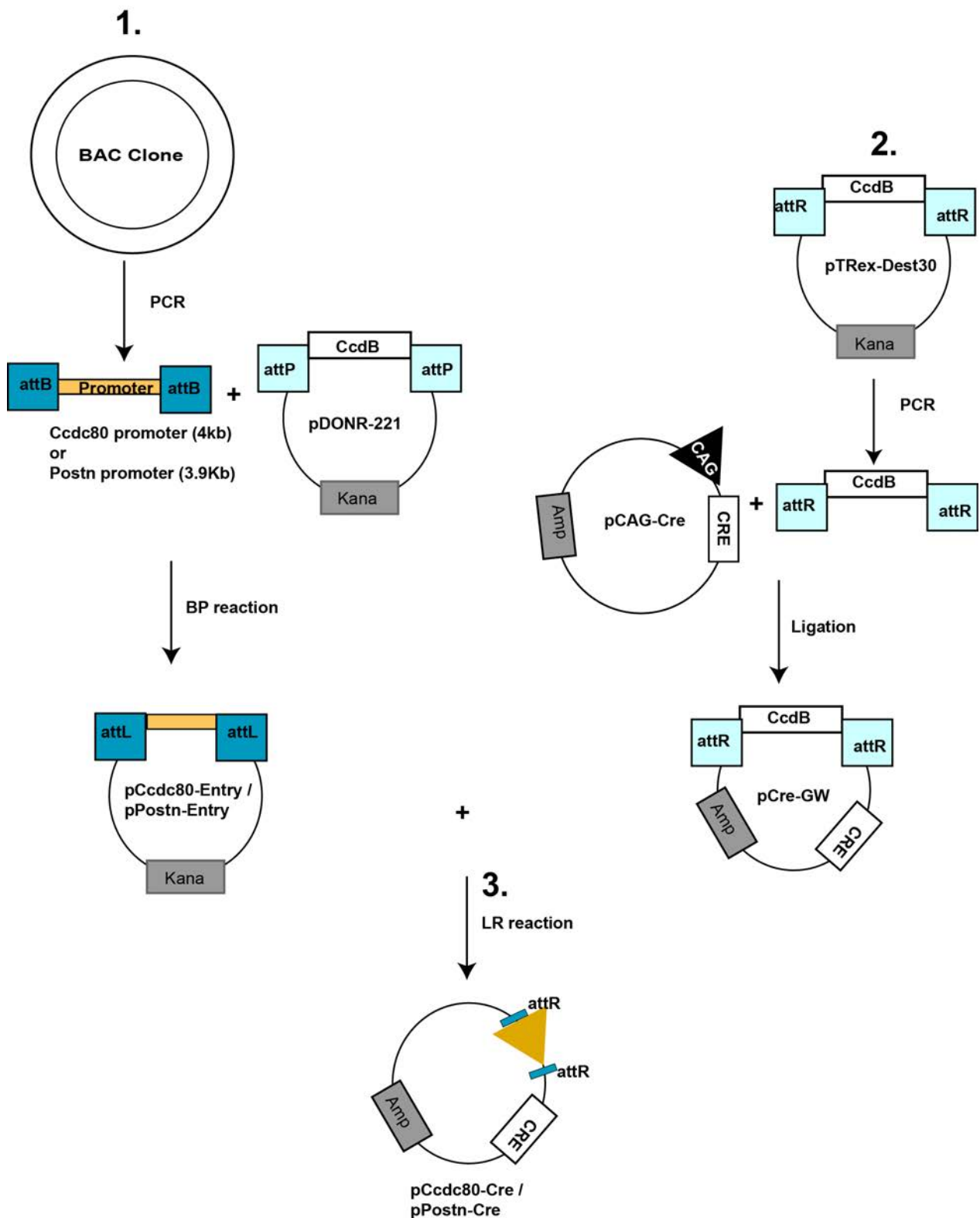


**Figure 4.5 Cloning strategies for generation of promoter-cre Constructs. 1.** Amplification of promoter sequences having attB sites from BAC clones using PCR and cloning of

promoter sequence to pDonR221 vector in order to generate Entry vector for the promoter sequences. **2.** pCAG-Cre vector adapted as a destination vector (pCre-GW) for LR reaction of gateway cloning. **3.** LR reaction between the different promoter-pEntry vector and pCre-GW (destination vector) for generation of Promoter-Cre constructs.

pCAG-Cre was adapted by removing its promoter region by restriction enzymes (Sall & XbaI) and ligation of the attb-ccdb-attb fragment (from pTREX-Dest30 vector) into the vector (Figure 4.5).

The Gateway System (Invitrogen) ensures a higher cloning efficiency than conventional cloning and is based on a two-step homologous recombination strategy for creating different reporters and expression plasmids (i.e. Destination vector) from a so-called Entry plasmid containing the relevant PCR product. Therefore, the two promoter fragments (Ccdc80 & Postn) were then amplified as described above (Figure 4.5). On each 5' end of the two primers, the attb-sites were added. The PCR product was cloned into an Entry clone by BP recombination and then into the above pCre-GW vector (destination vector) by LR recombination (Figure 4.5).

The correct integration and orientation of Ccdc80 and periostin promoter fragment into the adapted Cre vector was assured by analytical digestion with different restriction enzymes (Figure 4.6). Correctly oriented insert in pCcdc80-Cre vector lead to a digestion of the plasmid into a 3.6 kb, a 3.3 kb, and a 1.6 kb fragment while incorrect integration lead to a 3.5 kb, a 2.1 and a 1.2 kb fragment, as shown in Figure 4.6 A. On the other hand correctly oriented insert in pPostn-Cre vector leads to a 5kb and a 3 kb fragments when digested with two restriction enzymes (NheI & ClaI) while with no integration there was linearized 6kb fragment of empty pCre-GW vector (Figure 4.6 B). Positive clones of both vectors were selected, amplified in *E. coli* and purified. The correct junction from the promoter to the Cre gene and an unmutated transcription start site was confirmed by sequencing the plasmid.

To assess the efficiency of pCcdc-80-Cre and pPostn-Cre vectors, the vectors were transfected with an NIH-3T3 cell line that stably expresses the reporter pCALNL-GFP construct<sup>217</sup>. Both promoter sequences were capable of inducing efficient Cre recombination as seen by the GFP fluorescence in the cells similar to positive control (pCAG-Cre) (Figure 4.7 A).

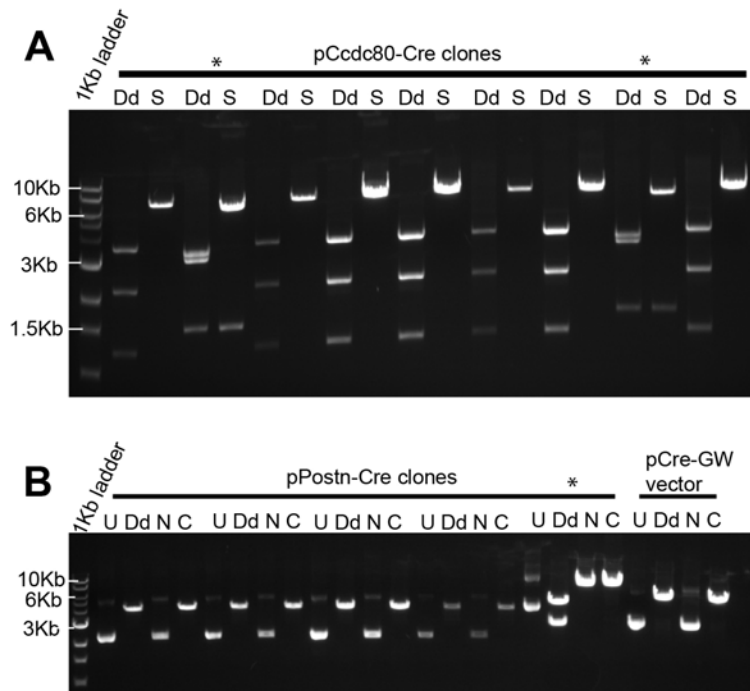


**Figure 4.6 Analytical digestion of *Ccdc80* and periostin promoter Cre constructs.** (A) 9 colonies were picked and plasmids were digested with *Sall* and *Clal* together (marked as Double digestion Dd) & with *Sall* alone (marked as S). Positive clones for *Ccdc80*-cre showed band with 3.6kb, 3.3kb, and 1.6kb. (B) Agarose gel of digested plasmids with *NheI* & *Clal* together (Dd), with *NheI* alone (marked as N) and with *Clal* alone (marked as C) along with undigested plasmids (U). Digested empty vector (pCre-GW) was loaded as control. Only one clone was positive clone for Postn-Cre showed band with 5kb and 3Kb. The positives clones in the figure shown were labeled with an asterisk.

In order to control the time of Cre induction in CFs *in vivo*, tamoxifen-inducible Cre vectors were also generated. Temporal control of Cre recombinase activity in transgenic mice has been demonstrated utilizing Cre recombinase fused with the mutated hormone-binding domain of the estrogen receptor (ERT<sup>T</sup>). Such transgene can be activated by the synthetic estrogen analog like tamoxifen or 4-OHT, but not by the physiological ligand 17 $\beta$ -estradiol. Therefore, such an inducible Cre recombinase system is further able to facilitate conditional gene knockout analysis in transgenic mice. It also permits the analysis of gene function at specific time points in a highly controlled manner. *In vitro* efficiency of tamoxifen-inducible Cre vectors (pCcdc80-ERT2CreERT2 & pPostn-ERT2CreERT2) was tested using stably transfected pCALNL-GFP reporter NIH-3T3 cells as above. **Solely upon stimulation with tamoxifen, a significant induction of GFP was observed with both the Cre constructs (Figure 4.7 B), demonstrating efficiently induced recombination by these two constructs *in vitro*.**



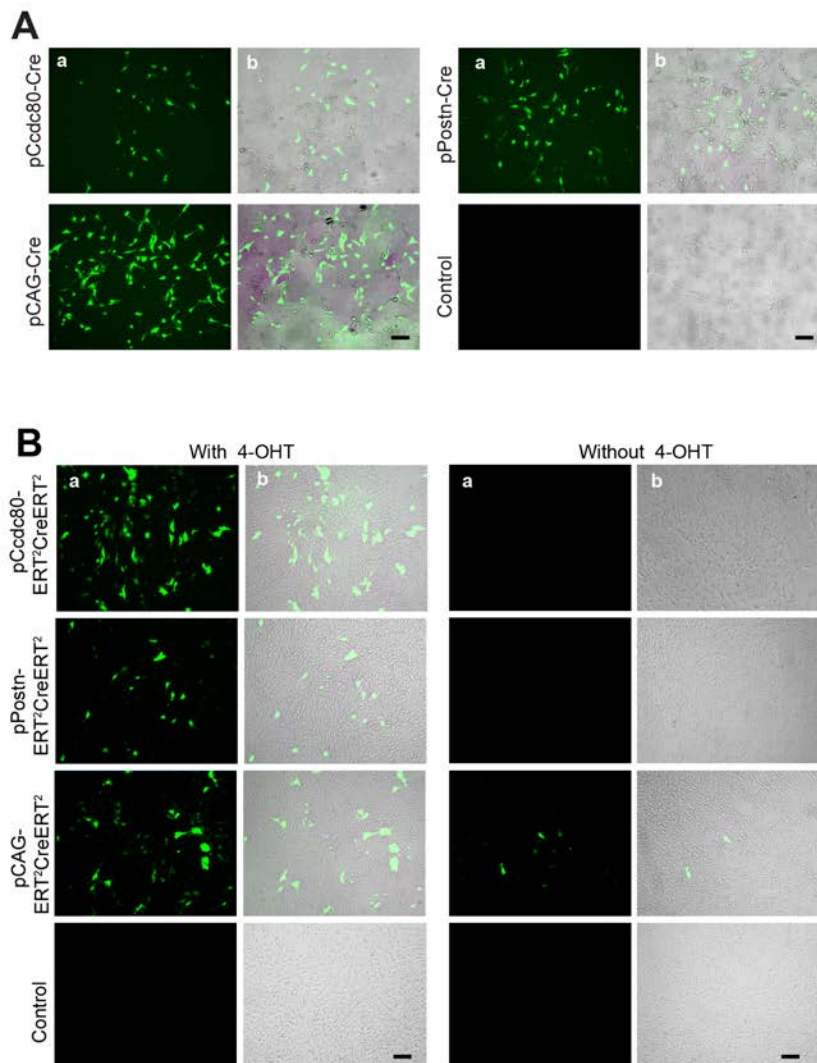


**Figure 4.7 Verification of promoter vector for efficient expression of Cre recombination *in vitro*.** (A) Photograph of the representative field showing NIH-3T3 stable cell line expressing GFP when transfected with pCcdc80-Cre, pPostn-Cre & pCAG-Cre vectors. The presence of endogenous GFP fluorescence accounts for the successful promoter activity in driving Cre expression *in vitro*. (B) GFP fluorescence observed in GFP-expressing stable NIH-3T3 cell line when transfected with promoter vectors expressing tamoxifen inducible-Cre recombinase in the presence (left panel) or in the absence (right panel) of 200nM 4-Hydroxy tamoxifen 48 hours post transfection. (a) GFP channel (b) overlay of GFP fluorescence and bright field image. Non-transfected cells were treated as control. Magnification: X20; Scale bar represents 50 $\mu$ m.

#### 4.1.3 Generation of a mouse line that expresses Cre recombinase under the control of the Ccdc80 promoter

As the ultimate goal was to generate transgenic mice to specifically knockout or overexpress a specific protein in cardiac fibroblasts, mice expressing Cre gene under the control of the Ccdc80 promoter were generated. For this study, Ccdc80 promoter was

chosen over periostin as periostin promoter (3.9Kb) had already been shown to drive tissue-specific expression in the neural crest-derived Schwann cell lineage and in a subpopulation of periostin-expressing cells in the cardiac outflow tract and endocardial cushions<sup>72</sup>. In addition, increased expression of periostin has been shown in the embryonic heart, restricted to mesenchymal cells, in pathological conditions and very low in adult hearts<sup>76,141,73</sup>. It is not feasible to have such a promoter whose activity is age dependent or condition dependent and can only be used for lineage mapping<sup>66, 67,72</sup>. The gene expression data and promoter sequence validation *in vitro*, so far (shown in Figure 4.2) showed Ccdc80 as a more promising candidate for the study.

To obtain a linearized construct for integration in the mouse genome and also to get rid of the extra unnecessary fragment, the pCcdc80-Cre plasmid was digested in front of the Ccdc80 promoter and after the Cre gene. The linearized fragment was then purified by dialysis. The construct was then integrated into the mouse genome by pronuclear injection and subsequent homologous recombination. The F<sub>0</sub> generation of the transgenic mice was genotyped for the presence of the Cre gene. 5 founders were received from our partner transgenic facility where only one animal was identified as transgenic having intense amplicon for Cre gene (Figure 4.8). The transgenic mice were bred with FVB mice to give rise to independent transgenic mouse lines.

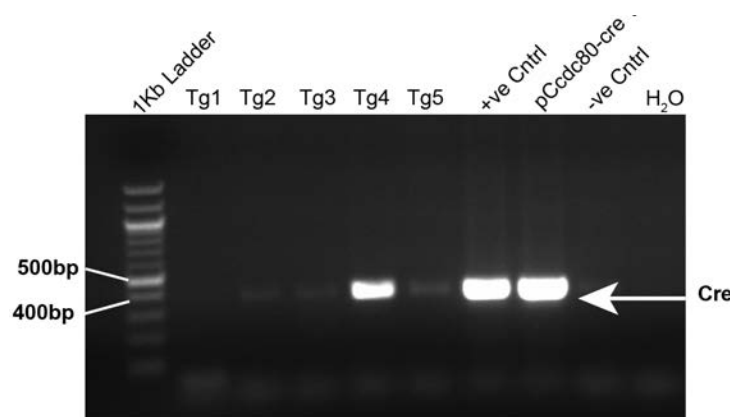


**Figure 4.8 Genotyping of Ccdc80-Cre founders by PCR.** Litters were genotyped after microinjection using primers for Cre gene. Out of five transgenic founders received only one founder showed intense band for Cre gene. The animal identified gave rise to the transgenic line (Tg4) for further study.

#### 4.1.4 Efficacy of the Ccdc80-Cre transgene *in vivo*

To analyze the Ccdc80 promoter efficiency *in vivo*, Ccdc80-Cre mice were bred with the homozygous Rosa26<sup>LacZ</sup> reporter mice<sup>218</sup>. The Rosa26<sup>LacZ</sup> reporter mice carries a bacterial β-

galactosidase gene (*lacZ*) flanked by *LoxP* sites<sup>218</sup>. When crossed with Cre-driver mice, *lacZ* is expressed in cells/tissues where Cre is expressed.  $\beta$ -Gal staining was performed, to investigate the site of Cre recombinase activity in frozen heart section of 6-7 weeks old *Ccdc80-Cre<sup>tg/0</sup>; Rosa26<sup>LacZ</sup>* mice. Cells stained in blue were observed indicating successful Cre recombination in the heart tissue (Figure 4.9).

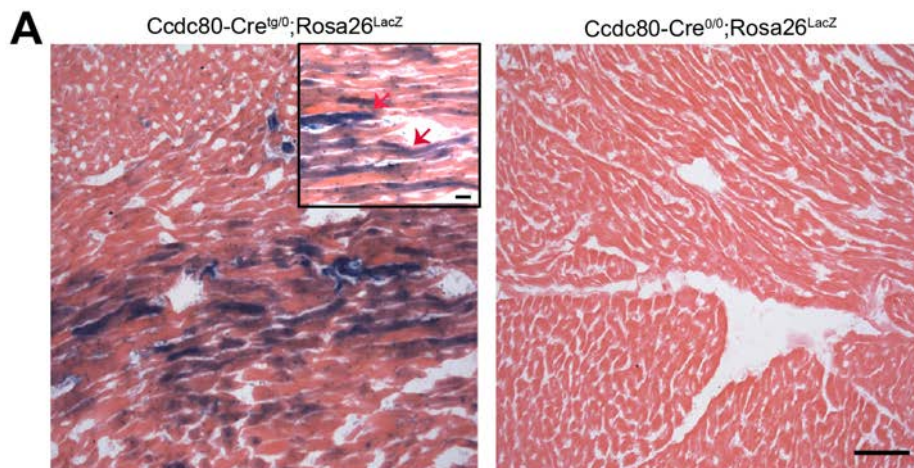


**Figure 4.9 Cre recombination in *Ccdc80-Cre<sup>tg/0</sup>; Rosa26<sup>LacZ</sup>* bitransgenic mice. (A)** Representative image of  $\beta$ -Gal staining in a transverse section from an adult mouse heart *Ccdc80-Cre<sup>tg/0</sup>; Rosa26<sup>LacZ</sup>* and its littermate control (*Ccdc80-Cre<sup>0/0</sup>; Rosa26<sup>LacZ</sup>*) obtained after crossing *Ccdc80-Cre<sup>tg/0</sup>* and *Rosa26<sup>LacZ</sup>* mice. The tissue was counterstained with eosin (red) for contrast. *Ccdc80-Cre* expression was observed in cardiomyocytes in the myocardium (as shown by an arrow) based on anatomical and morphological characterization. Scale bar represents 50 $\mu$ m.

However, unexpectedly, the  $\beta$ -gal staining was observed in the cardiomyocytes (blue cells) and not in the interstitial spaces in the heart as shown in Figure 4.9.

## 4.2 Characterization of VimCreERT2 transgenic mice expressing Cre recombinase in the heart

### 4.2.1 Vimentin promoter activity in heart tissue in comparison to Fsp1 promoter activity

Vimentin (the intermediate filament protein) has been extensively used to label fibroblast (in heart, all the CFs are positive) although they also label various other cell types including endothelial cells. In order to validate the vimentin promoter activity in the heart, a Vim-CreER BAC transgenic mouse line was provided by our collaborator Robert F. Schwabe, MD (Columbia University, New York). This mouse line has a CreERT2 cassette inserted in a BAC containing the mouse vimentin locus (Figure 4.10).

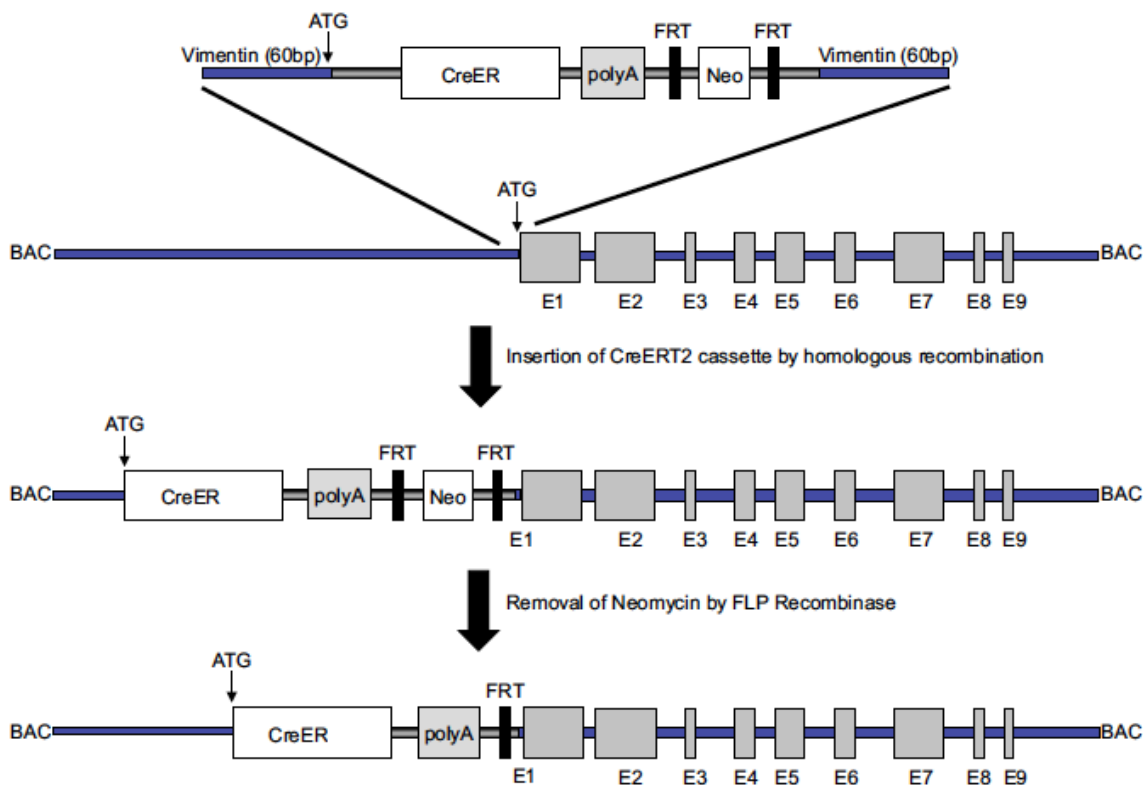
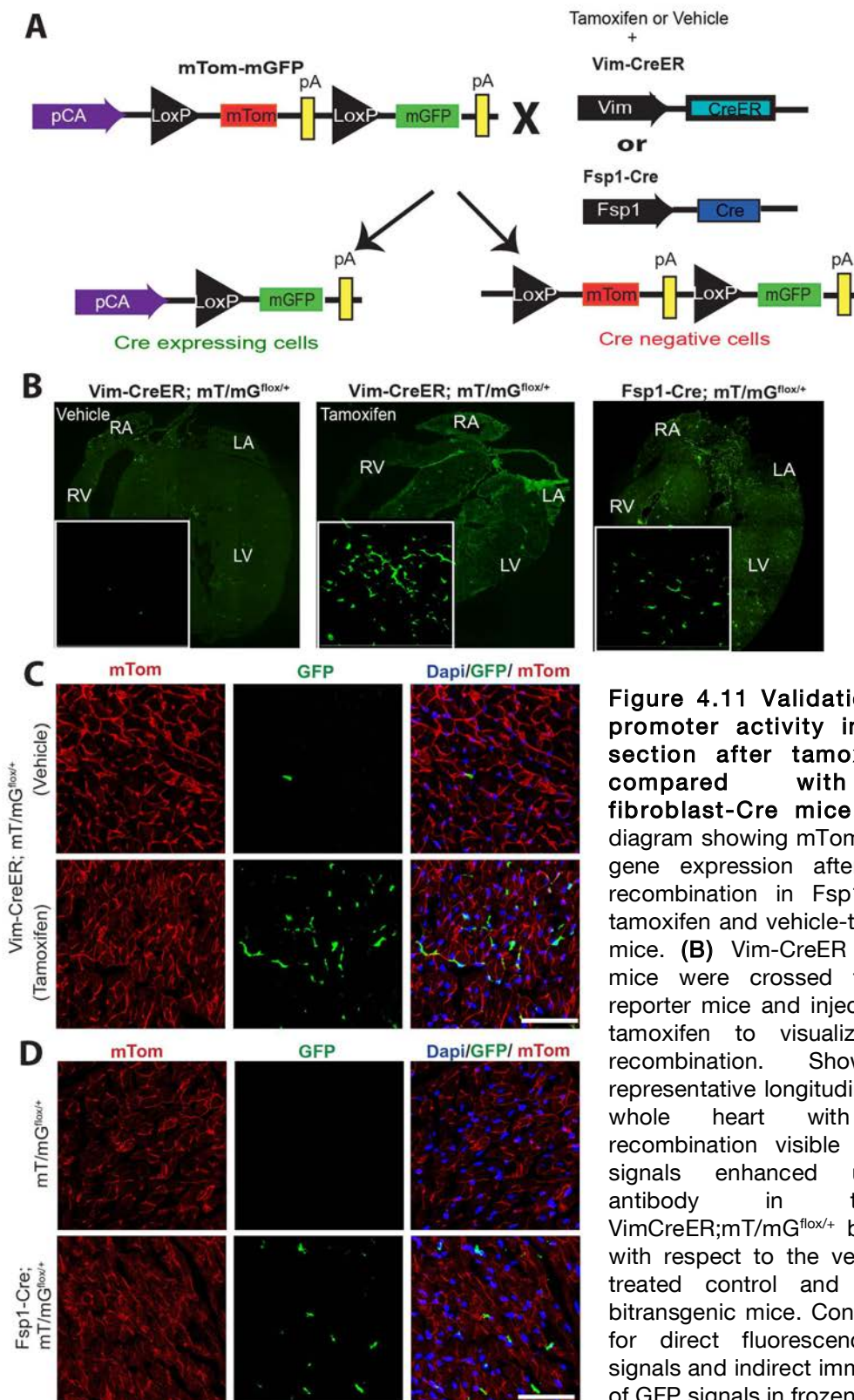


Figure 4.10 Shown is the construct for generation of VimCreERT2 transgenic mice by BAC recombination (Ref: Troeger JS *et al.* 2012) <sup>233</sup>.

Using the mTom-mGFP (mT/mG) dual fluorescent reporter mouse<sup>234</sup>, VimCreER marked cell population was analyzed in the heart with respect to known fibroblast promoter (Fsp1-Cre). The mT/mG reporter mouse has a consecutive expression of a membrane-targeted tdTomato (mTom) gene in cells without Cre activity and membrane-targeted EGFP (mGFP) expression in cells with Cre activity (Figure 4.11 A). For analyzing Cre-mediate



**Figure 4.11 Validation of Vimentin promoter activity in frozen heart section after tamoxifen injection compared with described fibroblast-Cre mice. (A)** Schematic diagram showing mTom -mGFP reporter gene expression after Cre mediated recombination in Fsp1-Cre mice and tamoxifen and vehicle-treated VimCreER mice. **(B)** Vim-CreER BAC transgenic mice were crossed to mTom-mGFP reporter mice and injected 6 times with tamoxifen to visualize Cre-mediated recombination. Shown are the representative longitudinal section of the whole heart with Cre-mediated recombination visible as green (GFP) signals enhanced using anti-GFP antibody in tamoxifen-treated VimCreER;mT/mG<sup>flox/+</sup> bitransgenic mice with respect to the vehicle (peanut oil) treated control and Fsp1Cre;mT/mG bitransgenic mice. Confocal microscopy for direct fluorescence of mtomato signals and indirect immunofluorescence of GFP signals in frozen heart sections of **(C)** tamoxifen-injected or vehicle-injected VimCreER; mT/mG<sup>flox/+</sup> mice & **(D)** Fsp1-cre;mT/mG<sup>flox/+</sup> mice with its littermate control mT/mG<sup>flox/+</sup> mice.

Scale bar = 100 $\mu$ m. The Vimentin marked cell population expresses GFP in the interstitial spaces of heart section and not in cardiomyocytes. Fsp1-Cre tagged cell also shows the GFP positive cells restricted to interstitial spaces, but the amount of cells expressing GFP was less as compared to tamoxifen induced VimCreER tagged cells.

recombination cryosections of heart tissue from 6-7 weeks old VimCreER;mT/mG bitransgenic mice were examined by immunofluorescence using the anti-GFP antibody. GFP-positive cells were observed in the interstitial spaces of frozen heart section after six-tamoxifen injection in VimCreER;mT/mG bitransgenic mice with respect to the vehicle (peanut oil) injected VimCreER;mT/mG mice (Figure 4.11 B&C). Due to non-availability of Fsp1 inducible Cre mouse line, Fsp1-Cre, the known fibroblast-Cre mouse line was used for comparison. Immunofluorescence staining in frozen heart section of Fsp1-Cre; mT/mG bitransgenic mice also show immuno-reactivity for GFP in interstitial spaces as compared to its littermate control (Figure 4.11 B&D). In spite of consecutive expression of Cre driven under Fsp1 promoter, the recombination observed in these bitransgenic mice were lower than tamoxifen-treated VimCreER;mT/mG bitransgenic mice (Figure 4.11 B&D) targeting around 20% of the interstitial cells in whole heart sections.

### 4.2.2 VimCreER marks non-myocytes in the heart.

In order to characterize VimCreER lineage- tagged cells, dual antibody immunofluorescent labeling was performed on frozen heart sections of tamoxifen or vehicle-injected VimCreER;mT/mG bitransgenic mice. For dual antibody immunofluorescent labeling different cell markers were used: P4HB and Vimentin (fibroblast marker), SM22a (smooth muscle cell marker) & CD31 (endothelial cell marker) along with GFP. As known from the literature, vimentin is found to be expressed by all fibroblasts and at a lower level by endothelial cell, we observed **the GFP-positive cells in tamoxifen-injected VimCreER;mT/mG bitransgenic mice co-stained with fibroblast markers (Figure 4.12 A) and this overlay was almost 80%**. We also observed some GFP-positive cells were co-stained with endothelial cell marker (CD31) (Figure 4.12 E), and most of them were seen lying in close proximity to CD31 positive cells. Several previous Immunofluorescence studies have demonstrated endogenous vimentin expression in blood vessels of human<sup>220, 222</sup> and of rabbit<sup>221</sup>. Consistently, the data presented indicate **an overlay between GFP-positive cells and smooth muscle cell marker in the blood vessels of tamoxifen-injected VimCreER;mT/mG mice (Fig 4.12 C)**. In comparison to tamoxifen-injected VimCreER;mT/mG mice and its littermate control mT/mG<sup>flox/+</sup> mice, the GFP positive cells in Fsp1-Cre;mT/mG mice were co-stained with fibroblast marker (Fig 4.12 B) and with endothelial cell marker but not with smooth muscle

cell markers (Fig 4.12 D, F).

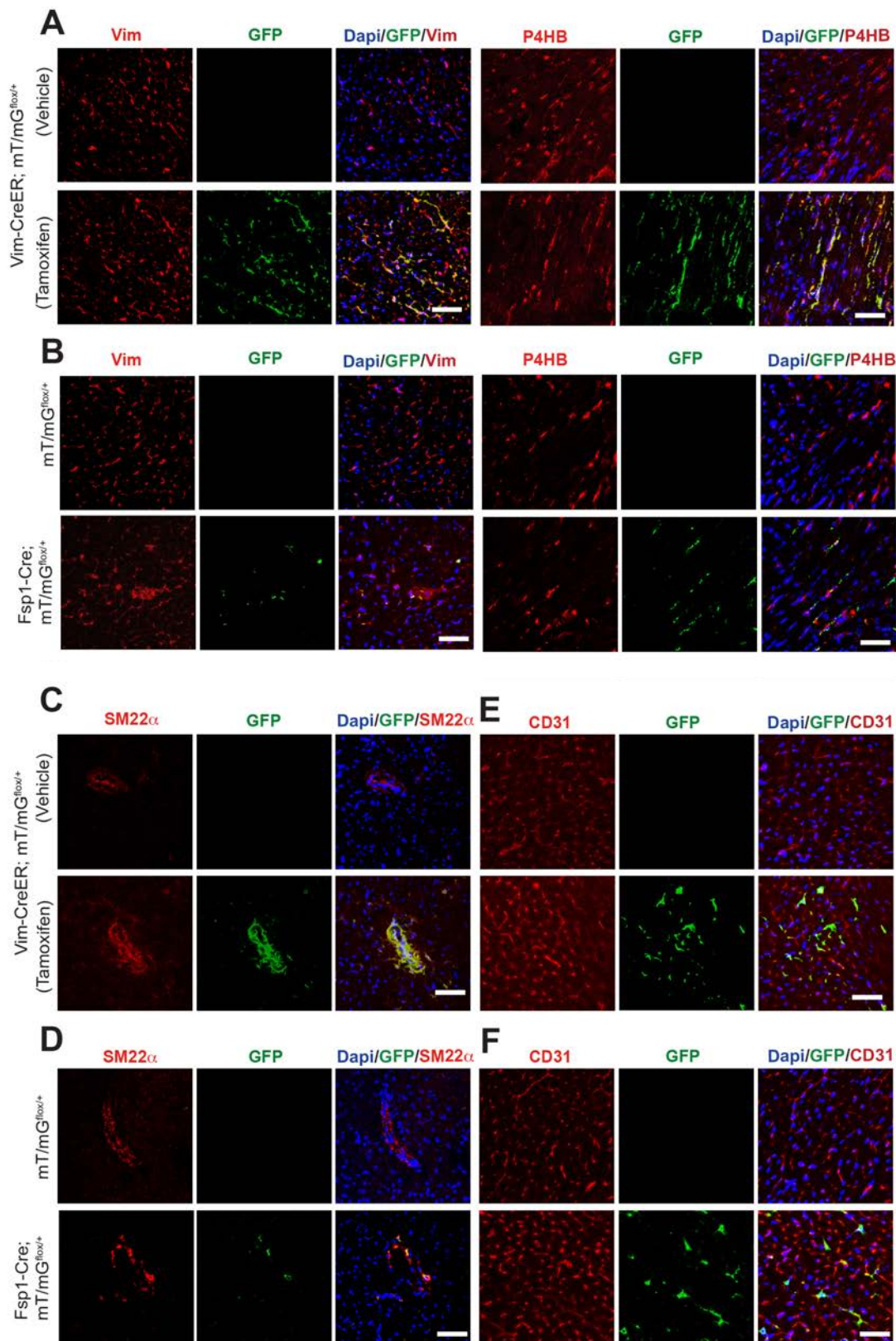


**Figure 4.12 Characterization of VimCreER lineage-tagged cells in heart sections by immunofluorescence.** Confocal microscopy of frozen heart section of tamoxifen or vehicle-injected VimCreER;mT/mG<sup>flox/+</sup> bitransgenic mice and Fsp1-Cre; mT/mG<sup>flox/+</sup> along with its littermate

control mT/mG<sup>fllox/+</sup> mice, co-stained for (A&B) Fibroblast marker (Vimentin & P4HB); (C&D) Smooth muscle marker (SM22 $\alpha$ ) & (E&F) Endothelial marker (CD31) along with anti-GFP antibody. Scale bar =50 $\mu$ m. VimCreER marked cells expressing GFP co-stains with fibroblast markers (Vim & P4HB), smooth muscle cell marker (in some big vessels as shown above), and not with endothelial cells (except for few cells). However, the Fsp1-Cre marked cells were co-stain with fibroblast markers and with endothelial cell marker but not with smooth muscle cell marker as compared to its littermate control mT/mG<sup>fllox/+</sup> mice.

### 4.2.3 Cardiac fibroblast specific Cre recombination in VimCreER bitransgenic mice

In order to verify that vimentin promoter has indeed a CF-specific expression, CFs and CM were isolated from tamoxifen-injected VimCreER;mT/mG and Fsp1-cre;mT/mG bitransgenic mice.

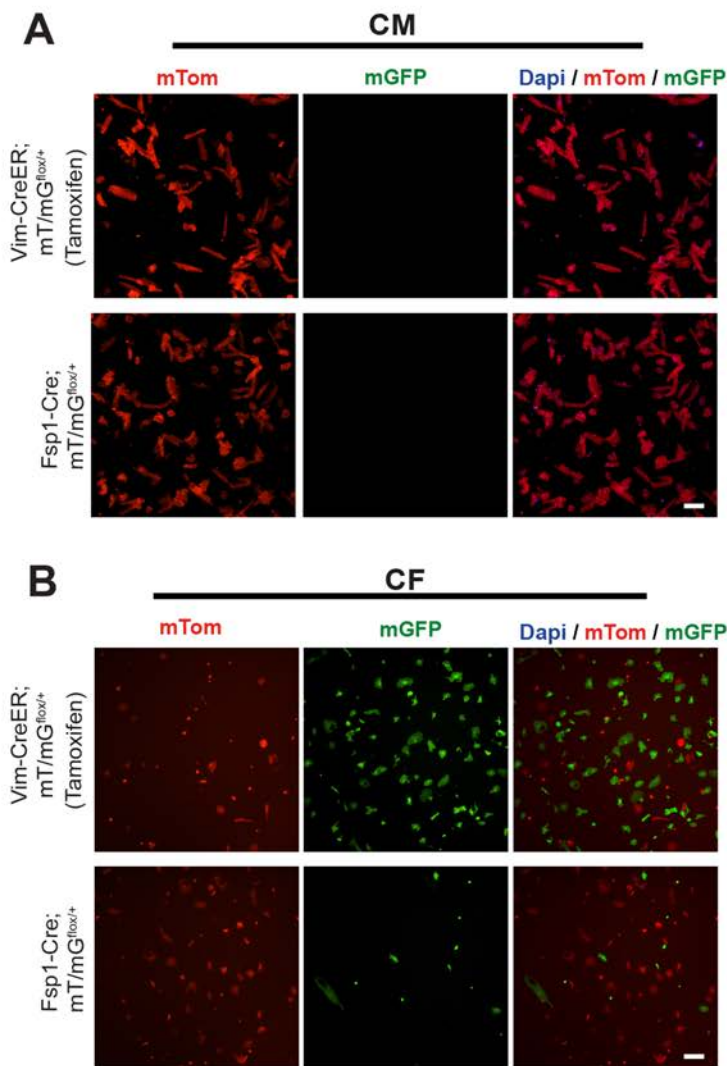


**Figure 4.13 Cell-specific expression of Vimentin promoter compared to described fibroblast promoter.**

(A) mTomato and mGFP signals detected in isolated and 32hrs cultured cardiac fibroblast (CF) and cardiomyocyte (CM) from the two bitransgenic mice. Images captured using a fluorescent microscope. Magnification 20X; Scale bar =50 $\mu$ m. Vimentin promoter activity is specifically in CF and not in CM isolated from tamoxifen-treated VimCreER;mT/mG mice with respect to vehicle-treated mice. Only a few CF appeared green in case of Fsp1-cre;mT/mG that accounts for weak Fsp1 promoter activity.

Cre-mediated recombination was observed by direct fluorescence for mGFP signals. The majority of cultured CFs (32hrs cultured) from tamoxifen-injected VimCreER;mT/mG



bitransgenic mice had mGFP signals as compared to Fsp1-cre;mT/mG bitransgenic mice, where only a few cells had mGFP signals (Fig 4.13 A). This observation was similar to whole heart tissue. In contrast, in the CM, isolated from both bitransgenic animals had only mTomato fluorescence. This demonstrated that **Cre-mediated recombination is restricted to CFs and not to CM in both the bitransgenic animals** (Fig 4.13 B).

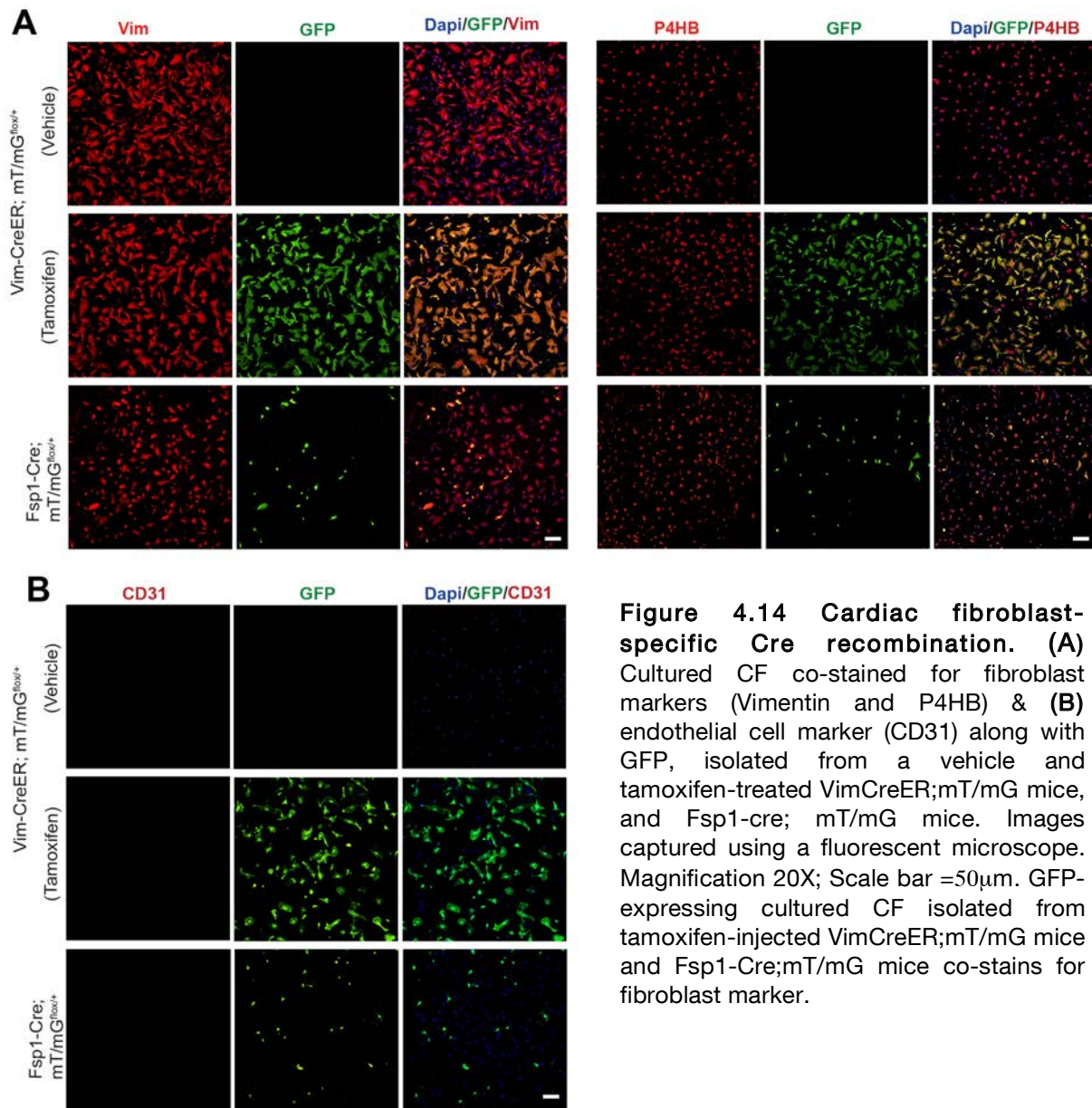


**Figure 4.14 Cardiac fibroblast-specific Cre recombination.** (A) Cultured CF co-stained for fibroblast markers (Vimentin and P4HB) & (B) endothelial cell marker (CD31) along with GFP, isolated from a vehicle and tamoxifen-treated VimCreER;mT/mG mice, and Fsp1-cre; mT/mG mice. Images captured using a fluorescent microscope. Magnification 20X; Scale bar =50µm. GFP-expressing cultured CF isolated from tamoxifen-injected VimCreER;mT/mG mice and Fsp1-Cre;mT/mG mice co-stains for fibroblast marker.

To further confirm that the GFP-expressing cultured CFs were fibroblast cells and not any other cell type, co-staining was performed for different cell markers along with anti-GFP antibody. **Cultured CFs positive for GFP were co-stained only with the fibroblast marker** (Vimentin and P4HB) (Figure 4.14 A) and not with endothelial cell

marker (Figure 4.14 B) or myocytes marker (data not shown). There was no mGFP fluorescence detected in cultured CFs, isolated from vehicle-treated control mice. This accounts for the tight regulation of vimentin promoter activity to drive tamoxifen inducible Cre expression in CFs. Also co-staining with fibroblast marker confirmed that the cultured CFs as fibroblast cells.

**Thus, concluding that presence of bright mGFP fluorescence restricted to cultured CFs signifies successful and specific vimentin promoter activity in driving Cre expression *in vivo*.**

#### **4.2.4 Vimentin promoter activity in the TAC model for chronic cardiac pressure overload**

TAC in the mouse is a commonly used experimental model of pressure overload-induced cardiac hypertrophy and fibrosis. In order to determine whether vimentin promoter has altered activity and specificity after cardiac injury, the endogenous level of Vimentin and Fsp1 genes under pathological cardiac hypertrophy were first analyzed. For this analysis, C57BL/6N mice were randomized for transverse aortic constriction (TAC) and sham surgery. Expressions of Vimentin (Vim) and Fsp1 genes were then quantified in CFs and CM isolated from C57BL/6N mice that were challenged with TAC for 6 weeks along with Sham-operated mice as the control (Figure 4.15 (A)). **Increased expression of vimentin and Fsp1 was observed in isolated CFs of C57BL/6N wild-type mice as compared to CM.** Moreover, this difference was significant for vimentin expression between CFs and CM isolated from TAC-operated mice. Though there was no significant difference observed in the expression of vimentin between CFs isolated from Sham and TAC operated mice. On the other hand, a difference in Fsp1 expression was significant between CFs from Sham and TAC operated mice Figure 4.15 (A). In addition, the expression of Fsp1 was more than Vimentin in CFs isolated from sham and TAC operated mice.

To further investigate the vimentin promoter activity in pressure overload myocardium, the 6-week-old VimCreER;mT/mG mice were first injected with vehicle (peanut oil) and tamoxifen (2mg /mouse /day dissolved in peanut oil) i.p. for 5 consecutive days and then subjected to thoracic aortic constriction (TAC; causing chronic pressure overload) or control surgery (sham) for 3 weeks. The animals were then sacrificed and hearts sections were used for immunofluorescence staining. Sham-operated mice hearts were treated as the control in each case. Confocal microscopy of immunostaining with the anti-GFP antibody on the heart sections showed an increased number of GFP-positive cells in the TAC-operated tamoxifen

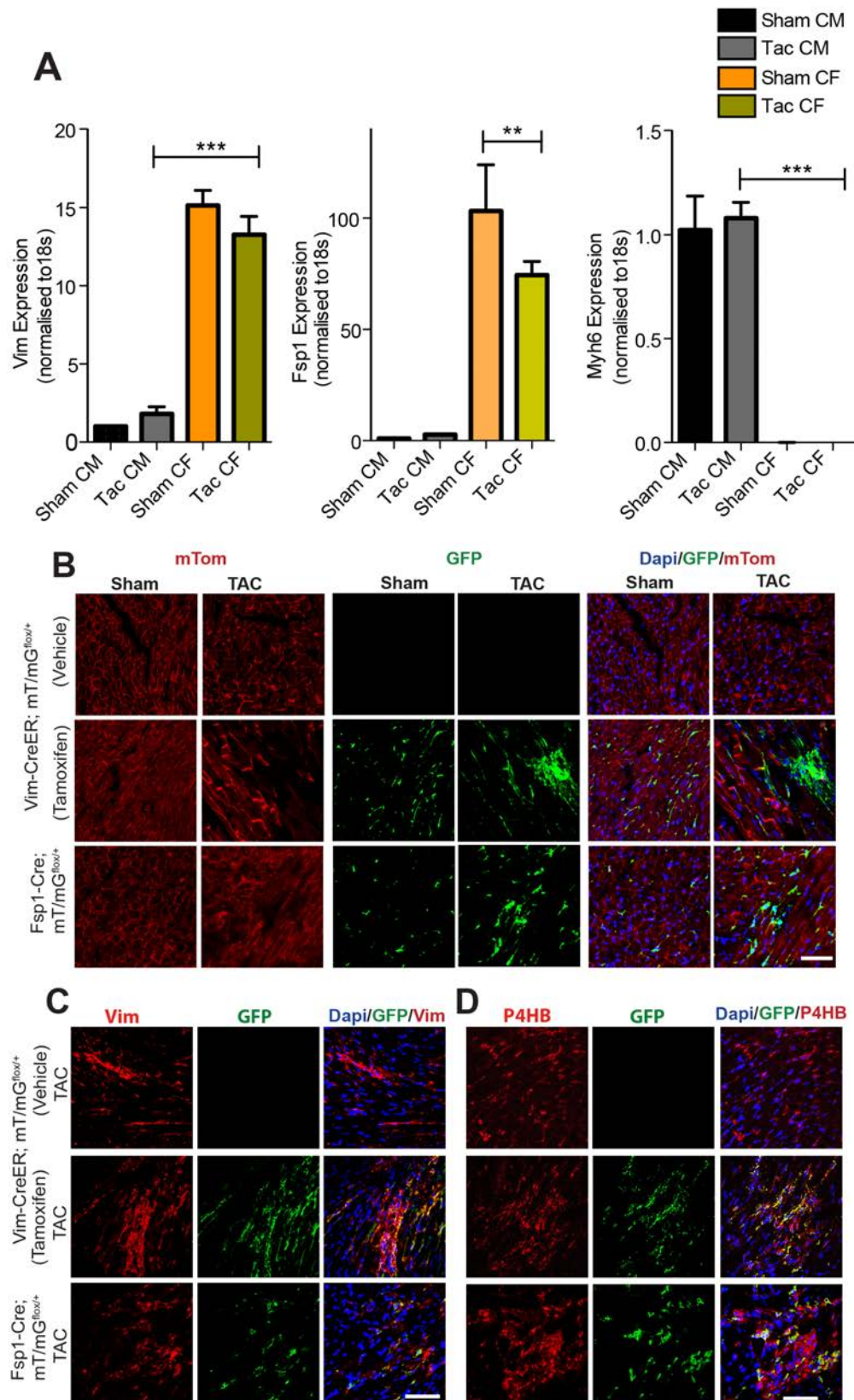


**Fig 4.15** Vimentin promoter activity in TAC-operated heart. Comparison with described fibroblast promoter (Fsp1). (A) Relative gene expression data of Vimentin and Fsp1 in isolated cardiac fibroblast (CF) and cardiomyocytes (CM) from C57BL/6N mice challenged with TAC for 6 weeks. Gene expression data of Myh6 and Sham-operated mice are taken as control for

analysis. Sham and TAC (n=3 each). All data were evaluated by 1-way ANOVA/ Bonferroni paired test. Statistical significance is shown as \*P<0.05, \*\*P<0.01, \*\*\*P<0.001. **(B)** Confocal microscopy of frozen heart sections for mTomato-mGFP signals after 3 weeks of TAC in the two bi-transgenic mice with respect to the vehicle-treated (Sham and TAC) control. **(C&D)** Confocal microscopy images of frozen heart section of TAC-operated bitransgenic mice with respect to TAC Vehicle-treated control mice co-stained with fibroblast marker (anti-Vimentin & anti-P4HB). Scale bar =50µm.

injected VimCreER;mT/mG bitransgenic mice with respect to the Sham & TAC-operated vehicle-injected VimCreER;mT/mG control mice (Figure 4.15 B). The TAC- operated Fsp1Cre: mT/mG mice also showed an increase in the number of GFP-positive cells compared to its sham control group. Although this increase was not as much as observed in the case of TAC-operated tamoxifen-injected VimCreER;mT/mG bitransgenic mice (Figure 4.15 B).

Fibroblasts in the injured heart are thought to have diverse origins. Recent studies on organs such as the kidney, lung and liver, heart and on metastatic tumors showed that during fibrosis, in addition to the proliferation of resident fibroblasts, bone marrow-derived fibroblasts, epithelial cells contribute to fibroblast accumulation through an epithelial-mesenchymal transition (EMT)<sup>55</sup>. Likewise, endothelial cells contribute to fibroblast via Endothelial-mesenchymal transition (EndMT)<sup>20</sup>, which is also a form of EMT as observed during formation of the atrioventricular cushion in an embryonic heart. To determine whether the GFP expression in the hearts of TAC-operated VimCreER;mT/mG mice was limited to fibroblasts, co-staining was performed on frozen hearts sections for fibroblast or endothelial cell markers along with anti- GFP antibody. **In comparison with TAC-operated Fsp1-Cre;mT/mG and TAC-operated vehicle control mice, a majority of the GFP-positive cells were identified as fibroblasts in TAC-operated, tamoxifen-injected VimCreER;mT/mG mice hearts (Figure 4.15 C&D). There was also no overlay observed with the endothelial cells marker (CD31) (Figure 4.16).** In contrast, in TAC-operated Fsp1-Cre;mT/mG mice, the GFP-positive cells showed a co-localization both with the fibroblast marker (Figure 4.15 D) and the endothelial cell marker (Figure 4.16).

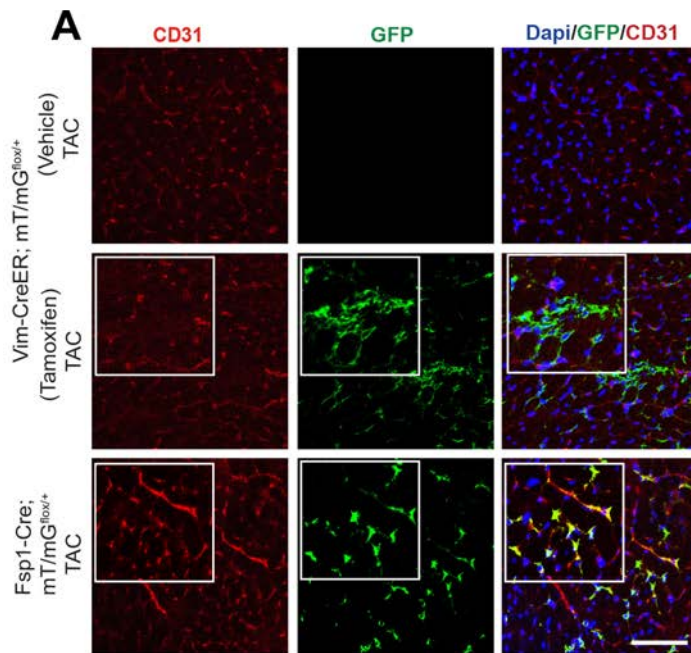


**Fig 4.16** Immunofluorescence staining for endothelial cell marker (CD31) along with GFP in frozen heart section of TAC-operated bi-transgenic mice. In comparison with TAC-operated Fsp1-Cre;mT/mG bitransgenic mice and vehicle-treated control mice, no overlay was observed between GFP-positive and CD31 positive cells in TAC-operated VimCreER;mT/mG bitransgenic mice. Scale bar =50 $\mu$ m.

Echocardiography was conducted to assess the cardiac phenotype in tamoxifen-injected Vim-CreER;mT/mG mice compared to vehicle-injected control mice post TAC (Figure 4.17 A). Change in the ratio of heart weight to body weight or heart weight to tibia length is one of the parameters for measuring cardiac hypertrophy in response to pressure overload. Here we observed an **insignificant change in the ratio of heart to body weight & heart weight to tibia length in Vim-CreER;mT/mG bitransgenic mice post TAC. Equally, we could not find any significant differences in contractility, as measured by the change in the ejection fraction (%) or fractional shortening (%)** (Figure 4.17B). Likewise, **in the case of Fsp1-cre;mT/mG mice post TAC no significant changes were observed in the heart to body weight & heart weight to tibia length compared to its littermate mT/mG<sup>fl/+</sup> control** (Figure 4.17 C). This could be because a lower number of both types of animals were used in this study. However, **an increase was noticed in HW/BW and HW/TL after TAC compared to Sham-operated mice, which account for cardiac hypertrophy induced in response to TAC in these mice. A significant difference in the percentage of fractional shortening and ejection fraction in TAC-operated Fsp1-Cre bitransgenic mice with respect to its TAC-operated control mice indicate a loss of function or failing condition in hearts of Fsp1Cre mice.** No change in the percentage of ejection fraction and fractional shortening was observed in TAC and Sham-operated mT/mG<sup>fl/+</sup> control mice. This indicates a delay in loss of function or occurrence of some compensation in these control animals.

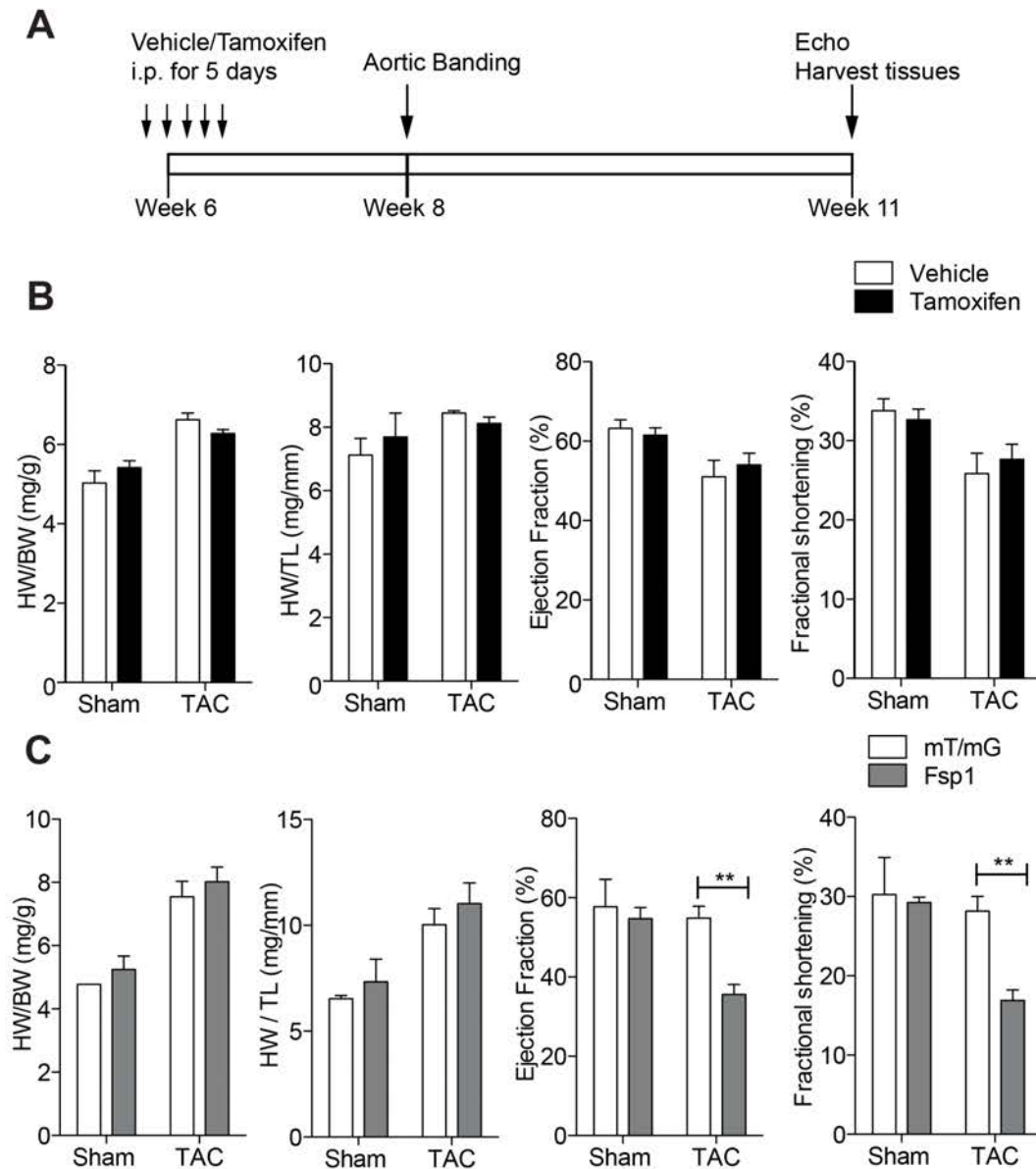


**Figure 4.17 Cardiac phenotyping in VimCreER mice post TAC.** (A) Experimental strategy for TAC study. The 6-week-old VimCreER;mT/mG mice were injected with vehicle (peanut oil) and tamoxifen (2mg /mouse /day dissolved in peanut oil) i.p. for 5 consecutive days and then subjected to thoracic aortic constriction (TAC; causing chronic pressure overload) or control surgery (sham). At week 11, echocardiographic measurements were taken, and animals were euthanized for further analysis (B) Ratio of the heart weight (HW) to body weight (BW) and heart weight (HW) to tibia length (TL) in vehicle-injected and tamoxifen-injected VimCreER;mT/mG mice post TAC. Sham and TAC n=3 each group. Ejection fraction (%) and left ventricular shortening fraction (fractional shortening (%)) as two parameters of the echocardiographic analysis post TAC. Sham (n=3) & TAC (n=5) each. (C) The ratio of HW to BW and HW to TL in Fsp1-cre: mT/mG and littermate control mice post TAC. Sham (n=3) & TAC (n=4-5) each. Left ventricular shortening fraction (fractional shortening (%)) and ejection fraction (%) calculation was done based on Sham (n=3) & TAC (n=4-5) mice. All data were evaluated by 2-way ANOVA/ Bonferroni posttest. Statistical significance is shown as \*P<0.05, \*\*P<0.01, \*\*\*P<0.001.

#### 4.2.5 Tamoxifen-independent recombination in the Vim-CreER mouse heart

In order to determine the tamoxifen-independent recombination, cryosections of heart tissue from 3- and 4-month-old vehicle-injected VimCreER;mT/mG bitransgenic mice were examined by immunofluorescence staining using the anti-GFP antibody. In principle, in a progeny containing both (VimCreER & mT/mG) transgenes, the mGFP expression in the cells should be detected only upon tamoxifen-induced removal of the floxed mTomato Stop cassette (Figure 4.18 A).

However, **positive reactivity for GFP was detected in heart tissues of some vehicle-injected mice** (Figure 4.18 B) similar to tamoxifen-injected VimCreER;mT/mG bitransgenic mice (Figure 4.18 A) demonstrating tamoxifen independent Cre recombination in these mice. While some vehicle-injected mice were negative for GFP (Figure 4.18 C). The specificity of this labeling was confirmed by the absence of immunoreactivity for GFP in heart sections of mT/mG<sup>fl/+</sup> reporter and BL/6N wild-type control mice (Figure 4.18 D, E).

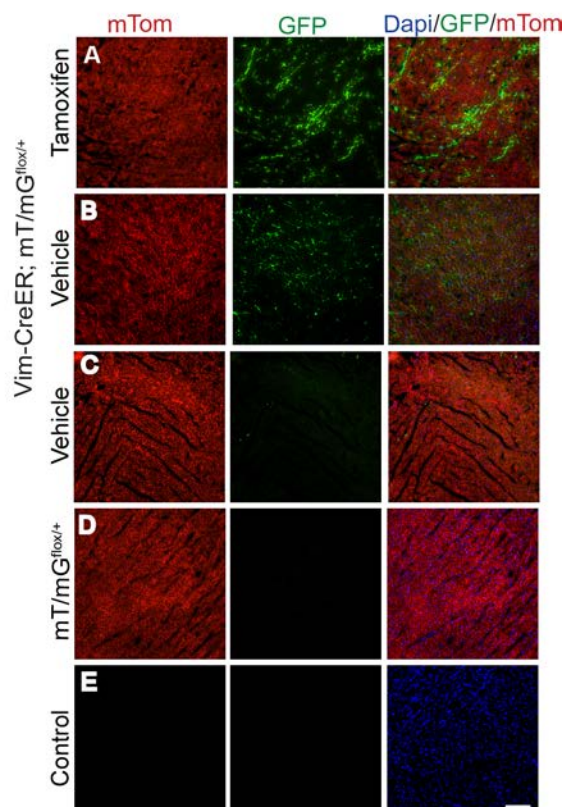


**Figure 4.18 Tamoxifen-independent Cre recombination in VimCreER;mT/mG bitransgenic mice.**

Immunofluorescence microscopy for GFP in frozen heart sections from 4-month-old (A) tamoxifen-injected, (B-C) vehicle-injected, (D) mT/mG<sup>fl/+</sup> & (E) BL/6N wild-type control mice. GFP fluorescence detected in frozen heart section of vehicle-injected mouse (B) compared to vehicle-injected mouse (C) demonstrates tamoxifen-independent recombination in these mice. A similar effect was observed in the case of an untreated mouse (D). The absence of GFP signals in mT/mG<sup>fl/+</sup> account for proper regulation of tamoxifen inducible Cre. Scale bar =50µm.

Additionally, other tissue sections from these vehicle-injected bitransgenic mice were also examined for tamoxifen independent recombination where except for lung, other tissue

sections had no mGFP fluorescence compared to tamoxifen-injected *VimCreER;mT/mG* mice and *mT/mG* reporter mice as control (Figure 4.19).

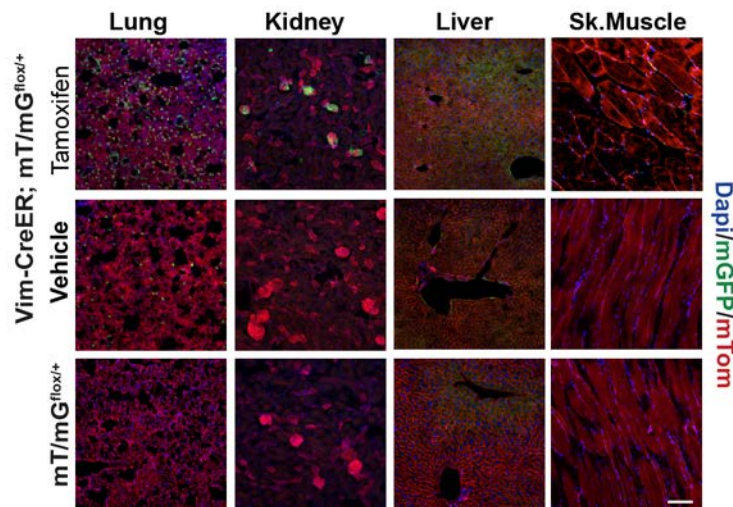


**Figure 4.19 Direct fluorescence for mTom-mGFP signals in different tissue sections of *VimCreER;mT/mG* mice.** Microscopy images of direct fluorescence of mGFP and mTom signals in fixed tissue sections from various organs after tamoxifen injection, vehicle injection in adult *VimCreER;mT/mG<sup>flox/+</sup>* mouse along with *mT/mG<sup>flox/+</sup>* reporter mouse. Tamoxifen injection in adult *VimCreER;mT/mG<sup>flox/+</sup>* mouse results in mosaic expression of mTom and mGFP in multiple tissue types while vehicle injection results in ubiquitous mTom expression in all tissues except for lung tissue section having tamoxifen independent mGFP expression. Fixed tissue sections of various organs from an adult *mT/mG<sup>flox/+</sup>* reporter mouse demonstrate ubiquitous mTom labeling as a control. Scale bar =50 $\mu$ m.

#### 4.2.6 Recombination in the heart of *VimCreER;mT/mG* mice during postnatal development

To further investigate feasibility of tamoxifen-inducible recombination during early and late postnatal development, and to elude the tamoxifen independent recombination in *VimCreER;mT/mG<sup>flox/+</sup>* bitransgenic mice, *VimCreER<sup>tg/0</sup>* males were crossed with *mT/mG<sup>flox/flox</sup>* females. Lactating mothers (*mT/mG<sup>flox/flox</sup>*) were then injected with tamoxifen (1mg/mouse/day) for five consecutive days starting at postnatal day 1 (P1; Figure 4.20 A).

It was predicted that the tamoxifen would be provided to the nurtured offspring through the milk. Intraperitoneal injections were well tolerated by lactating mothers and all their offspring were alive during the tamoxifen treatment. One-week (P7) old *VimCreER;mT/mG<sup>flox/+</sup>* and its littermate control (*mT/mG<sup>flox/+</sup>*) neonates were then analyzed for cell-specific expression of mGFP fluorescence and generalized expression of mTomato. As expected, **bright mGFP fluorescence was observed in the interstitial spaces in the myocardium of *VimCreER;mT/mG<sup>flox/+</sup>* neonates indicating successful Cre recombination.** While the littermate control neonates (*mT/mG<sup>flox/+</sup>*) have only mTomato fluorescence



in heart, indicating an absence of Cre recombination in these pups (Figure 4.20 B).

In conclusion, administration of tamoxifen to lactating mothers allows sufficient recombination during early postnatal development.

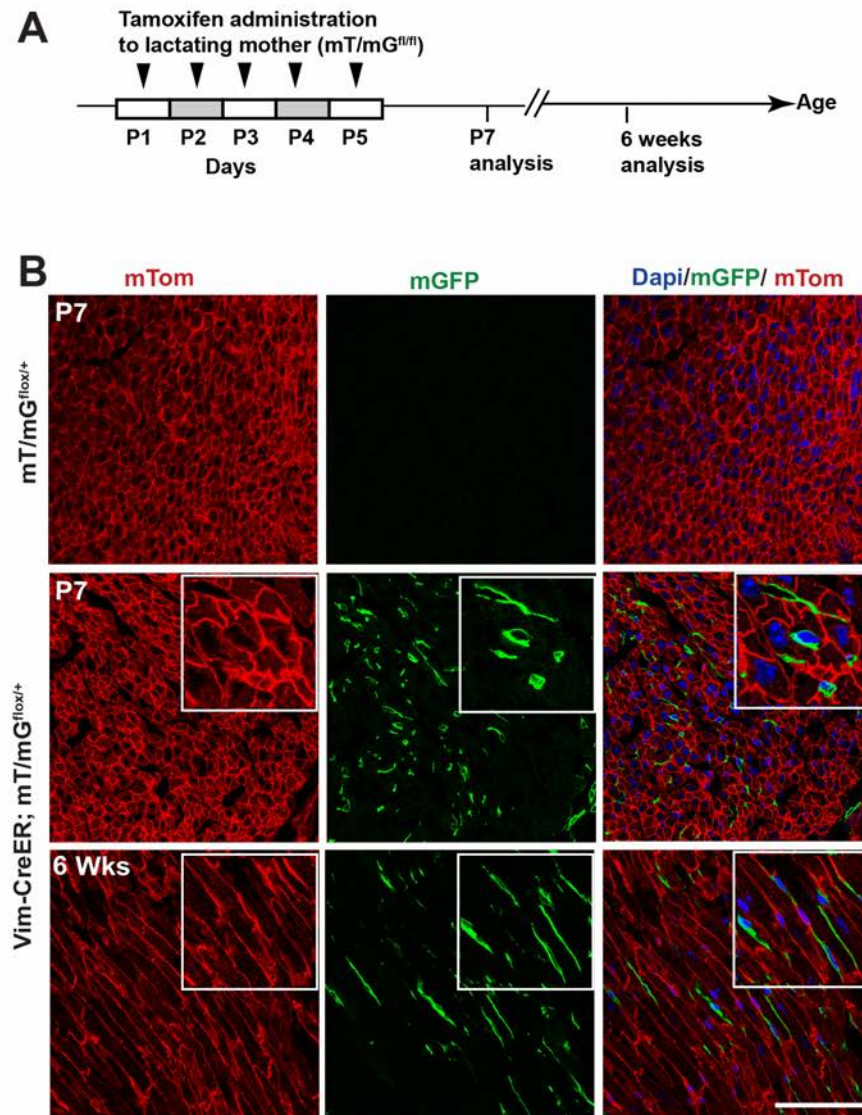


**Figure 4.20 Administration of tamoxifen (TM) to lactating mT/mG<sup>flox/flox</sup> mice leads to efficient recombination in the nourished pups. (A)** Scheme of administration protocol and subsequent analysis. Lactating mothers (mT/mG<sup>flox/flox</sup>) were injected with 1 mg of TM daily for 5 consecutive days starting on the day of birth of the litter. VimCreER;mT/mG<sup>flox/+</sup> bi-transgenic litters were analyzed at the age of postnatal day 7 and at 6 weeks for expression of mGFP. **(B)** Confocal Images of direct fluorescence of mGFP signals along with mTom in the frozen heart sections at 7-day-old neonate and 6 weeks old VimCreER;mT/mG<sup>flox/+</sup> mice along with their littermate control. Scale bar =100μm.

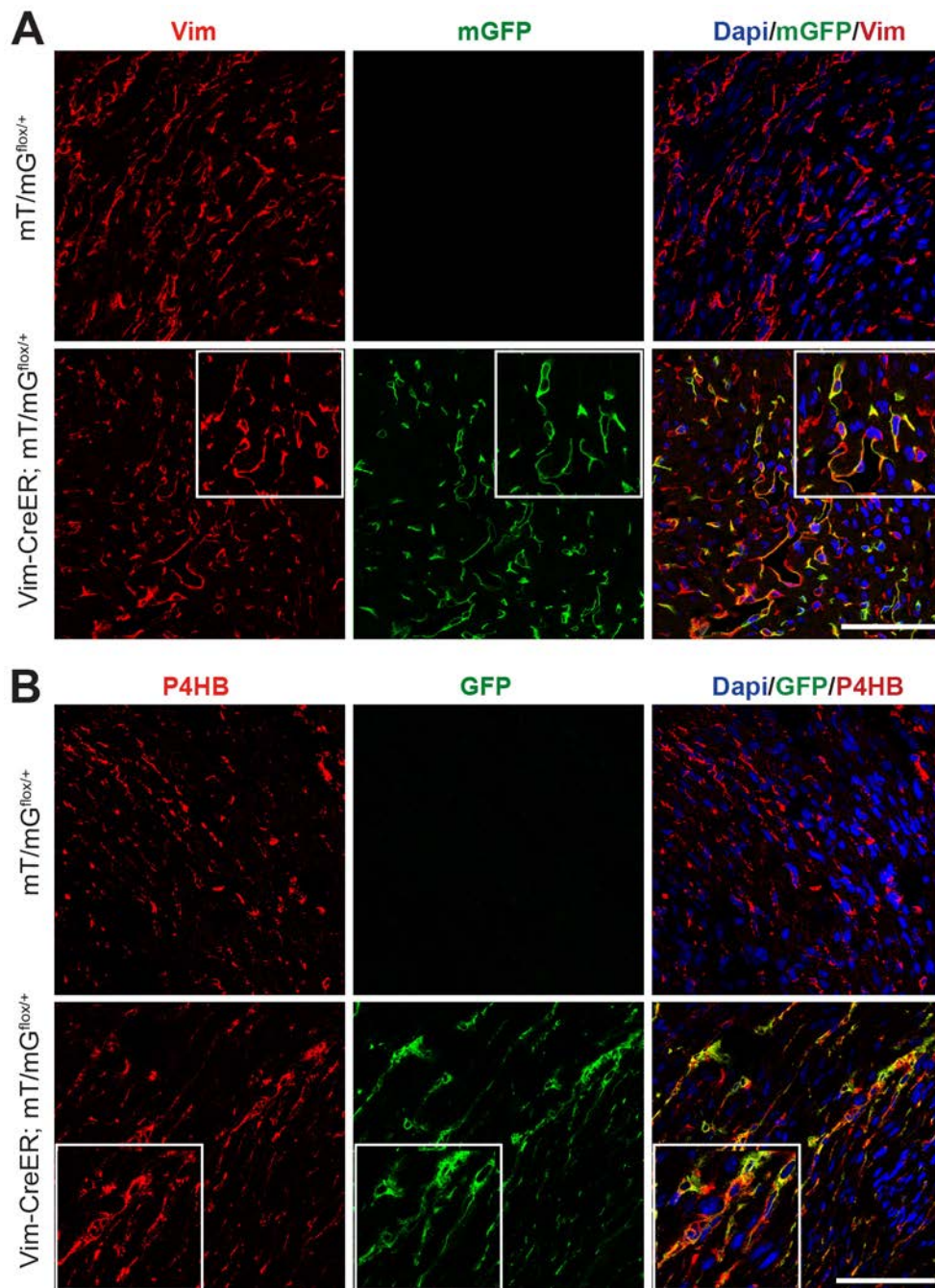


**Figure 4.21 Immunofluorescence for fibroblast cell markers at postnatal day 7 (P7).** (A) Confocal images showing colocalization of membrane tagged GFP (mGFP) expressing cells with vimentin & (B) P4HB in the frozen heart sections of seven-day-old VimCreER; mT/mG<sup>flox/+</sup> neonates along with their mT/mG<sup>flox/+</sup> littermate control. Scale bar =100 $\mu$ m.

As reported in previous studies, vimentin is found to expressed from embryonic day E7.5 onwards (Scherholz *et al.* (2013))<sup>171</sup> and shown to localize in interstitial spaces in later stages of heart development (Bennett *et al.* (1979)<sup>223</sup>; Gard and Lazarides, (1980); Speiser *et al.* (1992), Kim *et al.* (1996)<sup>169</sup>). We hypothesized that activating vimentin promoter at an

early stage will have mGFP expression restricted to fibroblasts in the heart. Immunostaining on frozen heart sections of neonates (P7) for fibroblast marker was performed. Colocalization of the GFP positive cells with fibroblast cell markers (Vimentin and P4HB) confirmed that the recombination occurred in fibroblast cells (Figure 4.21 A&B).

Consistent with previous studies demonstrating expression of vimentin in smooth muscle cells of blood vessels, mGFP-expressing cells around the vessels were observed in 7-day-old pups during the study. However, reduced number of the mGFP-expressing cells was observed in the heart sections of 6-weeks old animals (Figure 4.22).

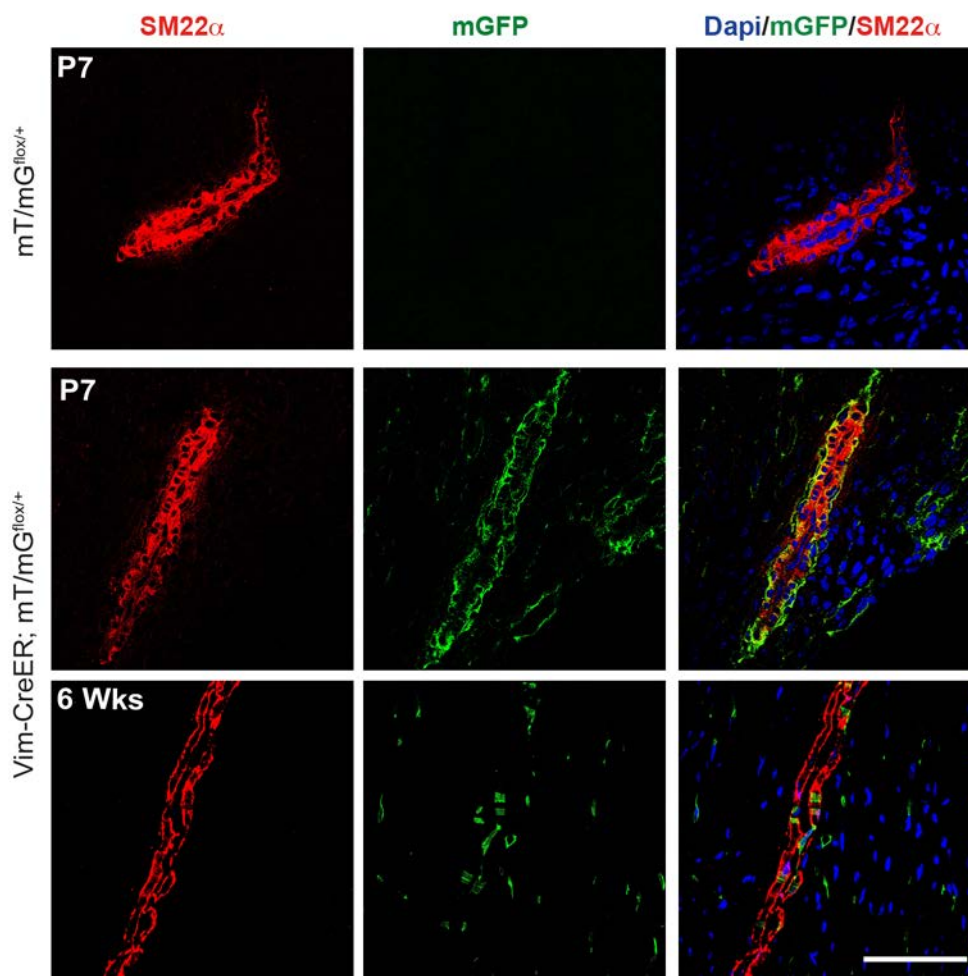


**Figure 4.22 Immunofluorescence staining for vascular smooth muscle cell marker in postnatal day 7 and 6 weeks old hearts.** Confocal images showing co-localization of membrane tagged GFP (mGFP) expressing cells with SM22 $\alpha$  antibody in frozen heart section of postnatal day 7 (P7) & of 6-week-old VimCreER;mT/mG<sup>flox/+</sup> bitransgenic animals along with their mT/mG<sup>flox/+</sup> littermate control. Scale bar =100 $\mu$ m

It has been shown through in situ hybridization that SM22  $\alpha$  transcripts were first expressed at about embryonic day (E) 9.5 in vascular smooth muscle cells and thereafter continued to

express in all smooth muscle cells in adulthood<sup>224</sup>. In contrast to its smooth muscle specificity in adult tissues, SM22  $\alpha$  was expressed transiently in the heart between E8.0 and E12.5 and in skeletal muscle cells in the myotomal compartment of the somites between E9.5 and E12.5. The expression of SM22  $\alpha$  in smooth muscle cells, as well as early cardiac and skeletal muscle cells, suggests that there may be commonalities between the regulatory programs that direct muscle-specific gene expression in these three myogenic cell types. Further analysis of GFP-expressing cells near the vessel is done by staining for smooth muscle cell marker (SM22 $\alpha$ ). An overlay between mGFP-expressing cell and SM22 $\alpha$  around the vessels in 7-day old pups was observed but in 6-weeks old VimCreER;mT/mG animal the number of cells was very low. This suggests that, in later stages of development, the vimentin promoter is mainly active in fibroblasts and to significantly lower extent in smooth muscle cells.

To test for vimentin promoter activity in endothelial cells, immunostainings with an antibody against the surface marker CD31 was carried out. This analysis revealed colocalization of mGFP-expressing cells (around 80%) with CD31 not only in 7-day-old pups (P7) but also in the later stage in 6 weeks old adult VimCreER;mT/mG bitransgenic mice hearts (Figure 4.23 A&B). This indicates that the recombination had also occurred in the endothelial cells along with fibroblasts during development, and somehow the vimentin promoter activity was not restricted to cardiac fibroblasts in the heart when induced in an early stage as observed in the case of adult recombination.

**In conclusion, insubstantial recombination occurred in the cardiac fibroblasts of VimCreER;mT/mG offspring from tamoxifen-injected lactating mothers during early and postnatal development.**

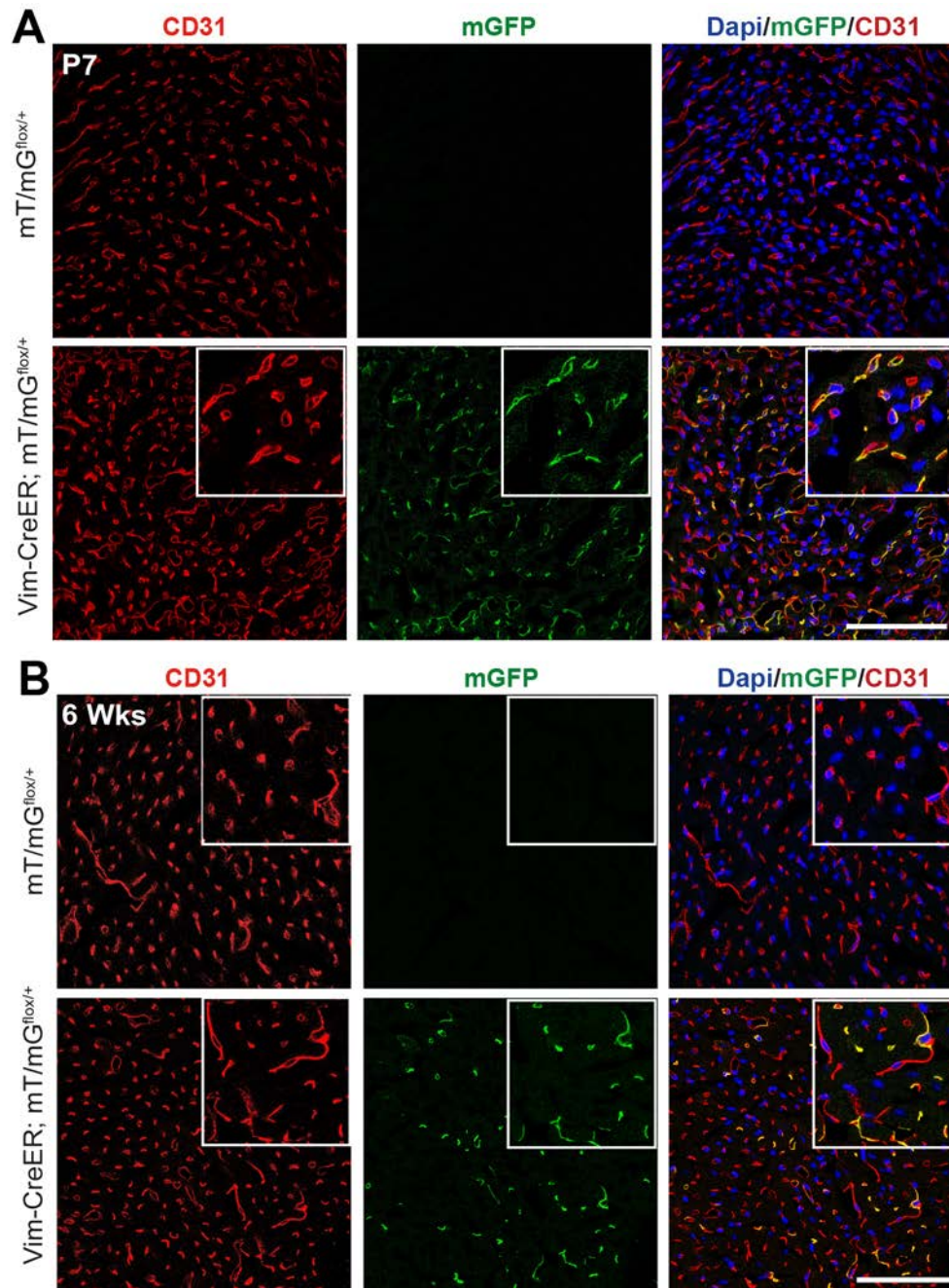


**Figure 4.23 Cre mediated recombination in endothelial cells in postnatal day 7 and 6 weeks old hearts.** Confocal images showing co-localization of membrane tagged GFP (mGFP) expressing cells with CD31 antibody in frozen heart section (A) of postnatal day 7 (P7) & (B) of 6-week-old VimCreER;mT/mG<sup>flx/+</sup> bitransgenic animals along with their mT/mG<sup>flx/+</sup> littermate control. Scalebar =100μm.

## 5 DISCUSSION

### 5.1 Screening for cardiac fibroblast specific genes

A primary goal of this project was to search for and to characterize gene promoters that are specifically active in cardiac fibroblasts (CFs). CFs represent one of the largest cell population in the heart, are a key source of components of the extracellular matrix (ECM) that regulates the structure of the heart and hence mechanical, chemical and electrical signals between the cellular and non-cellular components. More recently their active involvement in both normal cardiovascular biology and many other aspects of cardiac pathophysiology besides fibrosis have been recognized. Though cardiac fibroblasts play a critical role in the maintenance of normal cardiac function in the heart, the analysis of cardiac fibroblasts in heart tissue has been hampered by the absence of a fibroblast-specific surface marker.

Several fibroblast-specific transgenic lines, although not organ specific, have been established that express Cre and are driven by a Postn promoter (Postn-Cre mice)<sup>48,67</sup>, a S100a4 [Fibroblast Specific Protein 1 (Fsp1)] promoter<sup>67, 70</sup>, and Transcription Factor 21 [Tcf21, also known as Podocyte-Expressed 1 (Pod1) combination, or a Capsulin or Class A Basic Helix-Loop-Helix 23 (bHLHa23)] promoter, have been reported<sup>71</sup> but none of them seems to be specific for cardiac fibroblasts. Here we studied in two parts the promoters of candidate genes with potential specificity for cardiac fibroblasts, both *in vitro* and *in vivo*.

**The first part was based on microarray database screening** approach where we found out some cardiac specific genes based on their enrichment in heart and specifically in CFs in comparison with other tissue and CM. In this screening, we found Ccdc80 as a potential candidate for the study and also included Periostin, which has been used as a marker of activated fibroblasts in the remodeling myocardium<sup>66,76</sup>. Periostin, an extracellular matrix protein is highly expressed in embryonic myocardium<sup>73</sup> and is absent from cells of cardiomyocyte lineage, but is localized in cardiac mesenchymal cells<sup>65,72,74</sup>. In this study we demonstrated enrichment of an adipocyte-secreted protein Ccdc80 (also known as Cl2, DRO1, equarin, Ssg1, and Urb) in heart tissue as compared to other mice tissues that goes well with previous findings in literature about distribution or expression of Ccdc80 in heart tissue in mice, rat and human<sup>225, 226</sup>. Consistent with previous findings where periostin (Postn), have been found to be expressed, both at the mRNA and protein level by majority of normal adult tissues, including the aorta, stomach, lower gastrointestinal tract, placenta, uterus, adrenal glands, lung, thyroid, stomach, colon, ovary, testis and prostate and

breast<sup>227, 228</sup>. We also found periostin to be expressed more in the lung than in mouse heart tissue when quantified using qPCR.

## **5.2 Ccdc80 promoter activity in cardiomyocytes *in vivo***

In last ten years, there are only a few studies published on Ccdc80 function. Ccdc80 (also known as Cl2, DRO1, equarin, Ssg1, and Urb) was initially identified as an estrogen-induced gene in rat uterus and mammary gland<sup>229</sup>. It is expressed in a number of tissues in both the embryo and adult<sup>229, 230, 231</sup>. It is a novel adipocyte-secreted protein<sup>237, 225, 230</sup> and revealed to be abundantly expressed in adipose tissues<sup>231</sup>. Ccdc80 is deregulated in obesity<sup>236</sup> thereby, regulating adipogenesis through the down-regulation of Wnt/b-catenin signaling and induction of C/EBP $\alpha$  and PPAR $\gamma$ <sup>237</sup>. It is down-regulated in thyroid, ovarian, pancreatic, colon cancer cell lines and tumors<sup>236</sup>. Overexpression of Ccdc80 in colorectal and pancreatic cancer cell lines inhibits malignant growth and suppresses anchorage-independent growth<sup>232</sup>, suggesting that Ccdc80 may be a tumor-suppressor. In addition, Ccdc80 is also expressed in dermal papilla cells<sup>234</sup>, in bone marrow stromal cells<sup>235</sup> and in eye formation<sup>230</sup>. During mouse development, Ccdc80 RNA is barely detectable in 9dpc embryos. Though, in later stages, its expression is increased. The temporal and spatial expression pattern of Ccdc80 suggests its role in mouse skeletogenesis<sup>225</sup>. Ccdc80 has also been proposed to be a component of the extracellular matrix owing to its ability to bind various extracellular matrix proteins and promote cell adhesion<sup>238</sup>. A recent study showed Ccdc80 knockout (KO) mouse are hyperglycemic and glucose intolerant and display impaired insulin secretion *in vivo* when fed a HF diet thereby suggesting Ccdc80 as a novel modulator of glucose and energy homeostasis in mice<sup>226</sup>.

Since there is no literature published so far reporting, the function of Ccdc80 in the heart tissue, we are the first one to study the expression of Ccdc80 in the two major cell types (isolated CFs and CM) in the heart. Here we found the expression of Ccdc80 was significantly enriched in isolated CFs as compared to isolated CM, in both neonatal rat and adult mouse hearts. This also confirms our microarray expression data. Most of the cardiac diseases are coupled with fibrosis in the heart. In general, Fibrosis is a scarring process, which is characterized by fibroblast accumulation and accumulation of extracellular matrix (ECM) proteins that lead to distorted organ framework and function<sup>137</sup>. Ccdc80 has also been reported to be a component of the extracellular matrix owing to its ability to bind various extracellular matrix proteins, and promote cell adhesion<sup>238</sup>. An up-regulation of Ccdc80 gene expression in failing heart with respect to the healthy heart and also in

isolated CF indicates that *Ccdc80* gene is expressed by cardiac fibroblast in the heart in both normal and diseased conditions.

*In vitro* validation of *Ccdc80* promoter sequence upstream (approx. 4.2kb) by  $\beta$ -gal staining or by Cre recombination suggested that the promoter sequence amplified was efficient enough to drive the expression of Cre in transfected fibroblast cell line (NIH-3T3 cells). On the other hand, *in vivo* validation of *Ccdc80*-Cre transgenic mice upon crossing with *Rosa26<sup>LacZ</sup>* reporter mice demonstrated Cre recombination under *Ccdc80* promoter in cardiomyocytes and not in cardiac fibroblast of heart tissues. However, the promoter activity was active only in a small population of CM in the heart where only 20% of CM appeared blue after  $\beta$ -gal staining (Figure 4.9). We also found a strong and stable *Ccdc80* promoter activity in other organs like Lung, kidney, and liver of *Ccdc80*-Cre<sup>tg/0</sup>;*Rosa26<sup>LacZ</sup>* double transgenic mice (data not shown). To our understanding the reason for such a different activity of *Ccdc80* promoter in heart targeting CM *in vivo* can be because of the pronucleus microinjection technique used for generation of transgenic mice which is an old method and also include frequent random integration of multiple copies of a transgene that can results in silencing of our transgene, probably because of a positional effect and/or repeat-induced gene silencing. Another reason can be the promoter sequence, maybe it would have been better to use a BAC construct having all the important regulatory elements that are required to recapitulate endogenous *Ccdc80* gene expression.

### 5.3 Vimentin promoter activity in non-myocyte cells in heart tissue

The second part of this study characterized *VimCreERT2* transgenic mice as a candidate CF-specific Cre-expressing mouse line in comparison with *Fsp1*-Cre mouse line, which has been reported as a CF-specific line. Current analyzes of the origins of CF lineages during development and in disease have been established without the use of specific markers or systematic quantitative analysis of fibroblast lineages present in the heart. Markers used to identify fibroblasts, such as fibroblast specific protein 1 (*Fsp1*), not only marks only a subset of fibroblasts but, is also expressed by several other cell types, including endothelial and immune cells<sup>20,76, 188,152</sup>. Nowadays, vimentin has been extensively used to label cardiac fibroblasts in the heart. It is a major structural component of intermediate filaments (IFs) in many cell types and plays an important role in vital mechanical and biological functions in cells such as cell contractility, migration, stiffening, and proliferation. It is shown that the primary fibroblast derived from a vimentin-deficient mouse embryo compared with those from wild-type mouse embryo exhibit decreased motility, chemotactic migration, and



delayed wound healing<sup>165</sup>. More studies on Vimentin-deficient (Vim<sup>-/-</sup>) mice have revealed that loss of vimentin leads to failures in vascular adaptation resulting in pathological conditions, such as reduction of renal mass<sup>163</sup>, malformation of glia cells<sup>164</sup>, reduced resistance of arteries to shear stress<sup>166</sup>, and disturbance of leukocytes homing to lymph nodes<sup>167</sup>. During the past 2 decades, advances in the use of site-specific recombinase have added greatly to our ability to manipulate cells and gene expression. These site-specific recombinases bind to and recombine specific sequences of DNA, allowing researchers to hereditarily label cells, conditionally inactivate or activate genes, and even ablate cells based on their gene expression. Further use of dual-fluorescent reporter system that permits direct live visualization of both recombined and non-recombined cells at single cell resolution, offers an internal control for phenotypic analysis of Cre-induced mosaic mutants. Thereby, also providing a second marker for lineage tracing applications. **Here by using tamoxifen-inducible Cre system and dual fluorescent reporter mice (mTomato-mGFP), we have demonstrated through Cre recombination the vimentin promoter activity in heart tissue of the VimCreER:mT/mG bitransgenic mice. Immunofluorescence staining for recombined cells (i.e. GFP positive cells) in tamoxifen-injected VimCreER;mT/mG bitransgenic mice heart tissues showed the vimentin promoter activity restricted to cardiac interstitium, targeting nearly 80% of cells of interstitial spaces (Figure 4.11). Co-labeling with GFP and two fibroblast cell markers identified the majority of GFP-positive cells as fibroblasts (Figure 4.12).**

A number of studies have reported an expression of vimentin within endothelial cells, but to a lower extent<sup>135, 239</sup>. Here we also found very few VimCreER marked cells (GFP positive cells) positive for endothelial cell markers (CD31) in VimCreER:mT/mG bitransgenic mice heart sections following co-staining. In our observations, the majority of GFP-positive cells were lying in close proximity to CD31 positive cells suggesting that the vimentin promoter is active only in a very small population of endothelial cells in VimCreER:mT/mG bitransgenic mice.

The smooth muscle cell is the most abundant cell type in the blood vessel walls. It occurs in all vessels except capillaries and pericytic venules. Vascular SMCs have been divided into (at least) two distinct states of differentiation, usually referred to as synthetic and contractile phenotypes<sup>240, 241</sup>, the latter being predominant in the blood vessels of adult organisms. Previous studies show vimentin and desmin, as major constituents of the network in the smooth muscle cells and tissues. Vimentin insufficiency impairs contractile ability of various smooth muscle preparations, implying their important role for smooth muscle force

development<sup>242</sup>. Vascular smooth muscle cells mainly express vimentin that is widely distributed in various blood vessels ranging from the elastic arteries to micro arteries. Immunofluorescence studies demonstrate the presence of vimentin on vascular smooth muscle cells of blood vessels in different organs and species<sup>220-222</sup>. Consistent with immunofluorescence studies, we also found an overlay between VimCreER marked cells (GFP+) and smooth muscle cell marker (SM22 $\alpha$ ) in the myocardial arteries and the vessels of VimCreER:mT/mG bitransgenic mice hearts (Figure 4.12).

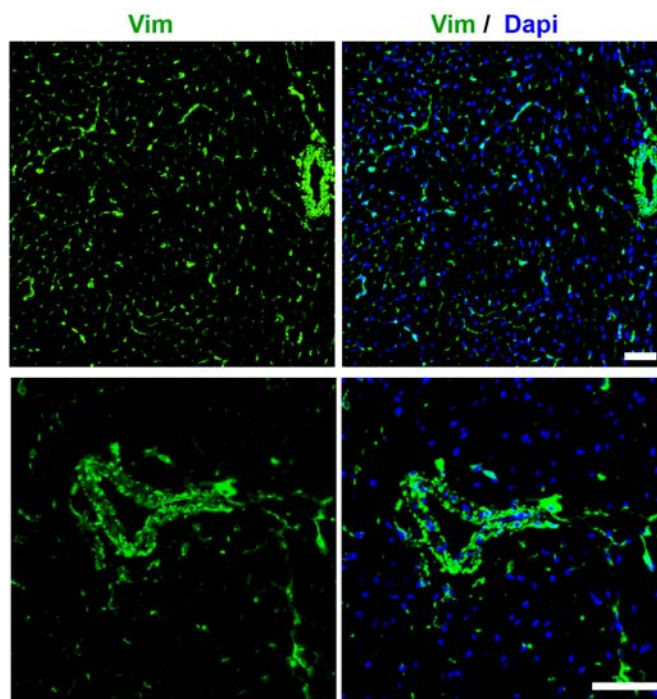


**Figure 5.1 Vimentin is expressed in the blood vessels in the heart.** Immunostaining against vimentin (Green) in frozen heart sections of C57BL/6N mice demonstrates the presence of vimentin expressing cells in blood vessels. Scale bar =50 $\mu$ m, 100 $\mu$ m.

C57BL/6N wild-type mice heart tissues stained for anti-vimentin (Fig 5.1) also demonstrates and confirms our finding along with previous findings regarding the expression of vimentin in the blood vessel-associated vascular smooth muscle cells in heart tissue.

In agreement with previous reports using FSP1 as a known fibroblast promoter<sup>20, 187</sup>, we found FSP1 marked cells (GFP positive cells) to be rare in the normal adult myocardium of Fsp1-Cre;mT/mG bitransgenic mice suggesting the limited activity of Fsp1 promoter in the heart (Figure 4.11). Also co-labeling with different cell markers demonstrates Fsp1-cre marked cells (GFP positive cells) mostly as endothelial cells or fibroblasts cells.

## **5.4 Cardiac fibroblast-specific Cre recombination in VimCreER; mT/mG bitransgenic mice**

Confirmation of CF-specific expression of vimentin promoter in comparison with Fsp1 promoter activity has been demonstrated by detecting the direct fluorescence for mGFP and mTomato signal in isolated CM and CFs of the two-bitransgenic mice. Here we have found mostly all CFs isolated from tamoxifen-treated VimCreER;mT/mG bitransgenic mice underwent Cre-mediated recombination (as shown in Figure 4.13) and had mGFP fluorescence thereby confirming efficient vimentin promoter activity. Whereas, the number of CFs isolated from Fsp1-Cre; mT/mG bitransgenic mice showing mGFP fluorescence were low. In addition, the CM isolated from both the bitransgenic mice has only mTomato fluorescence confirming strict cell-specific activity of both promoters (Figure 4.13).

Further double-staining with GFP and fibroblast cell markers (Vimentin and P4HB) showed a 100% overlay between the GFP-positive cell and the fibroblast cell markers in tamoxifen-injected VimCreER;mT/mG and Fsp1-cre:mT/mG mice (Figure 4.14), thereby confirming that the cells isolated and cultured were purely CFs and not contaminated with any other cell type, as we have also not found any cell positive for CD31 antibody in these cultures. There was also no overlap between GFP and myocytes marker (ACTN) in this culture (data not shown). All these data suggest that the vimentin promoter efficiency and CF-specific Cre-mediated recombination is much higher in VimCreER mice than Fsp1-Cre mice.

## **5.5 Vimentin promoter activity in the pressure-overloaded myocardium**

Fibroblast activation and expansion of the cardiac interstitium through deposition of matrix proteins are hallmarks of the myocardial response to pressure overload<sup>20,7</sup>. Increased expression of vimentin has been demonstrated in the interstitial space in fibrotic heart tissues<sup>176-179</sup>. Several lines of evidence suggest that cardiac fibroblasts are a heterogeneous population and derive from various distinct tissue niches in physiological and pathological conditions. Conventionally, adult fibroblasts considered to be derived directly from resident embryonic, mesenchymal cells and epithelial-mesenchymal transition (EMT), and their increase in number is only as a result of the proliferation of resident fibroblasts. Zeisberg and colleague have revealed that endothelial cells undergo the Endothelial-mesenchymal transition (EndMT) and contribute to the total pool of cardiac fibroblasts during fibrosis<sup>20</sup>. On the contrary, a very recent study showed that fibroblast accumulation associated with pressure overload hypertrophy resulted from activation and proliferation of these resident

lineages and not EndoMT, hematopoietic progenitor recruitment, or epicardial activation<sup>78</sup>. In line with a previous study, an increase in the number of cells expressing GFP in the cardiac interstitium of VimCreER:mT/mG bitransgenic mice post TAC was observed with respect to sham control (Figure 4.15 B). Further analysis of **these accumulated GFP-expressing cell in the fibrotic area of pressure overload myocardium of VimCreER:mT/mG bitransgenic mice** showed no co-localization between endothelial cell marker (CD31) and GFP-positive cells suggesting that the increased VimCreER marked cells **are not of EndMT origin** (Figure 4.16). **Rather co-labeling with different fibroblast markers (Vimentin or P4HB) along with GFP showed double positive cells for GFP and fibroblast markers (Fig 4.15 C&D) in these mice, thereby confirming the accumulated GFP-expressing cells as fibroblasts.**

Several high-profile studies have used Fsp1 as a fibroblast-specific marker to investigate the role of fibroblasts in the pathophysiology of disease through the development of fibroblast-specific knockout mice<sup>187</sup> or to study the origin of fibroblasts in fibrotic conditions<sup>20</sup>. However, Fsp1 was found to expressed in other cell types entering injured tissues, such as inflammatory macrophages<sup>188</sup>, dendritic cells<sup>189</sup>, lymphocytes<sup>190</sup>, and vascular smooth muscle cells<sup>191</sup>. Because of the foregoing issues with Fsp1 as a fibroblast marker, we analyzed the Fsp1 promoter activity in fibrotic areas in heart sections of Fsp1-cre: mT/mG bitransgenic mice post TAC. We found there was a slight increase in the number of GFP-expressing cells in interstitial spaces, but this was still lower than what was observed in case TAC operated VimCreER bi-transgenic mice. Co-labeling of these GFP-expressing cells in pressure overload myocardium of Fsp1Cre bi-transgenic mice with fibroblast markers confirmed some of the GFP-expressing cells as fibroblasts. **Also presence of GFP and CD31 double positive cells indicate that a population of the GFP-expressing cells were endothelial cells that might have the EndMT origin in Fsp1-cre mice.** Our results were consistent with the recent findings of Kong et al. (2014)<sup>76</sup>, where a large number of Fsp1 positive cells were identified as endothelial cells, inflammatory leukocytes, and arteriolar smooth muscle cells in pressure overload myocardium of Fsp1-GFP reporter mice<sup>76</sup>.

In terms of cardiac phenotype, we have observed decreased ejection fraction and fractional shorting in case of Fsp1-Cre mice post TAC with respect to its littermate control. On the other hand, insignificant change and difference in cardiac functions were observed in tamoxifen or vehicle-injected VimCreER mice post TAC. **Thereby, suggesting that following TAC VimCreER mice are less susceptible to heart failure than Fsp1-Cre mice.**

## 5.6 Vimentin promoter activity in endothelial cell of VimCreER; mT/mG bitransgenic mice during postnatal development

In the developing murine heart by E12.5 days post fertilization (dpf), cardiac fibroblasts were observed, and their numbers progressively increase throughout development<sup>22</sup>. Using flow cytometry, Banerjee *et al.* (2007)<sup>22</sup> estimated that cardiac fibroblasts comprise approximately 14% of all murine heart cells at E18.5 dpf and their number progressively increases in the heart in postnatal life comprising 27% of the total number of cells in the adult murine heart<sup>22</sup>. Similarly during murine development, vimentin expression commences on embryonic day 7.5 (E7.5)<sup>171</sup> and becomes predominant in the primitive streak stage<sup>172, 173</sup>, while in adult mice, vimentin expression was reported to be limited to connective tissue mesenchymal cells in the central nervous system and muscle<sup>174</sup>. We determined the vimentin promoter activity during early and late postnatal development hypothesizing that activation of vimentin promoter at the earlier stage would have more specific and restricted recombination in cardiac fibroblast in the heart. In addition, the tamoxifen-independent Cre recombination observed was eluded. Here we found successful recombination induced in cells of cardiac interstitium but not in the cardiomyocytes in heart sections of VimCreER; mT/mG pups at postnatal day 7 (P7) and 6 weeks old adults as measured by the mGFP direct fluorescence (Figure 4.20). **Further immunostaining with different fibroblast markers confirmed a high number of the GFP-expressing (i.e recombined) cells as fibroblasts. However, a large fraction of these GFP-expressing cells was also identified as endothelial cells by staining with CD31 (endothelial cell marker) both at P7 and in 6 weeks old mice hearts.**

Cellular switching from an epithelial-to-mesenchymal (EMT) phenotype, and conversely from a mesenchymal-to-epithelial (MET) phenotype, are important biological programs that are functioning throughout the life of a mammalian organism. The heart forms via a remarkable series of sequential waves of EMT/MET. All cells in the heart arise from one or more EMTs<sup>243</sup>. During heart development, cardiogenic mesodermal cells give rise to two types of heart cells, myocardial and endocardial cells. Most of the endocardial cells express endothelial markers, such as VE-cadherin and CD31. A population of endocardial cells in the atrioventricular canal differentiates into the mesenchymal heart cushion cells, forming cardiac septa and valves. Similarly, several studies have shown that endocardial-endothelial cells might transdifferentiate into mesenchymal cells during the formation of endocardial cushion tissue in the early embryonic chick heart<sup>244, 121</sup>. Since endothelial cells undergoing

EndoMT during embryonic heart development they have been shown to express markers of mesenchymal cells, this could be one of the explanations for activation of vimentin promoter in endothelial cells in VimCreER;mT/mG bitransgenic mice during postnatal development. Another reason could be the expression of vimentin in a wide range of cells. Since our objective was to check for the maintenance of specificity by vimentin promoter when activated early during mouse development we discovered that the promoter was active in the vimentin-expressing endothelial cells along with fibroblasts. In conclusion, significant recombination efficiencies could not be attained in VimCreER;mT/mG bitransgenic offspring from tamoxifen-injected lactating mothers as shown in adult recombination (70%).

### 5.7 Challenges and limitations of study

In our understanding, it may be that the diverse origins of cardiac fibroblasts preclude the discovery of a universal “one size fits all” marker. But by better understanding which markers are reliable under certain conditions and which combinations of markers best encompass the normal, quiescent cardiac fibroblast versus the transient, activated fibroblast, we may begin to probe this intricate system in greater detail and with increased precision. All fibroblast-specific transgenic mouse lines studied so far have considerable limitations. The recently identified fibroblast promoter fibroblast-specific protein 1 (FSP1, also known as S100A4), labels only a subset of fibroblasts and is expressed by several other cells including endothelial and immune cells which is also confirmed by our study along with other recent studies. Periostin, a matricellular protein, and another mesenchymal cell marker are found to be expressed in connective tissues including the periodontal ligament, tendons, skin and bone, in neoplastic tissues, cardiovascular disease, as well as in connective tissue wound repair. At present, Postn-Cre<sup>66</sup> and inducible Tcf21 (iCre) MerCreMer<sup>71</sup> transgenic mouse lines are two of the most promising tools for lineage mapping and genetically manipulating CFs, and particularly cardiac fibroblasts. However, considering the negligible expression of periostin in normal hearts, these animals are of limited value for targeting gene expression in normal cardiac fibroblasts.

Vimentin expression, on the other hand, is often reported in a wide range of other cell types including endothelial cells, vascular smooth muscle cells lining the blood vessels, macrophages, neutrophils, and leukocytes<sup>25</sup>. Despite this drawback here we found Vimentin promoter as more promising promoter and VimCreER<sup>tg/0</sup> mouse line as another genetic means to investigate the function of cardiac fibroblast cells *in vivo*. **As compared to other identified fibroblast-specific transgenic mouse lines expressing Cre-recombinase driven under Periostin (Postn) or Fibroblast specific protein-1**

(Fsp1), VimCreER<sup>tg/0</sup> mouse line had Cre recombination in the cells of interstitial spaces mostly cardiac fibroblast in heart tissue of adult mouse and also in pressure overload myocardium of these mice. This specificity was also observed in isolated cells (CFs) from this transgenic mouse. In addition, unlike Fsp1-Cre mice, VimCreER<sup>tg/0</sup> mice also showed fibroblast accumulation associated in response to TAC that might result from activation and proliferation of the resident CFs lineages and not EndoMT. Some missing experiments in this study have become one of its limitations. It would have been useful if through FACS further analysis of GFP-expressing cells as hematopoietic progenitor recruitment, or as epicardial activated cells can be done which can be helpful in confirming the origin of these accumulated fibroblasts in TAC-operated VimCreER mice. Another limitation was the tamoxifen independent recombinase activity observed in heart tissue of some animals from this transgenic mouse line. The possible explanations for this discrepancy is that maybe after many generations of backcrossing to the C57BL/6 background, the expression of the randomly integrated VimCreER transgene is enhanced, thereby increasing its probability of nuclear entry, even in tamoxifen untreated cells or it's the old CreERT2 system which has disadvantage of showing some leak in the animals as published by few authors. Maybe the use of ERT2CreERT2 system instead of CreERT2 would ensure tight regulation. As ERT2CreERT2 double fusion has a higher affinity for Hsp90 to form a tighter complex. It is having less activity due to the double fusion, and thus, less background activity. It is also possible that degradation of CreERT2 results in the generation of "active Cre" lacking the regulatory domain, whereas ERT2CreERT2 is still inactive even after losing one regulatory domain. Thus, use of ERT2CreERT2 system would have been a better option for studying inducible Cre activity.

## 5.8 Conclusions

Past several years have yielded remarkable insights and progress in identifying and mapping the various cell lineages which initially give rise to the developing heart and deciphering many of the key morphological events that are required for both normal heart development and the underlying causes of congenital heart defects. Despite this recent progress, our understanding of the mechanisms of induction and lineage specification of early non-cardiomyocyte cell fate is still rudimentary, and the signals that instruct key precursors to select a CFs cell-lineage remains unclear. In this study, we analyze the Vimentin promoter activity in heart tissue. In our understanding, vimentin promoter can serve as a useful tool for studying CFs in both physiological and pathophysiological conditions. Characterization of VimCreER<sup>tg/0</sup> mouse line demonstrated vimentin promoter

drive Cre recombination in the interstitial cells in heart specifically in the majority of CFs. However, recombination was also documented in other tissues including Liver, lung, kidney and skeletal muscle. Recombination in endothelial cells along with fibroblast in VimCreER<sup>tg/0</sup> mice during postnatal development somehow hinders the use of this mouse line for development studies. With some drawbacks and in comparison with other known fibroblast-Cre mouse line, this mouse line is still highly efficient and specific to cardiac fibroblast in the heart.



## 6 SUMMARY/ ZUSAMMENFASSUNG

Cardiac fibroblasts comprise a substantial component of the mammalian heart and are intimately involved in both normal cardiac development and injury through paracrine, mechanical, and potentially electrical interactions with cardiomyocytes. While there has been a steady increase in research investigating these interactions, further *in vivo* work is critical for addressing the functional contribution of each element both in utero and following injury to more aptly describe the dynamic roles of cardiac fibroblasts in development and disease. Obstacles such as the absence of a comprehensive cardiac fibroblast marker have hindered *in vivo* analysis of these interactions to date; however, new techniques such as utilizing the 3.9kbPeriostin-Cre and Fsp1-Cre lines for lineage mapping and genetic modification of in utero and adult cardiac fibroblasts, as well as an increasing number of fibroblast markers are emerging to help address these challenges.

Here we tried to study the CF-specific transgenesis by characterizing two transgenic mouse lines (Ccdc80-Cre<sup>tg/0</sup> and VimCreER<sup>tg/0</sup>). The study was conducted in two parts. The first part of the study was based on microarray database approach where Ccdc80 gene was found out as a promising candidate in search for CF-specific genes. Validation of Ccdc80 promoter sequence constructs confirms the promoter activity *in vitro*. Further, a mouse line where Ccdc80 promoter consecutively drives the expression of Cre recombinase was generated. Furthermore, validation of promoter activity in frozen heart section of Ccdc80-Cre<sup>tg/0</sup>;Rosa26<sup>LacZ</sup> bitransgenic mice through  $\beta$ -gal staining showed Cre recombination in a small subset of CM instead of CF that somehow question about the different *in vitro* and *in vivo* promoter activity of Ccdc80.

In the second part of the study, we characterised the VimCreER<sup>tg/0</sup> mouse line as CF-specific in comparison with Fsp1-Cre<sup>tg/0</sup> mouse line (a known fibroblast promoter) by using dual fluorescent reporter mice (mTom/mGFP<sup>flox/flox</sup>). In comparison with Fsp1-Cre;mT/mG<sup>flox/+</sup> bitransgenic mice, VimCreER;mT/mG<sup>flox/+</sup> bitransgenic mice upon tamoxifen injection showed Cre recombination (i.e GFP-expressing cells) in a majority of interstitial cells in the myocardium. Co-staining of these VimCreER marked cells with different cell markers along with GFP both in heart tissue and in isolated cardiac cells confirms them as fibroblasts. Furthermore, validation of vimentin promoter activity in response to pressure overload (TAC) showed an increase in the VimCreER marked cells in the cardiac interstitium in these mice where a majority of them were stained for fibroblast markers. On the other hand, TAC-operated Fsp1-Cre;mT/mG<sup>flox/+</sup> bitransgenic mice showed a slight increase in the number of

Fsp1-Cre marked cells in these mice, and most of these cells were labeled as endothelial cells along with fibroblasts. Cre recombination in early and postnatal development in VimCreER<sup>tg/0</sup> mice is somehow not able to attain the significant efficiency as observed in adult recombination. In our understanding and also in comparison with other fibroblast-specific established transgenic mouse line expressing Cre-recombinase driven under Fibroblast specific protein-1 or Periostin promoters, VimCreER<sup>tg/0</sup> mice may represent as another genetic mean to investigate the function of cardiac fibroblast cells both in physiological and pathophysiological conditions *in vivo*.

Kardiale Fibroblasten stellen eine zentrale Komponente des Säugerherzens dar und spielen sowohl in der normalen Entwicklung des Herzens als auch im Falle kardialen Fehlfunktionen eine zentrale Rolle, indem sie über parakrine, mechanische und potentiell auch elektrische Interaktion mit Kardiomyozyten kommunizieren. Die Interaktion von Fibroblasten und Myozyten im Herzen wurde in den letzten Jahren vermehrt untersucht. Um die funktionelle Beteiligung beider Zelltypen in utero und im Krankheitsmodell zu adressieren und die dynamische Rolle der kardialen Fibroblasten in der Herzentwicklung und im Krankheitsmodell zu beschreiben, ist ein Fibroblasten-spezifischer Promotor erforderlich. Um den idealen Promotor zu finden, können Cre-Linien für die Expressionsanalyse und die genetische Manipulation kardialer Fibroblasten in utero und in der adulten Maus verwendet werden. Zusätzlich können Fibroblasten-spezifische Marker zur Charakterisierung eines Fibroblasten-spezifischen Promotors herangezogen werden.

In dieser Arbeit wurden zwei transgene Mauslinien auf ihre Spezifität für kardiale Fibroblasten charakterisiert: *Ccdc80-Cre<sup>tg/0</sup>* and *VimCreER<sup>tg/0</sup>*. Zunächst wurde basierend auf einer Microarray Datenbank nach einem Gen gesucht, das spezifisch in kardialen Fibroblasten exprimiert wird. *Ccdc80* erwies sich als vielversprechender Kandidat. Der *Ccdc80*-Promotor war in vitro aktiv. Im Folgenden wurde eine Mauslinie generiert, in der der *Ccdc80*-Promotor, wenn aktiv, konstitutiv die Expression der Cre-Rekombinase induziert. Die Validierung des Promotors in  $\beta$ -gal gefärbten Herz-Gefrierschnitten von *Ccdc80-Cre<sup>tg/0</sup>;Rosa26LacZ* Mäusen ergab eine Cre Expression in wenigen Kardiomyozyten und nicht in Fibroblasten, was eine kritische Beurteilung der Übertragbarkeit der Aktivität des *Ccdc80*-Promotors von in vitro nach in vivo aufwirft.

In einem zweiten Teil wurde die *VimCreER<sup>tg/0</sup>* Mauslinie mit der *Fsp1-Cre<sup>tg/0</sup>* (einem bekannten Fibroblastenpromotor) im Hinblick auf die Spezifität für kardiale Fibroblasten verglichen. Hierzu wurde die duale Fluoreszenz-Reporterlinie *mTom/mGFP<sup>flox/flox</sup>* verwendet. Die *VimCreER;mT/mG<sup>flox/+</sup>* Mäuse zeigten nach Injektion von Tamoxifen Cre-Rekombination (i.e. GFP-positive Zellen) in der Mehrheit der interstitiellen Zellen im Myokard. Co-Färbungen dieser GFP-positiven Zellen mit Markern für verschiedene Zelltypen zeigte, dass es sich dabei sowohl im Herzgewebe als auch in isolierten kardialen Zellen um Fibroblasten handelte. Darüber hinaus stieg die Zahl der positiven Zellen im Interstitium nach induzierter Aortenkonstriktion (TAC). Auch hier war die Mehrheit positiv für Fibroblastenmarker. Dagegen zeigten *Fsp1-Cre;mT/mG<sup>flox/+</sup>* Mäuse nach TAC nur einen leichten Anstieg in der Zahl an GFP-positiven Zellen, wobei die meisten davon Endothelzellen waren.

In der frühen und postnatalen Entwicklungsphase in VimCreER<sup>tg/0</sup> ist die Rekombination signifikant weniger effizient als in adulten Tieren. Im Vergleich zu anderen etablierten Fibroblasten-spezifischen transgenen Cre-Rekombinase exprimierenden Linien wie Fsp1-Cre scheint VimCreER<sup>tg/0</sup> gut geeignet, um die Funktion kardialer Fibroblasten in vivo unter physiologischen und pathophysiologischen Bedingungen zu untersuchen.

---

## 7 REFERENCE

1. Mathers CD, Loncar D. 2006. Projections of Global Mortality and Burden of Disease from 2002 to 2030. *PLoS Med.* 3:e442.
2. Creemers EE, Wilde AA, Pinto YM. 2011. Heart failure: advances through genomics. *Nat Rev Genet.* 12:357-362.
3. Baudino TA, Carver W, Giles W, Borg TK. 2006. Cardiac fibroblasts: friend or foe? *Am J Physiol Heart Cir Physiol.* 291: 1015-1026.
4. Kalluri R, Zeisberg M. 2006 Fibroblasts in cancer. *Nat Rev Cancer.* 6:392-401.
5. Chang HY, Chi JT, Dudoit S, Bondre C, van de Rijn D, Brown PO. 2002. Diversity, topographic differentiation, and positional memory in human fibroblasts. *PNAS.* 99:12877-12882.
6. Brown, R.D., Ambler, S.K., Mitchell, M.D., & Long, C.S. 2005. The cardiac fibroblast: therapeutic target in myocardial remodeling and failure. *Annu Rev Pharmacol Toxicol* 45, 657-687.
7. Krenning G, Zeisberg EM, Kalluri R. 2010. The origin of fibroblasts and mechanism of cardiac fibrosis. *J Cell Physiol.* 225:631-637.
8. Manner J, Perez-Pomares JM, Macias D, Munoz-Chapuli R. 2001. The origin, formation and developmental significance of the epicardium: a review. *Cells Tissues Organs.*169:89-103.
9. Juan Manuel Gonzalez-Rosa NM. 2009. The epicardium: development, differentiation and its role during heart development. *Nat Rev Cardiol.* 6:1-6.
10. Lie-Venema H, van den Akker NMS, Bax NAM, Winter EM, Maas S, Kekarainen T, et al. 2007. Origin, fate, and function of epicardium-derived cells (EPDCs) in normal and abnormal cardiac development. *Sci World J.* 7:1777-98.
11. Manner J. 1999. Does the subepicardial mesenchyme contribute myocardioblasts to the myocardium of the chick embryo heart? A quail-chick chimera study tracing the fate of the epicardial primordium. *Anat Rec.* 255: 212-226.
12. Perez-Pomares JM, Carmona R, Gonzalez-Iriarte M, Atencia G, Wessels A, Munoz-Chapuli R. 2002. Origin of coronary endothelial cells from epicardial mesothelium in avian embryos. *Int J Dev Biol.* 46: 1005-1013.
13. Gittenberger-de Groot AC, Vrancken Peeters MP, Mentink MM, Gourdie RG, Poelmann RE. 1998. Epicardium-derived cells contribute a novel population to the myocardial wall and the atrioventricular cushions. *Circ Res.* 82: 1043-1052.
14. Kovacic JC, Mercader N, Torres M, Boehm M, Fuster V. 2012. Epithelial-to-mesenchymal and endothelial-to-mesenchymal transition: from cardiovascular development to disease. *Circulation.* 125: 1795-1808.

15. Eisenberg LM, Markwald RR. 1995. Molecular regulation of atrioventricular valvuloseptal morphogenesis. *Circ Res.* 77:1-6.
16. Markwald RR, Fitzharris TP, Manasek FJ. 1977. Structural development of endocardial cushions. *Am J Anat.* 148:85-119.
17. Goldsmith EC, Hoffman A, Morales MO, Potts JD, Price RL, McFadden A, Rice M, Borg TK. 2004. Organization of fibroblasts in the heart. *Dev Dyn.* 230: 787-794.
18. Kohl, P., Camelliti, P., Burton, F.L., & Smith, G.L. 2005. Electrical coupling of fibroblasts and myocytes: relevance for cardiac propagation. *J Electrocardiol.* 38: 45-50.
19. Camelliti P, Borg TK, Kohl P. 2005. Structural and functional characterization of cardiac fibroblasts. *Cardiovasc Res.* 65:40-51.
20. Zeisberg EM, Tarnavski O, Zeisberg M, Dorfman AL, McMullen JR, Gustafsson E, Chandraker A, Yuan X, Pu WT, Roberts AB, Neilson EG, Sayegh MH, Izumo S, Kalluri R. 2007. Endothelial-to-mesenchymal transition contributes to cardiac fibrosis. *Nat Med.* 13:952-961.
21. Banerjee I, Yekkala K, Borg TK, Baudino TA. 2006. Dynamic interactions between myocytes, fibroblasts and extracellular matrix. *Ann N Y Acad Sci.* 1080:76-84.
22. Banerjee I, Fuseler JW, Price RL, Borg TK, Baudino TA. 2007. Determination of cell types and numbers during cardiac development in the neonatal and adult rat and mouse. *Am J Physiol Heart Circ Physiol.* 293:1883-1891.
23. Zak R. 1974. Development and proliferative capacity of cardiac muscle cells. *Circ Res.* 32(Suppl 2): 17-26.
24. Adler CP, Ringlage WP, Bohm N .1981. (DNA content and cell number in heart and liver of children. Comparable biochemical, cytophotometric and histological investigations (author's transl)). *Pathol Res Pract.* 172: 25-41.
25. Cochard P, Paulin D. 1984. Initial expression of neurofilament and vimentin in the central and peripheral nervous system of the mouse embryo in vivo. *J Neurosci.* 4: 2080-2094.
26. de Souza PC, Katz SG. 2001. Coexpression of cytokeratin and vimentin in mice trophoblastic giant cells. *Tissue Cell.* 33:40-45.
27. Ko SH, Suh SH, Kim BJ, Ahn YB, Song KH, Yoo SJ, Son HS et al. 2004. Expression of the intermediate filament vimentin in proliferating duct cells as a marker of pancreatic precursor cells. *Pancreas.* 28: 121-128.
28. Mahrle G, Bolling R, Osborn M, Weber K. 1983. Intermediate filaments of the vimentin and prekeratin type in human epidermis. *J Invest Dermatol.* 81: 46-48.
29. Carter V, Shenton BK, Jaques B, Turner D, Talbot D, Gupta A, Chapman CE et al. 2005. Vimentin antibodies: a non-HLA antibody as a potential risk factor in renal

- transplantation. *Transplant Proc.* 37:654-657.
30. Evans RM .1998. Vimentin: the conundrum of the intermediate filament gene family. *Bioessays.* 20: 79-86.
  31. Zhou B, von Gise A, Ma Q, Hu YW, Pu WT. 2010. Genetic fate mapping demonstrates contribution of epicardium-derived cells to the annulus fibrosis of the mammalian heart. *Dev Biol.* 338:251-261.
  32. Gaudesius G, Miragoli M, Thomas SP, Rohr S. 2003. Coupling of cardiac electrical activity over extended distances by fibroblasts of cardiac origin. *Circ Res.* 93:421-428.
  33. Camelliti P, Green CR, LeGrice I, Kohl P. 2004, Fibroblast network in rabbit sinoatrial node: structural and functional identification of homogeneous and heterogeneous cell coupling. *Circ Res.* 94:828–835.
  34. Porter KE, Turner NA. 2009. Cardiac fibroblasts: at the heart of myocardial remodeling. *Pharmacol Ther.* 123:255-278.
  35. Long CS. 2001.The role of interleukin-1 in the failing heart. *Heart Fail Rev.* 6:81-94.
  36. Torre-Amione G, Kapadia S, Benedict C, Oral H, Young JB, Mann DL. 1996. Proinflammatory cytokine levels in patients with depressed left ventricular ejection fraction: a report from the Studies of Left Ventricular Dysfunction (SOLVD). *J Am Coll Cardiol.* 27: 1201-1206.
  37. Souders CA, Bowers SL, Baudino TA. 2009. Cardiac fibroblast: the renaissance cell. *Circ Res.* 105:1164-1176.
  38. Spinale F. 2007. Myocardial matrix remodeling and the matrix metalloproteinases: influence on cardiac form and function. *Physiol Rev.* 87:1285-342.
  39. Polyakova V, Hein S, Kostin S, Ziegelhoeffer T, Schaper J. 2004. Matrix metalloproteinases and their tissue inhibitors in pressure-overloaded human myocardium during heart failure progression. *J Am Coll Cardiol.* 44:1609-18.
  40. Kuster GM, Kotlyar E, RudeMK, Siwik DA, Liao R, Colucci WS, et al. 2005. Mineralocorticoid receptor inhibition ameliorates the transition to myocardial failure and decrease oxidative stress and inflammation in mice with chronic pressure overload. *Circulation.* 111:420-7.
  41. Sun Y, Weber KT. 2000. Infarct scar: a dynamic tissue. *Cardiovasc Res.* 46:250-256.
  42. Ausma J, Cleutjens J, Thone F, Flameng W, Ramaekers F, Borgers M. 1995. Chronic hibernating myocardium: interstitial changes. *Mol Cell Biochem.*147: 35-42.
  43. Ottaviano FG, Yee KO. 2011. Communication signals between cardiac fibroblasts and cardiac myocytes. *J Cardiovasc Pharmacol.* 57(5): 513-521.
  44. Kawaguchi M, Takahashi M, Hata T, Kashima Y, Usui F, Morimoto H, Izawa A, Takahashi Y, Masumoto J, Koyama J, Hongo M, Noda T, Nakayama J, Sagara J, Taniguchi S, Ikeda U. 2011. Inflammasome activation of cardiac fibroblasts is

- essential for myocardial ischemia/reperfusion injury. *Circulation*. 123(6): 594-604.
45. Kakkar R, Lee RT. 2010. Intramyocardial fibroblast myocyte communication. *Circ Res*. 106(1): 47-57.
  46. Lie-Venema H, Gittenberger-de Groot AC, van Empel LJ, Boot MJ, Kerckdijk H, de Kant E, DeRuiter MC. 2003. Ets-1 and Ets-2 transcription factors are essential for normal coronary and myocardial development in chicken embryos. *Circ Res*. 92(7): 749-756.
  47. Smith CL, Baek ST, Sung CY, Tallquist MD. 2011. Epicardial-derived cell epithelial-to-mesenchymal transition and fate specification require PDGF receptor signaling. *Circ Res*. 108(12): e15-26.
  48. Snider P, Standley KN, Wang J, Azhar M, Doetschman T, Conway SJ. 2009. Origin of cardiac fibroblasts and the role of periostin. *Circ Res*. 105:934-947.
  49. Matsusaka T, Katori H, Inagami T, Fogo A, Ichikawa I. 1999. Communication between myocytes and fibroblasts in cardiac remodeling in angiotensin chimeric mice. *J Clin Invest*. 103(10): 1451-1458.
  50. Molkenkin JD, Lu JR, Antos CL, Markham B, Richardson J, Robbins J, Grant SR, Olson EN. 1998. A calcineurin-dependent transcriptional pathway for cardiac hypertrophy. *Cell*. 93(2): 215-228.
  51. Zhang Y, Kanter EM, Yamada KA. 2010 Remodeling of cardiac fibroblasts following myocardial infarction results in increased gap junction intercellular communication. *Cardiovasc Pathol*. 19(6):e233-240.
  52. Bellini A, Mattoli S. 2007. The role of the fibrocyte, a bone marrow-derived mesenchymal progenitor, in reactive and reparative fibroses. *Lab Invest*. 87: 858-70.
  53. van Amerongen MJ, Bou-Gharios G, Popa E, van Ark J, Petersen AH, van Dam GM, et al. 2008. Bone marrow-derived myofibroblasts contribute functionally to scar formation after myocardial infarction. *J Pathol*. 214: 377-86.
  54. Haudek SB, Xia Y, Huebener P, Lee JM, Carlson S, Crawford JR, et al. 2006. Bone marrow derived fibroblast precursors mediate ischemic cardiomyopathy in mice. *PNAS*. 103: 18284-9.
  55. Duan J, Gherghe C, Liu D, Hamlett E, Srikantha L, Rodgers L, et al. 2012. Wnt1/beta-catenin injury response activates the epicardium and cardiac fibroblasts to promote cardiac repair. *EMBO J*. 31:429-42.
  56. Russell JL, Goetsch SC, Gaiano NR, Hill JA, Olson EN, Schneider JW. 2011. A dynamic notch injury response activates epicardium and contributes to fibrosis repair. *Circ Res*. 108:51-9.
  57. Van den Borne SW, Diez J, Blankesteyn WM, Verjans J, Hofstra L, Narula J. 2010. Myocardial remodeling after infarction: the role of myofibroblasts. *Nat Rev Cardiol*. 7:30-37.



58. Deb A, Ubil E. 2014. Cardiac fibroblast in development and wound healing. *Journal of Molecular and Cellular Cardiology*. 70; 47-55.
59. Holmes JW, Borg TK, Covell JW. 2005. Structure and mechanics of healing myocardial infarcts. *Annu Rev Biomed Eng*. 7:223-53.
60. Christia P, Bujak M, Gonzalez-Quesada C, Chen W, Dobaczewski M, Reddy A, et al. 2013. Systematic characterization of myocardial inflammation, repair, and remodeling in a mouse model of reperfused myocardial infarction. *J Histochem Cytochem*. 61: 555-70.
61. Takahashi K, Yamanaka S. 2006. Induction of pluripotent stem cells from mouse embryonic and adult fibroblast cultures by defined factors. *Cell* 126:663-676.
62. Tapscott SJ, Davis RL, Thayer MJ, Cheng PF, Weintraub H, Lassar AB. 1988. MyoD1: a nuclear phosphoprotein requiring a Myc homology region to convert fibroblasts to myoblasts. *Science*. 242:405-411.
63. Vierbuchen T, Ostermeier A, Pang ZP, Kokubu Y, Sudhof TC, Wernig M. 2010. Direct conversion of fibroblasts to functional neurons by defined factors. *Nature*. 463:1035-1041.
64. Ieda M, Fu JD, Delgado-Olguin P, Vedantham V, Hayashi Y, Bruneau BG, Srivastava D. 2010. Direct reprogramming of fibroblasts into functional cardiomyocytes by defined factors. *Cell*. 142(3): 375-386.
65. Snider P, Hinton RB, Moreno-Rodriguez RA, Wang J, Rogers R, Lindsley A, et al. 2008. Periostin is required for maturation and extracellular matrix stabilization of noncardiomyocyte lineages of the heart. *Circ Res*.102: 752-60.
66. Takeda N, Manabe I, Uchino Y, Eguchi K, Matsumoto S, Nishimura S, et al. 2010. Cardiac fibroblasts are essential for the adaptive response of the murine heart to pressure overload. *J Clin Invest*. 120: 254-65.
67. Qian L, Huang Y, Spencer CI, Foley A, Vedantham V, Liu L, et al. 2012. In vivo reprogramming of murine cardiac fibroblasts into induced cardiomyocytes. *Nature*. 485: 593-598.
68. Jayawardena TM, Egemnazarov B, Finch EA, Zhang L, Payne JA, Pandya K, Zhang Z, Rosenberg P, Mirotsov M, Dzau VJ. 2012. MicroRNA-mediated in vitro and in vivo direct reprogramming of cardiac fibroblasts to cardiomyocytes. *Circ Res*. 110:1465-1473.
69. Heine HL, LeongHS, Rossi FM, Mc Manus BM, Podor TJ. 2005. Strategies of conditional gene expression in myocardium: an overview. *Methods Mol Med*. 112:109-54.
70. Jayawardena TM, Egemnazarov B, Finch EA, Zhang L, Payne JA, Pandya K, et al. 2012. MicroRNA-mediated in vitro and in vivo direct reprogramming of cardiac fibroblasts to cardiomyocytes. *Circ Res*. 110:1465-73.

71. Acharya A, Baek ST, Banfi S, Eskiocak B, Tallquist MD. 2011. Efficient inducible Cre-mediated recombination in Tcf21 cell lineages in the heart and kidney. *Genesis*. 49:870-877.
72. Lindsley A, Snider P, Zhou H, Rogers R, Wang J, Olaopa M, et al. 2007. Identification and characterization of a novel Schwann and outflow tract endocardial cushion lineage-restricted periostin enhancer. *Dev Biol*. 307: 340-355.
73. Kruzynska-Frejtag A, Machnicki M, Rogers R, Markwald RR, Conway SJ. 2001. Periostin (an osteoblast-specific factor) is expressed within the embryonic mouse heart during valve formation. *Mech Dev*. 103: 183-188.
74. Conway SJ, Molkentin JD. 2008. Periostin as a heterofunctional regulator of cardiac development and disease. *Curr Genomics*. 9: 548-55.
75. Stansfield WE, Andersen NM, Tang RH, Selzman CH. 2009. Periostin is a novel factor in cardiac remodeling after experimental and clinical unloading of the failing heart. *Ann Thorac Surg*. 88(6): 1916-21.
76. Kong P, Christia P, Saxena A, Su Y, Frangogiannis N. 2013. Lack of specificity of Fibroblast Specific Protein (FSP)1 in cardiac remodeling and fibrosis. *Am J Physiol Heart Circ Physiol*. 305:1363-1372.
77. Acharya A, Baek S, Huang G, Eskiocak B, Goetsch S, Sung C, et al. 2012. The bHLH transcription factor Tcf21 is required for lineage-specific EMT of cardiac fibroblast progenitors. *Development*. 139: 2139-49.
78. Moore-Morris T, Guimarães-Camboa N, Banerjee I, Zambon AC, Kisseleva T, Velayoudon A, Stallcup WB, Gu Y, Dalton ND, Cedenilla M, Gomez-Amaro R, Zhou B, Brenner DA, Peterson KL, Chen J, Evans SM. Resident fibroblast lineages mediate pressure overload-induced cardiac fibrosis. 2014. *J Clin Invest*. 124(7):2921-34.
79. Snider P, Conway SJ. 2011. Probing human cardiovascular congenital disease using transgenic mouse models. *Prog Mol Biol Transl Sci*. 100: 83-110.
80. Yutzey KE, Robbins J. 2007. Principles of genetic murine models for cardiac disease. *Circulation*. 115:792-799.
81. Molkentin JD, Robbins J. 2009. With great power comes great responsibility: using mouse genetics to study cardiac hypertrophy and failure. *J Mol Cell Cardiol*. 46:130 - 136.
82. Gittenberger-de Groot AC, Bartelings MM, DeRuiter MC, Poelmann RE. 2005. Basics of cardiac development for the understanding of congenital heart malformations. *Pediatr Res*. 57:169 -176.
83. Doetschman T, Barnett JV, Runyan RB, Camenisch TD, Heimark RL, Granzier HL, Conway SJ, Azhar M. 2012. Transforming growth factor beta signaling in adult cardiovascular diseases and repair. *Cell Tissue Res*. 347:203-223.

84. Robbins J. 2011. Twenty years of gene targeting: what we don't know. *Circ Res.* 109:722-723.
85. Doetschman T. 1999. Interpretation of phenotype in genetically engineered mice. *Lab Anim Sci.* 149:137-143.
86. Sauer B, Henderson N .1988. Site-specific DNA recombination in mammalian cells by the Cre recombinase of bacteriophage P1. *PNAS.* 85:5166-5170.
87. Soriano P. 1999. Generalized lacZ expression with the ROSA26 Cre reporter strain [Letter]. *Nat Genet.* 21: 70-71.
88. Kain SR, Adams M, Kondepudi A, Yang TT, Ward WW, Kitts P. 1995. Green fluorescent protein as a reporter of gene expression and protein localization. *Biotechniques.* 19:650-5.
89. Freem LJ, Escot S, Tannahill D, Druckenbrod NR, Thapar N, Burns AJ. 2010. The intrinsic innervation of the lung is derived from neural crest cells as shown by optical projection tomography in Wnt1-Cre; YFP reporter mice. *J Anat.* 217:651-64.
90. Wellershaus K, Degen J, Deuchars J, Theis M, Charollais A, Caille D, Gauthier B, Janssen-Bienhold U, Sonntag S, Herrera P, Meda P, Willecke K. 2008. A new conditional mouse mutant reveals specific expression and functions of connexin36 in neurons and pancreatic beta-cells. *Exp Cell Res.* 314: 997-1012.
91. Armstrong JJ, Larina IV, Dickinson ME, Zimmer WE, Hirschi KK. 2010. Characterization of bacterial artificial chromosome transgenic mice expressing mCherry fluorescent protein substituted for the murine smooth muscle alpha-actin gene. *Genesis.* 2010 48:457-63.
92. Giraldo, P. and L. Montoliu. 2001. "Size matters: use of YACs, BACs and PACs in transgenic animals. *Transgenic Res.* 10(2): 83-103.
93. Testa, G., Zhang, Y., Vintersten, K., Benes, V., Pijnappel, W. W., Chambers, I., Smith, A. J., Smith, A. G., Stewart, A. F. 2003. Engineering the mouse genome with bacterial artificial chromosomes to create multipurpose alleles. *Nat Biotechnol.* 21, 443-7.
94. Dymecki SM. 1996. Flp recombinase promotes site-specific DNA recombination in embryonic stem cells and transgenic mice. *PNAS.* 93:6191-6196.
95. Anastassiadis K, Fu J, Patsch C, Hu S, Weidlich S, Duerschke K, Buchholz F, Edenhofer F, Stewart AF. 2009. Dre recombinase, like Cre, is a highly efficient site-specific recombinase in E. coli, mammalian cells and mice. *Dis Model Mech.* 2:508 - 515.
96. Bockamp E, Maringer M, Spangenberg C, Fees S, Fraser S, Eshkind L, Oesch F, Zabel B. 2002. Of mice and models: improved animal models for biomedical research. *Physiol Genomics.* 11(3):115-32.
97. Kuhn R, Schwenk F, Aguet M, Rajewsky K. 1995. Inducible gene targeting in mice. *Science.* 269: 1427-1429.

98. Utomo AR, Nikitin AY, Lee WH. 1999. Temporal, spatial, and cell type specific control of Cre-mediated DNA recombination in transgenic mice. *Nat Biotechnol.* 17: 1091-1096.
99. Engelhardt, S., Hein, L., Wiesmann, F. & Lohse, M. J.1999. Progressive hypertrophy and heart failure in beta1-adrenergic receptor transgenic mice. *PNAS.* 96: 7059–64.
100. Feil R, Brocard J, Mascrez B, LeMeur M, Metzger D, Chambon P.1996. Ligand-activated site-specific recombination in mice. *PNAS.* 93:10887-10890.
101. Indra AK, Li M, Brocard J, Warot X, Bornert JM, Gerard C, Messaddeq N, Chambon P, Metzger D. 2000. Targeted somatic mutagenesis in mouse epidermis. *Horm Res.* 54:296 -300.
102. Feil, R., Wagner, J., Metzger, D., Chambon, P., 1997. Regulation of Cre recombinase activity by mutated estrogen receptor ligand-binding domains. *Biochem. Biophys. Res. Commun.* 237(3): 752-757.
103. Casanova, E., Fehsenfeld, S., Lemberger, T., Shimshek, D.R., Sprengel, R., Mantamadiotis, T., 2002. ER-based double iCre fusion protein allows partial recombination in forebrain. *Genesis.* 34:208-214.
104. Matsuda, T., Cepko, C.L., 2007. Controlled expression of transgenes introduced by in vivo electroporation. *PNAS.* 104:1027-1032.
105. Levin ER. Integration of the extranuclear and nuclear actions of estrogen.2005. *Mol Endocrinol.* 19:1951-1959.
106. Schwenk F, Kuhn R, Angrand PO, Rajewsky K, Stewart AF.1998. Temporally and spatially regulated somatic mutagenesis in mice. *Nucleic Acids Res.* 26:1427-1432.
107. Glaser S, Lubitz S, Loveland KL, Ohbo K, Robb L, Schwenk F, Seibler J, Roellig D, Kranz A, Anastassiadis K, Stewart AF. 2009. The histone 3 lysine methyltransferase, Mll2, is only required briefly in development and spermatogenesis. *Epigenetics Chromatin.* 2: 5.
108. Sohal DS, Nghiem M, Crackower MA, Witt SA, Kimball TR, Tymitz KM, Penninger JM, Molkentin JD. 2001. Temporally regulated and tissue specific gene manipulations in the adult and embryonic heart using tamoxifen-inducible Cre protein. *Circ Res.* 89:20 - 25.
109. Hameyer D, Loonstra A, Eshkind L, Schmitt S, Antunes C, Groen A, Bindels E, Jonkers J, Krimpenfort P, Meuwissen R, Rijswijk L, Bex A, Berns A, Bockamp E. 2007. Toxicity of ligand-dependent Cre recombinases and generation of a conditional Cre deleter mouse allowing mosaic recombination in peripheral tissues. *Physiol Genomics.* 31:32-41.
110. Danielian PS, Muccino D, Rowitch DH, Michael SK, McMahon AP.1998. Modification of gene activity in mouse embryos in utero by a tamoxifeninducible form of Cre recombinase. *Curr Biol.* 18:1323-1326.

111. Jung-Eun Kim. 2006. Functional Study of Gene using Inducible Cre System. *J Korean Endocr Soc.* 21(5): 364-369.
112. Vogt MA, Chourbaji S, Brandwein C, Dormann C, Sprengel R, Gass P. 2008. Suitability of tamoxifen-induced mutagenesis for behavioral phenotyping. *Exp Neurol.* 211: 25-33.
113. Moga MA, Nakamura T, Robbins J. 2008. Genetic approaches for changing the heart and dissecting complex syndromes. *J Mol Cell Cardiol.* 45:148 -155.
114. Gossen, M., Bujard, H., 1992. Tight control of gene expression in mammalian cells by tetracycline-responsive promoters. *PNAS.* 89: 5547-5551.
115. Gossen, M., Freundlieb, S., Bender, G., Muller, G., Hillen, W., Bujard, H., 1995. Transcriptional activation by tetracyclines in mammalian cells. *Science.* 268:1766-1769.
116. Schonig K, Bujard H. 2003. Generating conditional mouse mutants via tetracycline-controlled gene expression. *Methods Mol Biol.* 209: 69-104.
117. Belteki G, Haigh J, Kabacs N, Haigh K, Sison K, Costantini F, Whitsett J, Quaggin SE, Nagy A. 2005. Conditional and inducible transgene expression in mice through the combinatorial use of Cre-mediated recombination and tetracycline induction. *Nucleic Acids Res.* 33(5): e51.
118. Yu HM, Liu B, Chiu SY, Costantini F, Hsu W. 2005. Development of a unique system for spatiotemporal and lineage-specific gene expression in mice. *PNAS.* 102:8615-8620.
119. Badea TC, Hua ZL, Smallwood PM, Williams J, Rotolo T, Ye X, Nathans J. 2009. New mouse lines for the analysis of neuronal morphology using CreER(T)/loxP-directed sparse labeling. *PLoS One.* 4: e7859.
120. Sanbe A, Gulick J, Hanks MC, Liang Q, Osinska H, Robbins J. 2003. Reengineering inducible cardiac-specific transgenesis with an attenuated myosin heavy chain promoter. *Circ Res.* 92:609-616.
121. Lee P, Morley G, Huang Q, Fischer A, Seiler S, Horner JW, Factor S, Vaidya D, Jalife J, Fishman GI. 1998. Conditional lineage ablation to model human diseases. *PNAS.* 95:11371-11376.
122. Yutzey KE, Robbins J. 2007. Principles of genetic murine models for cardiac disease. *Circulation.* 115: 792-799.
123. Conway SJ, Kruzynska-Frejtag A, Kneer PL, Machnicki M, Koushik SV. 2003. What cardiovascular defect does my prenatal mouse mutant have, and why? *Genesis.* 35:1-21.
124. Minamino T, Gaussin V, DeMayo FJ, Schneider MD. 2001. Inducible gene targeting in postnatal myocardium by cardiac-specific expression of a hormone-activated Cre fusion protein. *Circ Res.* 88:587-592.

125. Wu B, Zhou B, Wang Y, Cheng HL, Hang CT, Pu WT, Chang CP, Zhou B. 2010. Inducible cardiomyocyte-specific gene disruption directed by the ratTnnt2 promoter in the mouse. *Genesis*. 48:63-72.
126. Forde A, Constien R, Grone HJ, Hammerling G, Arnold B. 2002. Temporal Cre-mediated recombination exclusively in endothelial cells using Tie2 regulatory elements. *Genesis*. 33:191-197.
127. Monvoisin A, Alva JA, Hofmann JJ, Zovein AC, Lane TF, Iruela-Arispe ML. 2006. VE-cadherin-CreERT2 transgenic mouse: a model for inducible recombination in the endothelium. *Dev Dyn*. 235:3413-3422.
128. Nakamura E, Nguyen MT, Mackem S. 2006. Kinetics of tamoxifen-regulated Cre activity in mice using a cartilage-specific CreER(T) to assay temporal activity windows along the proximodistal limb skeleton. *Dev Dyn*. 235: 2603-2612.
129. Wendling O, Bornert JM, Chambon P, Metzger D. 2009. Efficient temporally controlled targeted mutagenesis in smooth muscle cells of the adult mouse. *Genesis*. 47:14 -18.
130. Zervas M, Millet S, Ahn S, Joyner AL. 2004. Cell behaviors and genetic lineages of the mesencephalon and rhombomere 1. *Neuron*. 43:345-357.
131. Hoesl E, Stieber J, Herrmann S, Feil S, Tybl E, Hofmann F, Feil R, Ludwig A. 2008. Tamoxifen-inducible gene deletion in the cardiac conduction system. *J Mol Cell Cardiol*. 45: 62-69.
132. Beyer S, Kelly RG, Miquerol L. 2011. Inducible Cx40-Cre expression in the cardiac conduction system and arterial endothelial cells. *Genesis*. 49:83-91.
133. Arnolds DE, Moskowitz IP. 2011. Inducible recombination in the cardiac conduction system of minK: CreERT(2) BAC transgenic mice. *Genesis*. 49: 878-84.
134. Wilke A, Schonian U, Herzum M, Hengstenberg C, Hufnagel G, Brilla CG, Maisch B. 1995. The extracellular matrix and cytoskeleton of the myocardium in cardiac inflammatory reaction. *Herz*. 20: 95-108.
135. Franke WW, Schmid E, Osborn M, Weber K. 1979. Intermediate-sized filaments of human endothelial cells. *J Cell Biol*. 81: 570 -580.
136. Strutz F, Okada H, Lo CW, Danoff T, Carone RL, Tomaszewski JE, Neilson EG. 1995. Identification and characterization of a fibroblast marker: FSP1. *J Cell Biol*. 130:393-405.
137. Weber KT. 2000. Fibrosis and hypertensive heart disease. *Curr Opin Cardiol*. 15:264-272.
138. Visconti RP, Markwald RR. 2006. Recruitment of new cells into the postnatal heart: potential modification of phenotype by periostin. *Ann N Y Acad Sci*. 1080:19-33.
139. Katsuragi N, Morishita R, Nakamura N, Ochiai T, Taniyama Y, Hasegawa Y, et al. 2004.

- Periostin as a novel factor responsible for ventricular dilation. *Circulation*. 110: 1806-1813.
140. Wang D, Oparil S, Feng JA, Li P, Perry G, Chen LB, et al. 2003. Effects of pressure overload on extracellular matrix expression in the heart of the atrial natriuretic peptide-null mouse. *Hypertension*. 42: 88-95.
141. Kudo A. 2011. Periostin in fibrillogenesis for tissue regeneration: periostin actions inside and outside the cell. *Cell Mol Life Sci*. 68: 3201-3207.
142. Stanton LW, Garrard LJ, Damm D, Garrick BL, Lam A, Kapoun AM, et al. 2000. Altered patterns of gene expression in response to myocardial infarction. *Circ Res*. 86: 939-45.
143. Rossert J, Terraz C, Dupont S. 2000. Regulation of type I collagen gene expression. *Nephrol Dial Transplant* 15:66-8.
144. Rossert J, Eberspaecher H, de Crombrughe B. 1995. Separate cis-acting DNA elements of the mouse pro- $\alpha 1(I)$  collagen promoter direct expression of reporter genes to different type I collagen-producing cells in transgenic mice. *J Cell Biol*. 129:1421-32.
145. Ford CM, Li S, Pickering JG. 1999. Angiotensin II stimulates collagen synthesis in human vascular smooth muscle cells: involvement of the AT1 receptor, transforming growth factor  $\beta$  and tyrosine phosphorylation. *Arterioscler Thromb Vasc Biol*. 19:1843-51.
146. Schlumberger W, Thie M, Rauterberg J, Robenek H. 1991. Collagen synthesis in cultured aortic smooth muscle cells: modulation by collagen lattice culture, transforming growth factor- $\beta 1$  and epidermal growth factor. *Arterioscler Thromb*. 11:1660-6.
147. Ieda M, Tsuchihashi T, Ivey KN, Ross RS, Hong TT, Shaw RM, et al. 2009. Cardiac fibroblasts regulate myocardial proliferation through  $\beta 1$  integrin signaling. *Dev Cell*. 16(2): 233-44.
148. Hudon-David F, Bouzeghrane F, Couture P, Thibault G. 2007. Thy-1 expression by cardiac fibroblasts: lack of association with myofibroblast contractile markers. *J Mol Cell Cardiol*. 42(5): 991-1000.
149. Lane E, Hogan B, Kurkinen M, Garrels J. 1983. Co-expression of vimentin and cytokeratins in parietal endoderm cells of early mouse embryo. *Nature*. 303(5919): 701-4.
150. Duprey P, Paulin D. 1995. What can be learned from intermediate filament gene regulation in the mouse embryo. *Int J Dev Biol*. 39(3): 443-57.
151. Lajiness J, Conway S. 2012. The dynamic role of cardiac fibroblasts in development and disease. *J Cardiovasc Transl Res*. 5:739-48.
152. Zeisberg EM, Kalluri R. 2010 Origins of cardiac fibroblasts. *Circ Res*. 107:1304-12.

153. Baum J, Duffy HS. 2011. Fibroblasts and myofibroblasts: what are we talking about? *J Cardiovasc Pharmacol.* 57(4): 376-9.
154. Takakura N, Yoshida H, Ogura Y, Kataoka H, Nishikawa S. 1997. PDGFR alpha expression during mouse embryogenesis: immunolocalization analyzed by whole-mount immunohistostaining using the monoclonal anti-mouse PDGFR alpha antibody APA5. *J Histochem Cytochem.* 45(6): 883-93.
155. Niedermeyer J, Kriz M, Hilberg F, Garin-Chesa P, Bamberger U, Lenter M, et al. 2000. Targeted disruption of mouse fibroblast activation protein. *Mol Cell Biol.* 20(3): 1089-94.
156. H. Herrmann, B. Fouquet, W.W. Franke, Expression of intermediate filament proteins during development of *Xenopus laevis*. I. 1989. cDNA clones encoding different forms of vimentin. *Development.* 105: 279-298.
157. Schaffeld M1, Herrmann H, Schultess J, Markl J. 2001. Vimentin and desmin of a cartilaginous fish, the shark *Scyliorhinus stellaris*: sequence, expression patterns and in vitro assembly, *Eur. J. Cell Biol.* 80: 692-702.
158. Herrmann, H., and Aebi, U. 2004. Intermediate filaments: Molecular structure, assembly mechanism, and integration into functionally distinct intracellular scaffolds. *Annu. Rev. Biochem.* 73: 749-789.
159. Ivaska, J., Pallari, H. M., Nevo, J., and Eriksson, J. E. 2007. Novel functions of vimentin in cell adhesion, migration, and signaling. *Exp. Cell Res.* 313: 2050-2062.
160. Steinert, P. M., and Liem, R. K. 1990. Intermediate filament dynamics. *Cell.* 60: 521-523.
161. Olson, E. N., and Capetanaki, Y. G. 1989. Developmental regulation of intermediate filament and actin mRNAs during myogenesis is disrupted by oncogenic ras genes. *Oncogene.* 4: 907-913.
162. Capetanaki, Y., Smith, S., and Heath, J. P. 1989. Overexpression of the vimentin gene in transgenic mice inhibits normal lens cell differentiation. *J. Cell Biol.* 109: 1653-1664.
163. Terzi, F., Henrion, D., Colucci-Guyon, E., Federici, P., Babinet, C., Levy, B. I., Briand, P., and Friedlander, G. 1997. Reduction of renal mass is lethal in mice lacking vimentin. Role of endothelin-nitric oxide imbalance. *J. Clin. Invest.* 100:1520-1528.
164. Colucci-Guyon, E., Giménez, Y., Ribotta, M., Maurice, T., Babinet, C., and Privat, A. 1999. Cerebellar defect and impaired motor coordination in mice lacking vimentin. *Glia.* 25:33-43.
165. Eckes, B., Colucci-Guyon, E., Smola, H., Nodder, S., Babinet, C., Krieg, T. and Martin, P. 2000. Impaired wound healing in embryonic and adult mice lacking vimentin. *J. Cell Sci.* 113: 2455-2462.
166. Henrion, D., Terzi, F., Matrougui, K., Duriez, M., Boulanger, C. M., Colucci-Guyon, E., Babinet, C., Briand, P., Friedlander, G., Poitevin, P., and Le'vy, B. I. 1997. Impaired



- flow-induced dilation in mesenteric resistance arteries from mice lacking vimentin. *J. Clin. Invest.* 100: 2909-2914.
167. Nieminen, M., Henttinen, T., Merinen, M., Marttila-Ichihara, F., Eriksson, J. E., and Jalkanen, S. 2006. Vimentin function in lymphocyte adhesion and transcellular migration. *Nat. Cell Biol.* 8: 156-162.
168. Naq AC, Krehel W, Cheng M. 1986. Distribution of vimentin and desmin filaments in embryonic cardiac muscle cells in culture, *Cytobios.* 45(182-183): 195-209.
169. Kim HD, Expression of intermediate filament desmin and vimentin in the human fetal heart, *Anat Rec.* 246: 271-278.
170. Grigore A1, Arsene D, Filipoiu F, Cionca F, Enache S, Ceausu M, Comanescu M, Staniceanu F, Ardeleanu C. 2012. Cellular immunophenotypes in human embryonic, fetal and adult heart. *Rom J Morphol Embryol.* 53: 299-311.
171. Scherholz PL1, de Souza PC, Spadacci-Morena DD, Katz SG. 2013. Vimentin is synthesized by mouse vascular trophoblast giant cells from embryonic day 7.5 onwards and is a characteristic factor of these cells. *Placenta.* 34: 518-525.
172. Schaart G, Viebahn.C, Langmann.W and Ramaekers.F.1989. Desmin and titin expression in early postimplantation mouse embryos. *Development.*107: 585-596.
173. Franke WW, Grund C, Kuhn C, Jackson BW, Illmensee K. 1982. Formation of cytoskeletal elements during mouse embryogenesis. III. Primary mesenchymal cells and the first appearance of vimentin filaments. *Differentiation.* 23:43-59.
174. Larsson A, Wilhelmsson U, Pekna M, Pekny M. 2004. Increased cell proliferation and neurogenesis in the hippocampal dentate gyrus of old GFAP (-/-) Vim(-/-) mice. *Neurochem Res.* 29:2069-2073.
175. Tsutsui H, Tagawa H, Kent RL, McCollam PL, Ishihara K, Nagatsu M, Cooper G. 1994. Role of microtubules in contractile dysfunction of hypertrophied cardiocytes. *Circulation.* 90: 533-555.
176. Heling A, Zimmermann R, Kostin S, Maeno Y, Hein S, Devaux B, Bauer E, Klövekorn WP, Schlepper M, Schaper W, Schaper J. 2000. Increased Expression of Cytoskeletal, Linkage, and Extracellular Proteins in Failing Human Myocardium. *Circ Res.* 86:846-853.
177. Tagawa H, Wang N, Narishige T, Ingber DE, Zile MR, Cooper G. 1997. Cytoskeletal mechanics in pressure-overload cardiac hypertrophy. *Circ Res.* 80:281-289.
178. Schaper J, Froede TA, Hein St, et al. 1991 Impairment of the myocardial ultrastructure and changes of the cytoskeleton in dilated cardiomyopathy. *Circulation.* 83: 504-14.
179. Di Somma S1, Marotta M, Salvatore G, Cudemo G, Cuda G, De Vivo F, Di Benedetto MP, Ciaramella F, Caputo G, de Divitiis O.2000. Changes in myocardial cytoskeletal intermediate filaments and myocyte contractile dysfunction in dilated cardiomyopathy: an in vivo study in humans. *Heart.* 84: 659-667.

180. Tagawa H, Koide M, Sato H, Zile MR, Carabello BA, Cooper G. 1998. Cytoskeletal role in the transition from compensated to decompensated hypertrophy during adult canine left ventricular pressure overloading. *Circ Res.* 82:751-761.
181. Tarabykina S, Griffiths TR, Tulchinsky E, Mellon JK, Bronstein IB, Kriajevska M. 2007. Metastasis-associated protein S100A4: spotlight on its role in cell migration. *Curr Cancer Drug Targets.* 7:217-228.
182. Helfman DM, Kim EJ, Lukanidin E, Grigorian M. 2005. The metastasis associated protein S100A4: role in tumour progression and metastasis. *Br J Cancer.* 92:1955-1958.
183. Schneider M, Kostin S, Strom CC, Aplin M, Lyngbaek S, Theilade J, Grigorian M, Andersen CB, Lukanidin E, Lerche Hansen J, Sheikh SP. 2007. S100A4 is upregulated in injured myocardium and promotes growth and survival of cardiac myocytes. *Cardiovasc Res.* 75:40-50.
184. Pedersen MV, Kohler LB, Grigorian M, Novitskaya V, Bock E, Lukanidin E, Berezin V. 2004. The Mts1/S100A4 protein is a neuroprotectant. *J Neurosci Res.* 77: 777-786.
185. Okada H, Danoff TM, Kalluri R, and Neilson EG. 1997. Early role of Fsp1 in epithelial-mesenchymal transformation. *Am J Physiol.* 273: 563-574.
186. Lawson WE, Polosukhin VV, Zoia O, Stathopoulos GT, Han W, Plieth D, Loyd JE, Neilson EG, and Blackwell TS. 2005. Characterization of fibroblast-specific protein 1 in pulmonary fibrosis. *Am J Respir Crit Care Med.* 171: 899-907.
187. Bhowmick NA, Chytil A, Plieth D, Gorska AE, Dumont N, Shappell S, Washington MK, Neilson EG, and Moses HL. 2004. TGF-beta signaling in fibroblasts modulates the oncogenic potential of adjacent epithelia. *Science.* 303:848-851.
188. Osterreicher CH, Penz-Osterreicher M, Grivennikov SI, Guma M, Koltsova EK, Datz C, Sasik R, Hardiman G, Karin M, and Brenner DA. 2011. Fibroblast-specific protein 1 identifies an inflammatory subpopulation of macrophages in the liver. *PNAS.*108: 308-313.
189. Boomershine CS, Chamberlain A, Kendall P, Afshar-Sharif AR, Huang H, Washington MK, Lawson WE, Thomas JW, Blackwell TS, and Bhowmick NA. 2009. Autoimmune pancreatitis results from loss of TGFbeta signalling in S100A4-positive dendritic cells. *Gut.* 58: 1267-1274.
190. Le Hir M, Hegyi I, Cueni-Loffing D, Loffing J, and Kaissling B. 2005. Characterization of renal interstitial fibroblast specific protein 1/S100A4-positive cells in healthy and inflamed rodent kidneys. *Histochem Cell Biol.* 123: 335-346.
191. Brisset AC, Hao H, Camenzind E, Bacchetta M, Geinoz A, Sanchez JC, Chaponnier C, Gabbiani G, and Bochaton- Piallat ML. 2007. Intimal smooth muscle cells of porcine and human coronary artery express S100A4, a marker of the rhomboid phenotype in vitro. *Circ Res.*100: 1055-1062.
192. Inamoto S, Murao S, Yokoyama M, Kitazawa S, Maeda S. 2000. Isoproterenol-

- induced myocardial injury resulting in altered S100A4 and S100A11 protein expression in the rat. *Pathol Int.* 50:480-485.
193. Horiuchi K, Amizuka N, Takeshita S, Takamatsu H, Katsuura M, Ozawa H, Toyama Y, Bonewald LF, Kudo A .1999. Identification and characterization of a novel protein, periostin, with restricted expression to periosteum and periodontal ligament and increased expression by transforming growth factor beta. *J Bone Miner Res.* 14:1239-1249.
  194. Takeshita S, Kikuno R, Tezuka K, Amann E .1993. Osteoblast specific factor 2: cloning of a putative bone adhesion protein with homology with the insect protein fasciclin I. *Biochem J.* 294:271-278.
  195. Gillan L, Matei D, Fishman DA, Gerbin CS, Karlan BY, Chang DD. 2002. Periostin secreted by epithelial ovarian carcinoma is a ligand for alpha(V)beta(3) and alpha(V)beta(5) integrins and promotes cell motility. *Cancer Res.* 62(18): 5358-5364.
  196. Bao S, et al. 2004. Periostin potently promotes metastatic growth of colon cancer by augmenting cell survival via the Akt/PKB pathway. *Cancer Cell.* 5(4): 329-339.
  197. Lindner V, Wang Q, Conley BA, Friesel RE, Vary CP.2005.Vascular injury induces expression of periostin: implications for vascular cell differentiation and migration. *Arterioscler Thromb Vasc Biol.* 25(1): 77-83.
  198. Roy S, et al. 2007. Transcriptome-wide analysis of blood vessels laser captured from human skin and chronic wound-edge tissue. *PNAS.* 104(36): 14472-14477.
  199. Rios H, et al. 2005. Periostin null mice exhibit dwarfism, incisor enamel defects, and an early-onset periodontal disease-like phenotype. *Mol Cell Biol.* 25(24): 11131-11144.
  200. Nishiyama T, et al. 2011. Delayed re-epithelialization in periostin-deficient mice during cutaneous wound healing. *PLoS One.* 6(4): e18410.
  201. Elliott CG, et al. 2012. Periostin modulates myofibroblast differentiation during full-thickness cutaneous wound repair. *J Cell Sci.* 125(pt 1): 121-132.
  202. Ontsuka K, et al. 2012. Periostin, a matricellular protein, accelerates cutaneous wound repair by activating dermal fibroblasts. *Exp Dermatol.* 21(5): 331-336.
  203. Ruan K, Bao S, Ouyang G. 2009. The multifaceted role of periostin in tumorigenesis. *Cell Mol Life Sci.* 66(14): 2219-2230.
  204. Hayashi N, Yoshimoto T, Izuhara K, Matsui K, Tanaka T, Nakanishi K. 2007. T helper 1 cells stimulated with ovalbumin and IL-18 induce airway hyper-responsiveness and lung fibrosis by IFN- $\gamma$  and IL-13 production. *PNAS* 104(37): 14765-14770.
  205. Takayama G, et al. 2006. Periostin: a novel component of sub epithelial fibrosis of bronchial asthma downstream of IL-4 and IL-13 signals. *J Allergy Clin Immunol.* 118(1): 98-104.
  206. Katsuragi N, et al. 2004. Periostin as a novel factor responsible for ventricular dilation. *Circulation.* 110(13): 1806-1813.

207. Oka T, et al. 2007. Genetic manipulation of periostin expression reveals a role in cardiac hypertrophy and ventricular remodeling. *Circ Res.* 101(3): 313-321.
208. Lorts A, Schwanekamp JA, Elrod JW, Sargent MA, Molkentin JD. 2009. Genetic manipulation of periostin expression in the heart does not affect myocyte content, cell cycle activity, or cardiac repair. *Circ Res.* 104(1): e1-e7.
209. Shimazaki M, et al. 2008. Periostin is essential for cardiac healing after acute myocardial infarction. *J Exp Med.* 205(2): 295-303.
210. Teekakirikul P, eminaga S, Toka O, Alcalai R, wang L, wakimoto H, Naylor M, Konno T, Gorham JM, wolf CM, Kim JB, Schmitt JP, Molkentin JD, Norris RA, Tager AM, Hoffman SR, Markwald RR, Seidman Ce, Seidman JG. 2010. Cardiac fibro- sis in mice with hypertrophic cardiomyopathy is mediated by non-myocyte proliferation and requires Tgf-beta. *J Clin Invest.* 120: 3520-3529.
211. Norris RA, Moreno-Rodriguez R, Hoffman S, Markwald RR. 2009. The many facets of the matricellular protein periostin during cardiac development, remodeling, and pathophysiology. *J Cell Commun Signal.* 3:275-286.
212. Hakuno D, Kimura N, Yoshioka M, Mukai M, Kimura T, Okada Y, Yozu R, Shukunami C, Hiraki Y, Kudo A, Ogawa S, Fukuda K. 2010. Periostin advances atherosclerotic and rheumatic cardiac valve degeneration by inducing angiogenesis and MMP production in humans and rodents. *J Clin Invest.* 120: 2292-2306.
213. Asakura M, Kitakaze M. 2009. Global gene expression profiling in the failing myocardium. *Circ J* 73: 1568-1576.
214. Hixson Je, Shimmin LC, Montasser Me, Kim DK, Zhong Y, Ibarquen H, Follis J, Malcom G, Strong J, Howard T, Langefeld C, Liu Y, Rotter JI, Johnson C, Herrington D. 2011. Common variants in the periostin gene influence development of atherosclerosis in young persons. *Arterioscler Thromb vasc Biol.* 31: 1661-1667.
215. Henrichsen CN, Vinckenbosch N, Zöllner S, Chaignat E, Pradervand S, Schütz F, Ruedi M, Kaessmann H, Reymond A. 2009. Segmental copy number variation shapes tissue transcriptomes. *Nat Genet.* 41(4): 424-9.
216. Jiacheng Yang, Christine S. Moravec, Mark A. Sussman, Nicholas R. DiPaola, Dechen Fu, Lesley Hawthorn, Christina A. Mitchell, James B. Young, Gary S. Francis, Patrick M. McCarthy and Meredith Bond. 2000. Decreased SLIM1 Expression and Increased Gelsolin Expression in Failing Human Hearts Measured by High-Density Oligonucleotide Arrays. *Circulation.* 102: 3046-3052.
217. Matsuda T, Cepko CL. 2007. Controlled expression of transgenes introduced by in vivo electroporation. *PNAS.* 104(3):1027-32.
218. Soriano P. 1999. Generalized lacZ expression with the ROSA26 Cre reporter strain. *Nat Genet.* 21(1): 70-1.
219. Troeger JS, Mederacke I, Gwak GY, Dapito DH, Mu X, Hsu CC, Pradere JP, Friedman

- RA, Schwabe RF. 2012. Deactivation of hepatic stellate cells during liver fibrosis resolution in mice. *Gastroenterology*. 143(4):1073-83.
220. Gabbiani G, Schmid E, Winter S, Chaponnier C, de Ckhashtonay C, Vandekerckhove J, Weber K, Franke WW. 1981. Vascular smooth muscle cells differ from other smooth muscle cells: predominance of vimentin filaments and a specific alpha-type actin. *PNAS*. 78:298-302.
221. Frank ED, Warren L. 1981. Aortic smooth muscle cells contain vimentin instead of desmin. *PNAS*. 78:3020-4.
222. Johansson B, Eriksson A, Virtanen I, Thornell LE. 1997. Intermediate filament proteins in adult human arteries. *Anat Rec*. 247:439-48.
223. Tapscott, S. J., Bennett, G. S., Toyama, Y., Kleinbart, F., and Holtzer, H. 1981. Expression of a neural type of intermediate filament as a distinguishing feature between oat cell carcinoma and other lung cancers. *Dev. Biol.* 86: 40-54.
224. Li L, Miano JM, Cserjesi P, Olson EN. 1996. SM22 alpha, a marker of adult smooth muscle, is expressed in multiple myogenic lineages during embryogenesis. *Circ Res*. 78(2): 188-95.
225. Liu, Y., Monticone, M., Tonachini, L., Mastrogiacomo, M., Marigo, V., Cancedda, R. and Castagnola, P. 2004. URB expression in human bone marrow stromal cells and during mouse development. *Biochem. Biophys. Res. Commun.* 322:497-507.
226. Tremblay F, Huard C, Dow J, Gareski T, Will S, Richard AM, Syed J, Bailey S, Brennehan KA, Martinez RV, Perreault M, Lin Q, Gimeno RE. 2012. Loss of coiled-coil domain containing 80 negatively modulates glucose homeostasis in diet-induced obese mice. *Endocrinology*. 153: 4290-303.
227. Tai IT, Dai M, Chen LB. 2005 Periostin induction in tumor cell line explants and inhibition of in vitro cell growth by anti-periostin antibodies. *Carcinogenesis*. 26:908-915.
228. Hong LZ, Wei XW, Chen JF, Shi Y. 2013 Overexpression of periostin predicts poor prognosis in non-small cell lung cancer. *Oncol Lett*. 6:1595-1603.
229. Marcantonio, D., Chalifour, L.E., Alaoui-Jamali, M.A., Alpert, L. and Huynh, H.T. 2001. Cloning and characterization of a novel gene that is regulated by estrogen and is associated with mammary gland carcinogenesis. *Endocrinology*. 142: 2409-2418.
230. Mu, H., Ohta, K., Kuriyama, S., Shimada, N., Tanihara, H., Yasuda, K. and Tanaka, H. 2003. Equarin, a novel soluble molecule expressed with polarity at chick embryonic lens equator, is involved in eye formation. *Mech. Dev.* 120:143-155.
231. Aoki, K., Sun, Y.J., Aoki, S., Wada, K. and Wada, E. 2002. Cloning, expression, and mapping of a gene that is upregulated in adipose tissue of mice deficient in bombesin receptor subtype-3. *Biochem. Biophys. Res. Commun.* 290:1282-1288.
232. Bommer GT, Jäger C, Dürr EM, Baehs S, Eichhorst ST, Brabletz T, Hu G, Fröhlich T, Arnold G, Kress DC, Göke B, Fearon ER, Kolligs FT. 2005. DRO1, a gene down-

- regulated by oncogenes, mediates growth inhibition in colon and pancreatic cancer cells. *J. Biol. Chem.* 280:7962-7975.
233. Ohki-Hamazaki H, Watase K, Yamamoto K, Ogura H, Yamano M, Yamada K, Maeno H, Imaki J, Kikuyama S, Wada E, Wada K. 1997. Mice lacking bombesin receptor subtype-3 develop metabolic defects and obesity. *Nature.* 390:165-169.
234. Cha, S.Y., Sung, Y.K., Im, S., Kwack, M.H., Kim, M.K. and Kim, J.C. 2005. URB expression in human dermal papilla cells. *J. Dermatol. Sci.* 39:128-130.
235. Monticone M, Liu Y, Tonachini L, Mastrogiacomo M, Parodi S, Quarto R, Cancedda R, Castagnola P. 2004. Gene expression profile of human bone marrow stromal cells determined by restriction fragment differential display analysis. *J. Cell Biochem.* 92:733-744.
236. Okada T, Nishizawa H, Kurata A, Tamba S, Sonoda M, Yasui A, Kuroda Y, Hibuse T, Maeda N, Kihara S, Hadama T, Tobita K, Akamatsu S, Maeda K, Shimomura I, Funahashi T. 2008. URB is abundantly expressed in adipose tissue and dysregulated in obesity. *Biochem. Biophys. Res. Commun.* 367:370-376.
237. Tremblay, F., Revett, T., Huard, C., Zhang, Y., Tobin, J.F., Martinez, R.V. and Gimeno, R.E. 2009. Bidirectional modulation of adipogenesis by the secreted protein Ccdc80/DRO1/URB. *J. Biol. Chem.* 284:8136-8147.
238. Manabe R, Tsutsui K, Yamada T, Kimura M, Nakano I, Shimono C, Sanzen N, Furutani Y, Fukuda T, Oguri Y, Shimamoto K, Kiyozumi D, Sato Y, Sado Y, Senoo H, Yamashina S, Fukuda S, Kawai J, Sugiura N, Kimata K, Hayashizaki Y, Sekiguchi K. 2008. Transcriptome-based systematic identification of extracellular matrix proteins. *PNAS.* 105:12849-12854.
239. Dave JM, Bayless KJ. 2014 Vimentin as an integral regulator of cell adhesion and endothelial sprouting. *Microcirculation.* 21:333-44.
240. Thyberg J, Hedin U, Sjölund M, Palmberg L, Bottger BA. 1991. Regulation of differentiated properties and proliferation of arterial smooth muscle cells. *Atherosclerosis.* 10:966-990.
241. Owens GK. 1995. Regulation of differentiation of vascular smooth muscle cells. *Physiol Rev.* 75:487-517.
242. Tang DD. 2008 Intermediate filaments in smooth muscle. *Am J Physiol Cell Physiol.* 294(4): C869-78.
243. Kovacic JC, Mercader N, Torres M, Boehm M, Fuster V. 2012. Epithelial-to-mesenchymal and endothelial-to-mesenchymal transition: from cardiovascular development to disease. *Circulation.* 125(14): 1795-808.
244. Lin F, Wang N, Zhang TC. 2012 The role of endothelial-mesenchymal transition in development and pathological process. *IUBMB Life.* 6:717-23.
245. Muzumdar MD, Tasic B, Miyamichi K, Li L, Luo L. 2007. A global double-fluorescent

Cre reporter mouse. *Genesis*. 45(9): 593-605.

## INDEX

## Similar result of the Microarray analysis

ol	Gene Title	mNonfailing (NF) CF Log2	mFailing CF Log2	mNF CF vs mHeat Log2	mNF CF vs mNF CM Log2	mNF CF vs mLu Log2
	growth arrest specific 7	14.57	5.51	7.25	9.28	7.27
	gelsolin	14.10	14.26	6.75	4.37	3.69
ik	RIKEN cDNA 5031426D15 gene	14.07	8.57	11.78	5.01	3.28
	gelsolin	13.64	13.90	9.82	4.31	3.62
	colony stimulating factor 1 (macrophage)	13.63	6.39	6.59	6.13	3.03
	RNA binding motif protein 16	12.11	8.64	9.13	4.73	4.86
	procollagen, type VIII, alpha 1	12.03	8.58	9.27	5.13	-0.04
	complement component 5a receptor 1	11.90	9.15	9.44	6.49	0.53
	ribosomal protein L31 /// similar to ribosomal protein L31 ///	11.73	5.29	9.33	9.23	7.19
	hypermethylated in cancer 1	11.53	5.56	11.68	5.36	3.15
ik	RIKEN cDNA 9030425L15 gene	11.39	5.83	4.31	5.58	5.94

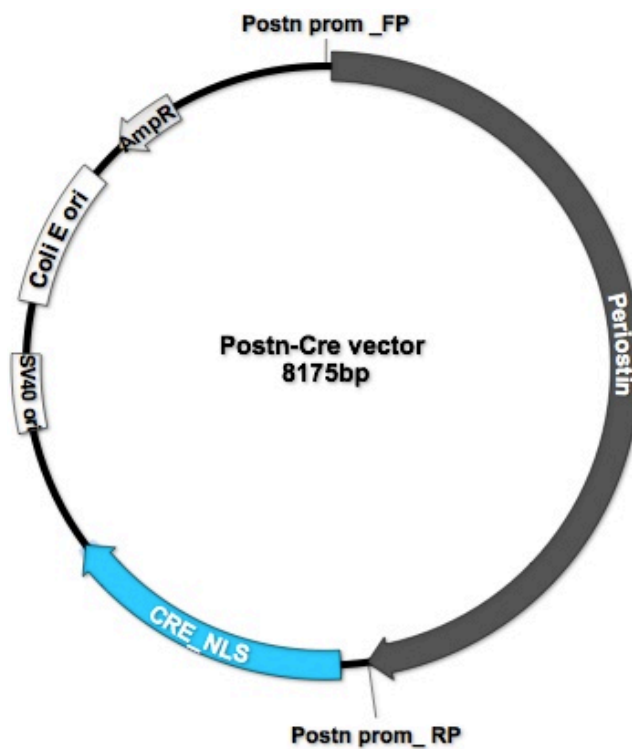
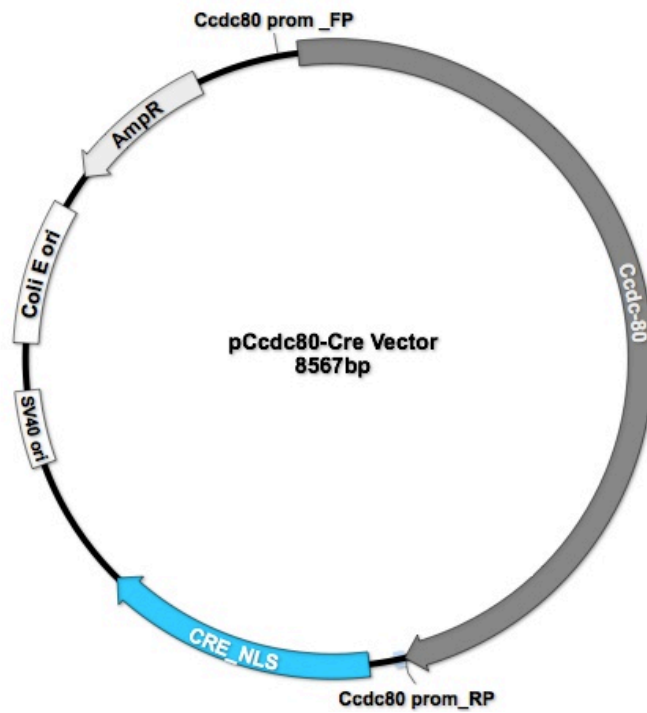


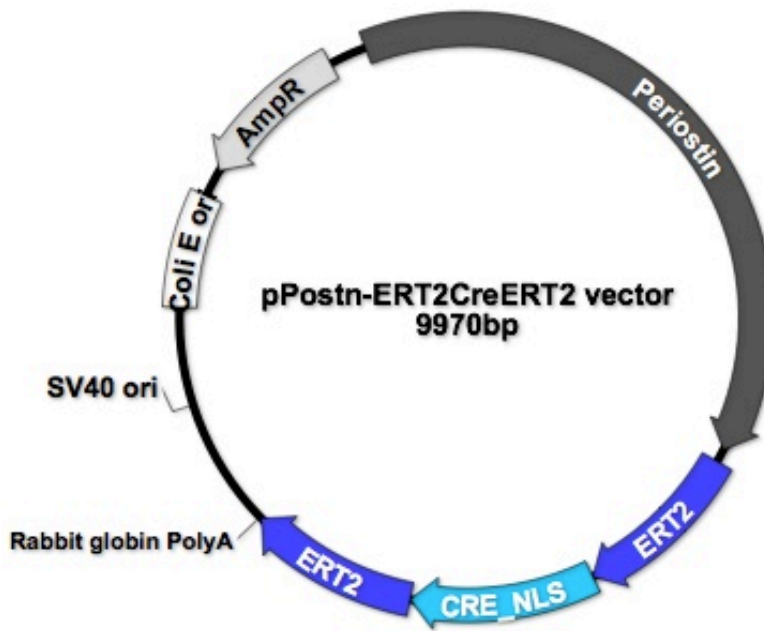
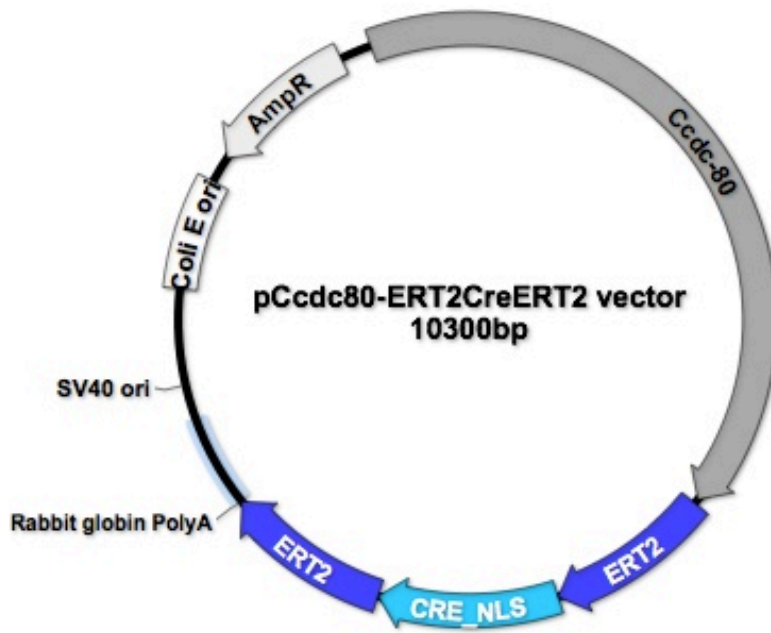
	procollagen, type VIII, alpha 1	11.33	10.53	4.63	9.45	1.63
	chondroitin sulfate proteoglycan 2	10.44	10.07	4.55	5.22	0.86
	inositol 1,4,5- trisphosphate 3-kinase B	10.35	5.85	7.44	8.54	4.21
	ninein	10.32	8.72	6.38	4.47	3.27
	sulfatase 1	10.09	8.78	10.41	4.75	-0.58
ik	RIKEN cDNA 2700055K07 gene	9.99	5.41	3.10	4.50	4.61
	sprouty homolog 2 (Drosophila)	9.74	9.02	6.70	4.47	1.82
k	RIKEN cDNA 6330406I15 gene	9.65	8.03	11.39	4.06	1.76
ik	RIKEN cDNA 1700027J05 gene	9.59	4.85	7.21	5.27	3.60
	HECT domain containing 2	9.59	7.94	11.33	4.94	7.38
ik	RIKEN cDNA 2610203C20 gene	9.56	8.65	6.13	8.08	1.95
	actinin, alpha 1	9.55	6.05	8.87	8.31	0.13
	predicted gene, EG227054 /// ribosomal protein L23a	9.49	7.88	4.42	6.50	4.77
	sodium channel, voltage-gated, type VII, alpha	9.48	8.63	5.59	7.28	7.79

	proline-rich coiled-coil 1	9.45	7.55	5.06	7.19	3.38
	cell cycle exit and neuronal differentiation 1	9.43	6.84	7.23	7.09	5.42
lik	RIKEN cDNA A330050F15 gene	9.40	6.05	4.30	4.47	4.42
	cysteine-rich secretory protein LCCL domain containing 2	9.40	8.31	4.34	5.49	2.34
	tribbles homolog 2 (Drosophila)	9.34	7.22	4.67	8.42	5.74
	Phosphodiesterase 4B, cAMP specific	9.29	8.06	8.71	8.29	6.80
	expressed sequence C87115	9.25	5.47	6.62	6.69	7.20
lik	RIKEN cDNA 4930483O08 gene	9.22	4.92	6.55	7.63	6.27
lik	RIKEN cDNA 5430416O09 gene	9.21	8.52	5.71	4.10	5.48
	opioid binding protein/cell adhesion molecule-like	9.20	8.09	4.74	5.21	3.41
lik	RIKEN cDNA 5830428H23 gene	9.20	6.42	5.36	5.40	6.41
	gamma-glutamyltransferase-like activity 1	9.19	6.01	3.67	4.13	4.29
	coiled-coil domain containing 80	9.19	7.28	5.04	4.14	0.13

coagulation factor XIII, A1 subunit	9.13	6.42	7.70	4.17	0.70
Protogenin homolog (Gallus gallus)	9.12	7.43	5.53	4.14	2.67
FK506 binding protein 5	9.08	6.60	12.41	6.71	2.96
RAB GTPase activating protein 1-like	9.07	5.79	4.58	6.78	3.72
angiopoietin-like 7	9.06	5.08	6.00	4.23	2.50
POU domain, class 2, associating factor 1	9.05	5.38	5.85	5.80	3.29
a disintegrin-like and metallopeptidase (reprolysin type) with thrombospondin type 1 motif, 7	9.05	7.36	6.54	6.10	5.81
LPS-responsive beige-like anchor	9.01	6.28	5.36	5.18	6.50
solute carrier family 25 (mitochondrial carrier, palmitoylcarnitine transporter), member 29	9.00	7.21	3.40	5.92	3.73
Vimentin	10.48	10.31	4.46	1.53	-1.23
S100 calcium binding protein A4	5.82	8.42	0.18	5.49	-5.91
prolyl 4-hydroxylase, beta polypeptide	7.72	8.40	-2.99	-2.31	-4.46

## 8.2 Map of Ccdc80 and Periostin promoter constructs used for study





### 8.3 DNA sequence of Ccdc80-Cre targeting Vector

```

0001 ACAAGTTTGT ACAAAAAGC AGGCTTCAGT TCCAGGATAC CCAGGGCTAT
    GTAAGGAGAC
0061 CCTGTCTCAA AAGACCAACC ACAAATCAA ACAACCCCTC TAAATTAATC
    CATGTATAGT
0121 TTTCCCTCTG GCTGAGTACA CACATCACCC AGCCTCAGTA TCTCCTCTGG
    ATCTGCCCAC
0181 CCCTATACAA GTCTTTCTTG GGTGTCAGGA AAATGGGCTG GTCTAGATGA
    GAAACTGTCA
0241 AAACTAGAAA TTCAGATCCT CATAAGCCAC AAATCATTCT AGGTCCCCCC
    ATAAAGGGGT
0301 AGATGTGAAC TTGTTCTATA AATTGCTCTT CGTAAACGCC CACATCCCAG
    ACATCCCTGA
0361 AGAGCTTTTC TGACGACCCA GTTAGGGTTT AGACAGCAAG ATGGAAAAC
    GAGCAAGCAG
0421 GAGAAATCCC AGTTGGCCCC TGATTGGGGC AGACCCTGAA AGGTCTGCTC
    CTGCTCGTGT
0481 GTTTAGTGCG CCACCTACTG ACATGGTGTC GGAGACTAGA AGGTGAGCCT
    GAGATCCCAG
0541 GAAGAGAAAG GCAGCTCAGG GTTGTGTGGG TCAGTGGCTT CCCCTCTGGA
    CACCCACGGC
0601 CAGCTTGCTG TTATAACTTC TCTCAACTCT ACTCCCTCAC GGAGCACGGG
    TGTCCAGTAC
0661 TGTTTCATATT GTTTGGGAGG GTTCATGAAA TACATGAGAA TTCAGGAAAT
    AGGATGAGAT
0721 TTTTAAGGAA CTACCGAGAA AGGCAAAAGG TAAGCTACAC GATTGTTTTA
    GAAAGCAGAG
0781 CTCCAAGAGG ATAAC TTTGC TCTGGCTGAA CAAATCAACG AGAGATCCTT
    TATGAAATCT
0841 TTATGAAAAC GGGAAACACA AAGAACTGA AAGCATATTT TAAAAAAGGA
    ACAGTGTGGG
0901 CAGAAAATGG AAAATGAAGG CAGGCAACCT CACTGCAGGA TACCACGTCT
    GAACTTCAGC
0961 GCCACCCAC TTAATTATTT GTGTGATAAC AAGAAATGTA TTGAAACATT
    CCAGGCCTCT
1021 GTCAAGCTAT AAATTGAGGA TGGGACTCAT CCTATTACCT CCCAGGTCTG
    TTAAATAACA
1081 GAGTCTACTA AAGTGCCAAG CCCTTGAAAA TACGTAGTAA ACTGATATCT
    GTTGTCATTA
1141 GGGGAAAAC TAGAAGAAAA TGGCAACAAC AAATAAGAGG AGAAGGCTCA
    GTAAGAGTAG
1201 TGTGAAACAT ATGGGGAAAT AATGAAAATA ACACAGAGAC TCTATTACCG
    GGCACGAGGA

```

1261 ACTAATGAGC TTTGCGGTTT GGATGAAATG GGATTTGTGA TGGTGGGCAT  
CATTCCCTGTT

1321 TGGCATCCTG TGCACCTCTAA ACAATGACAT AAGAGTGCTA TATCCAACAC  
CACCTACAGG

1381 AATTTCCCTCA ACTCTGTGCT CAGAGTTTTTC TTTATGTGCA GGAAGACGC  
CTGTAACTGG

1441 GAGGGATGGA GCTGGTTGTG GGATGGATGC AACTAGGGAT GAGGTTTTTCA  
CCCATCCAGG

1501 GGAGCTGTTT GTATGGCTTA GTTCACCGGG TTTTGGTGGA GCCTGGGCTG  
CCACTGTTGT

1561 CGACAGTTAA TATAAATTTG GAGAGTTTGG GAGAAATGCC CACGGGACCT  
GAGATATCTT

1621 CTCTTCTCCC CTAACGCTGA GTCCTCATGA CAGACCCAGA AGGTGAGTGG  
GAAAGCTGCC

1681 ATAGTCTCTC CTGTAGAGCC TTATATGACT ATTTCTTTGT GTGTTTGTGT  
GGCTGTGTGT

1741 CTTATGTGCA TCTGTTCACA TTCATATGTG TGCACACATT GCAGGGAGTG  
GAGTTAAGAT

1801 GCTGATGTCA GTAATATTCC TCAGCCACTC TCTACCTTAT TTATTTAATG  
TGTATGAAAG

1861 CCTTTCCTTT GTGTGTGTGT GTGTGTGTGT GTGTGTGTGT GTGTGTGTGT  
GTGTGTGTGC

1921 TCATGAACAC ACACACACAG GCAATGTCTG GTGACTGCAG AAGTCAGAAC  
GGTCCATATT

1981 GCCTGGACTG TAGCTGCAGA TGATTGTGAG CCACCATGTG GTGCTGGAAA  
TCAAACCCAA

2041 GTCTTCTTCA AGAGCAACTG ATGCTCTTAA CCAGTGAGTC CGACTAGCGC  
CTCCACCTTA

2101 CTTTTTTGAG ACAGGGGCTC CCATTGAGCC TAGAGCTGGT TGTATCAGCT  
AGAAAGGCTG

2161 AGGAGTGAGT TCCAGTGACC CACCTGCCTC TGCTCCTTTT CCCTCAGTGC  
CAGAGGTACA

2221 GCCTCAGTGC CCAGTTTTTC TGTAATGCT GGGATCTGA ATTCAGGCTC  
TCATACTGCG

2281 AGAAGCAAAG ACTTTACCAG CTGAGGCACC TTCCAGCCA AGCATAACATC  
TACTTCTAGG

2341 GACTGACTAA GCATTTTAGG TTCTTAAAGC ATCTGGAGAG CTGAATATTG  
TAACACACAC

2401 ACACACACAC ACACAAAAAA AGAGAGAGAG AGAGAGAGAA AAAGAGAGAG  
AGAGAGAGAG

2461 AGAGAGAGCT CACCATTTCT AGAGAAGCTG GGAGCCAGAA TGCCCATTC  
CTGATGTAAT

2521 GTCCAACCTGC AGTCTCAGGA GACAGCAGCC TTTGCCTGCA TTGCTAACCT  
TTTACCAGCT

2581 TCACCCCAT CCCAAGGAGA AATAAGGACC GAGAACACAG TAACTTGAGC  
CCCAATTAGC

2641 ATAATATAAA AACAACTTAG TCATGTTTTTC CATGGGCTTT TCCAACCCAG  
AACTCAAAGC

2701 ATAAAGCAGG CAGAAAGAGA TAAAAATATA CACGTGGAAC TATAAATAGA  
TGCATACTGT

2761 CTCGAAATGC AATGCCAATA TCTGTGGCCC AAATGAGCAG CTGTCTCTAG  
GGAACCCAGT

2821 CAGATGGAGC AACCTGACGA CTTTCCCCTT CTCAAACCTGT AGTGTGAGAA  
TCCACAGGAG

2881 GGGGAAGGTC CCGCCCCATG GCTCGGTACG GAAGGGGTTA AGTCCTCAGT  
CATCCTATTC

2941 TGAGGTGATT TACAATGATG TGTAGAGTTT CAAAACTTTT CCCAGCCCAA  
GCACAGCCCT

3001 CTCCTTCCTC GCCAGTTCA CAGACTCTCC ATGTACTGAG AGGGGAAGGA  
GGCGTGTFFF

3061 GCTGATCTGT TAAATTCTTA GTGAAGTTTT CTTGATTTCC AGTGCTGTTG  
TTTGAGTTTG

3121 GTTTGGAGCA AACCTGAAGT AGCCCTGACA TTTCTGGGAT GGAATCCAGA  
TGAGGAAAAA

3181 ATAGAAGGAG AAGGGGGAGA AAAGGGAGAA GAGAAGGTGG GGGGAAATAA  
AGGGAGGAGA

3241 GACGGAAGGG AAGGGGAAA TTGTCCCTTT TCACATTCAG GCTTCTCTGT  
TTTCCCTCAG

3301 CCTGGAAAAC ATATTAATCC TGGTGTTTTT TTTTTTTTTT TTTTTTTTTT  
TTTTTTTTTTA

3361 CGCTCGGAAA CAAAGGGACT CGGCCAGACT GCAGGAGGGG AAGGGTGATA  
AGAAGTTCTG

3421 GGAAAACCTC ACAGAAGGGA AGAGCGAGAT TCAGAAATCA CTAGGACTTC  
ACTTTCAGGA

3481 AGATCCCTGT GGCAACCAAG GACGGGCACA CACAGACCCA GGAGAACTG  
CAGACAAATG

3541 GAGATACAAA CGGTCCCAAG GACAGCAGCG TTCACCTCCT CCCACTGGAC  
CAGAAGGTAA

3601 AAGACACAGC CAGCAAAAGG AATCGGCCA GGCTGGGCTC CCTGGGGCTG  
CTTTGCAGAC

3661 AGACAAGGAG ACAGAGAGCG GGAAGGAACC GATCTCACCT AGGAAACTGT  
CCTGGGGACC

3721 AACCTTCACG TTTCTCTGGA AAGCCTCTGC AAGCATCTCC ATGAACCACT  
GTGTAAGTGT

3781 GCCAACCTTC CTCTCTGGTG CTTGTTTCCT TGTTGCTTGT TTGAAGACAT  
GAAGTGTGAA

3841 TGCACATTC AAGTTAGAAT TCATAATTAG CATGCTCAGT TTACACAGTC  
TCTGGTGCAT



3901 CTGGGCACAG CTGAGGCAGA GCAGGCGTGC CTCATGCCTG CCGCCTGTAA  
ATCAAAGCTG

3961 GATTTCCCTGC TTAAAGACTG ACTCTGCTAA GCACTGACAA TCGCAGCAGT  
TTAAGAGAAG

4021 CCCTCTCTCT GTTTGCCCTC CTCTGCTTGC CCTCCTTTTT CTTCCTTAAAC  
TATCTCCTGC

4081 CCTTTCTTTT TGGCCAGTTA GAGAAGAGAT CATGCCCAGC TCTGCTTGCA  
ATTAATGACT

4141 TTTTTTCCTT TCTTTTTCTC CCTTCTCATT TTATGTTATT TTCATTTTTG  
TATTATACCC

4201 CCTCTGCGCG TCCCCAAGTG GATAATACAG ACACCCAGCT TTCTTGTACA  
AAGTGGTTGA

4261 TGGGCGGCCG CTCTAGCTAG AGCCTCTGCT AACCATGTTT ATGCCTTCTT  
CTTTTTCTTA

4321 CAGCTCCTGG GCAACGTGCT GGTTATTGTG CTGTCTCATC ATTTTGGCAA  
AGAATTCTGA

4381 GCCGCCACCA TGGCCAATTT ACTGACCGTA CACCAAATTT TGCCTGCATT  
ACCGGTCGAT

4441 GCAACGAGTG ATGAGGTTTC CAAGAACCTG ATGGACATGT TCAGGGATCG  
CCAGGCGTTT

4501 TCTGAGCATA CCTGGAAAAT GCTTCTGTCC GTTTGCCGGT CGTGGGCGGC  
ATGGTGCAAG

4561 TTGAATAACC GGAAATGGTT TCCCGCAGAA CCTGAAGATG TTCGCGATTA  
TCTTCTATAT

4621 CTTCAGGCGC GCGGTCTGGC AGTAAAACT ATCCAGCAAC ATTTGGGCCA  
GCTAAACATG

4681 CTTTCATCGTC GGTCCGGGCT GCCACGACCA AGTGACAGCA ATGCTGTTTC  
ACTGGTTATG

4741 CGGCGGATCC GAAAAGAAAA CGTTGATGCC GGTGAACGTG CAAAACAGGC  
TCTAGCGTTC

4801 GAACGCACTG ATTTTCGACCA GGTTTCGTTCA CTCATGGAAA ATAGCGATCG  
CTGCCAGGAT

4861 ATACGTAATC TGGCATTCTT GGGGATTGCT TATAACACCC TGTTACGTAT  
AGCCGAAATT

4921 GCCAGGATCA GGGTTAAAGA TATCTCACGT ACTGACGGTG GGAGAATGTT  
AATCCATATT

4981 GGCAGAACGA AAACGCTGGT TAGCACCGCA GGTGTAGAGA AGGCACTTAG  
CCTGGGGGTA

5041 ACTAAACTGG TCGAGCGATG GATTTCCGTC TCTGGTGTAG CTGATGATCC  
GAATAACTAC

5101 CTGTTTTGCC GGGTCAGAAA AAATGGTGTT GCCGCGCCAT CTGCCACCAG  
CCAGCTATCA

5161 ACTCGCGCCC TGGAAGGGAT TTTTGAAGCA ACTCATCGAT TGATTTACGG  
CGCTAAGGAT

5221 GACTCTGGTC AGAGATACCT GGCCTGGTCT GGACACAGTG CCCGTGTCGG  
AGCCGCGCGA

5281 GATATGGCCC GCGCTGGAGT TTCAATACCG GAGATCATGC AAGCTGGTGG  
CTGGACCAAT

5341 GTAAATATTG TCATGAACTA TATCCGTAAC CTGGATAGTG AAACAGGGGC  
AATGGTGC GC

5401 CTGCTGGAAG ATGGCGATGG ACCGGTGGAA CAAAACTTA TTTCTGAAGA  
AGATCTGTGA

5461 TAGCGGCCGC ACTCCTCAGG TGCAGGCTGC CTATCAGAAG GTGGTGGCTG  
GTGTGGCCAA

5521 TGCCCTGGCT CACAAATACC ACTGAGATCT TTTCCCTCT GCCAAAAATT  
ATGGGGACAT

5581 CATGAAGCCC CTTGAGCATC TGA CTCTCTGG CTAATAAAGG AAATTTATTT  
TCATTGCAAT

5641 AGTGTGTTGG AATTTTTTGT GTCTCTCACT CGGAAGGACA TATGGGAGGG  
CAAATCATTT

5701 AAAACATCAG AATGAGTATT TGGTTTAGAG TTTGGCAACA TATGCCATAT  
GCTGGCTGCC

5761 ATGAACAAAG GTGGCTATAA AGAGGTCATC AGTATATGAA ACAGCCCCCT  
GCTGTCCATT

5821 CCTTATTCCA TAGAAAAGCC TTGACTTGAG GTTAGATTTT TTTTATATTT  
TGTTTTGTGT

5881 TATTTTTTTC TTAAACATCC CTAAAATTTT CCTTACATGT TTTACTAGCC  
AGATTTTTCC

5941 TCCTCTCCTG ACTACTCCCA GTCATAGCTG TCCCTCTTCT CTTATGAAGA  
TCCCTCGACC

6001 TGCAGCCCAA GCTTGGCGTA ATCATGGTCA TAGCTGTTTC CTGTGTGAAA  
TTGTTATCCG

6061 CTCACAATTC CACACAACAT ACGAGCCGGA AGCATAAAGT GTAAAGCCTG  
GGGTGCCTAA

6121 TGAGTGAGCT AACTCACATT AATTGCGTTG CGCTCACTGC CCGCTTTCCA  
GTCGGGAAAC

6181 CTGTCGTGCC AGCGGATCCG CATCTCAATT AGTCAGCAAC CATAGTCCCG  
CCCCTA ACTC

6241 CGCCCATCCC GCCCCTAACT CCGCCAGTT CCGCCATTC TCCGCCCAT  
GGCTGACTAA

6301 TTTTTTTTAT TTATGCAGAG GCCGAGGCCG CCTCGGCCTC TGAGCTATTC  
CAGAAGTAGT

6361 GAGGAGGCTT TTTTGGAGGC CTAGGCTTTT GCAAAAAGCT AACTTGTTTA  
TTGCAGCTTA

6421 TAATGGTTAC AAATAAAGCA ATAGCATCAC AAATTT CACA AATAAAGCAT  
TTTTTTCACT

6481 GCATTC TAGT TGTGGTTTGT CCAA ACTCAT CAATGTATCT TATCATGTCT  
GGATCCGCTG

6541 CATTAATGAA TCGGCCAACG CGCGGGGAGA GGCGGTTTGC GTATTGGGCG  
CTCTTCCGCT

6601 TCCTCGCTCA CTGACTCGCT GCGCTCGGTC GTTCGGCTGC GGCGAGCGGT  
ATCAGCTCAC

6661 TCAAAGGCGG TAATACGGTT ATCCACAGAA TCAGGGGATA ACGCAGGAAA  
GAACATGTGA

6721 GCAAAAGGCC AGCAAAAGGC CAGGAACCGT AAAAAGGCCG CGTTGCTGGC  
GTTTTTCCAT

6781 AGGCTCCGCC CCCCTGACGA GCATCACAAA AATCGACGCT CAAGTCAGAG  
GTGGCGAAAC

6841 CCGACAGGAC TATAAAGATA CCAGGCGTTT CCCCTGGAA GCTCCCTCGT  
GCGCTCTCCT

6901 GTTCCGACCC TGCCGCTTAC CGGATACCTG TCCGCCTTTC TCCCTTCGGG  
AAGCGTGGCG

6961 CTTTCTCAAT GCTCACGCTG TAGGTATCTC AGTTCGGTGT AGGTCGTTCCG  
CTCCAAGCTG

7021 GGCTGTGTGC ACGAACCCCC CGTTCAGCCC GACCGCTGCG CCTTATCCGG  
TAACTATCGT

7081 CTTGAGTCCA ACCCGGTAAG ACACGACTTA TCGCCACTGG CAGCAGCCAC  
TGGTAACAGG

7141 ATTAGCAGAG CGAGGTATGT AGGCGGTGCT ACAGAGTTCT TGAAGTGGTG  
GCCTAACTAC

7201 GGCTACACTA GAAGGACAGT ATTTGGTATC TCGCTCTGC TGAAGCCAGT  
TACCTTCGGA

7261 AAAAGAGTTG GTAGCTCTTG ATCCGGCAAA CAAACCACCG CTGGTAGCGG  
TGGTTTTTTT

7321 GTTTGCAAGC AGCAGATTAC GCGCAGAAAA AAAGGATCTC AAGAAGATCC  
TTTGATCTTT

7381 TCTACGGGGT CTGACGCTCA GTGGAACGAA AACTCACGTT AAGGGATTTT  
GGTCATGAGA

7441 TTATCAAAAA GGATCTTCAC CTAGATCCTT TTAAATTAAA AATGAAGTTT  
TAAATCAATC

7501 TAAAGTATAT ATGAGTAAAC TTGGTCTGAC AGTTACCAAT GCTTAATCAG  
TGAGGCACCT

7561 ATCTCAGCGA TCTGTCTATT TCGTTCATCC ATAGTTGCCT GACTCCCCGT  
CGTG TAGATA

7621 ACTACGATAC GGGAGGGCTT ACCATCTGGC CCCAGTGCTG CAATGATACC  
GCGAGACCCA

7681 CGCTCACCGG CTCCAGATTT ATCAGCAATA AACCAGCCAG CCGGAAGGGC  
CGAGCGCAGA

7741 AGTGGTCTTG CAACTTTATC CGCCTCCATC CAGTCTATTA ATTGTTGCCG  
GGAAGCTAGA

7801 GTAAGTAGTT CGCCAGTTAA TAGTTTGCGC AACGTTGTTG CCATTGCTAC  
AGGCATCGTG

7861 GTGTCACGCT CGTCGTTTGG TATGGCTTCA TTCAGCTCCG GTTCCCAACG  
 ATCAAGGCGA  
 7921 GTTACATGAT CCCCCATGTT GTGCAAAAAA GCGGTTAGCT CCTTCGGTCC  
 TCCGATCGTT  
 7981 GTCAGAAGTA AGTTGGCCGC AGTGTTATCA CTCATGGTTA TGGCAGCACT  
 GCATAATTCT  
 8041 CTTACTGTCA TGCCATCCGT AAGATGCTTT TCTGTGACTG GTGAGTACTC  
 AACCAAGTCA  
 8101 TTCTGAGAAT AGTGTATGCG GCGACCGAGT TGCTCTTGCC CGGCGTCAAT  
 ACGGGATAAT  
 8161 ACCGCGCCAC ATAGCAGAAC TTTAAAAGTG CTCATCATTG GAAAACGTTC  
 TTCGGGGCGA  
 8221 AAACCTCTCA GGATCTTACC GCTGTTGAGA TCCAGTTCGA TGTAACCCAC  
 TCGTGCACCC  
 8281 AACTGATCTT CAGCATCTTT TACTTTCACC AGCGTTTCTG GGTGAGCAAA  
 AACAGGAAGG  
 8341 CAAAATGCCG CAAAAAAGGG AATAAGGGCG ACACGGAAAT GTTGAATACT  
 CATACTCTTC  
 8401 CTTTTTCAAT ATTATTGAAG CATTATCAG GGTTATTGTC TCATGAGCGG  
 ATACATATTT  
 8461 GAATGTATTT AGAAAAATAA ACAAATAGGG GTTCCGCGCA CATTTCCCCG  
 AAAAGTGCCA  
 8521 CCTGGGTCGA CTAGAGGATC CCTACCGGTG ATATCCTCGA GCCCATCAA

Legend

ACAA -----	attB1 andattB2 gateway cloning site
TCAG -----	Ccdc80 promoter sequence forward and reverse
primers	
TGCG -----	Ccdc80 promoter sequence
AGAA -----	Cre_NLS sequence

## 8.4 Acknowledgement

First and foremost I would like to thank my supervisor Prof Dr. Dr. Stefan Engelhardt whose guidance, support and encouragement helped me to accomplish this work. I appreciate all his contributions of time, ideas, and funding to make my Ph.D. experience productive and stimulating. I would like to thank Prof Angelika Schnieke for being my first supervisor. My heartfelt thanks to Robert F. Schwabe, M.D., PD Dr. med. Michael Quante for providing us with VimCreERT2 mice and with the useful information time to time. I would like to acknowledge Dr Bernhard Laggerbauer for reviewing and for his valuable comments and support during my thesis writing. I would like to thank all former and present group members for the constant willingness to help and support in the daily laboratory work as well as for the really great atmosphere in the team. My special thanks to Isabell Flohrschütz and Lucia Koblitz for the neonatal rat and mouse cardiomyocytes and cardiac fibroblast cells isolation. Korneliya Sakac and Pascal for TAC operations, which represented an essential basis for numerous experiments. Andrea Ahles (Ph.D) for her immense support and useful guidance in understanding confocal microscopy and also for numerous joint ventures. Astrid Vens and Sabine Brummer for the professional collaboration and the great time in the laboratory and on private trips. Deepak Ramanujam (Ph.D), Simon Leierseder (Ph.D), Jaya Ganesan (Ph.D), Kathleen Meyer, Yassine Sassi (Ph.D.), Michael Regn, Katrin Domes (Ph.D), Xavier Loyer (Ph.D.) have also been very supportive of me in many ways and always had an open ear, which I am very grateful.

I would also like to acknowledge Deutscher Akademischer Austausch Dienst (DAAD), not only for providing the scholarship for my doctoral thesis but also for giving me the opportunity to meet and interact with interesting people in Germany. Finally, I must express my very profound gratitude to my parents and to my husband for providing me with unfailing support and continuous encouragement throughout my years of study and through the process of researching and writing this thesis. This accomplishment would not have been possible without them. Lastly, I want to thank God for his blessings. Thank you.

## 8.5 Curriculum vitae

**Name:** Megha Saraiya  
**Geburtstag/-ort:** 27.03.1981 in Berasia, India  
**Adresse:** Hansjakobstraße 95, 81825 München  
**Telefon:** 017632041581  
**Email:** [saraiyamegha@gmail.com](mailto:saraiyamegha@gmail.com)

### Studium und Praktika

**2003-2005** M.Sc. (Microbiology), Barkatullah University, India

Master thesis: Isolation and cloning of therapeutic protein gene Alpha-1 antitrypsin. (01/2005-06/2005)

Betreuer: Dr. A.K. Shasany and Dr.M.P.Darokar.

**2001-2003** B.Sc. (Biotechnology) Barkatullah University, India

Bachelors training: On Plant Tissue Culture Techniques at Tissue Culture Laboratory, Plant Resource Center, Obaidullaganj, MP (2003).

Advanced Instrumental Training at Central Laboratory Center of M.P Council of Science & Technology, Bhopal, MP (2001).

### Arbeit

**01/2006–02/2008** Als Projektassistentin im Projekt gearbeitet  
Title: Spermato-transgenesis in Primates for developing animal model to study HIV/AIDS.  
Betreuer: National Institute of Immunology, New Delhi.

### Promotion

**10/2009- heute** Doktorarbeit am Institut für Pharmakologie und Toxikologie der Technische Universität München.  
Title: Cardiac-fibroblast specific transgenesis.  
Betreuer: Prof. Dr. Dr. Stefan Engelhardt.

**04/2013-04/2014** Mitglied der TUM Graduate School der Technische Universität München.

### Honor & Award

**10/2009 –03/2013** Awarded **DAAD (Deutscher Akademischer Austausch Dienst) Scholarship** for Doctoral studies in Germany

**Publications**

Wadhwa N, Kunj N, Tiwari S, **Saraiya M**, Majumdar SS. 2009. Optimization of Embryo Culture Conditions for Increasing Efficiency of Cloning in Buffalo (*Bubalus bubalis*) and Generation of Transgenic Embryos via Cloning. *Cloning and Stem Cells*, 11(3): 387-95.

Shasany AK, Shukla AK, Darokar MP, **Saraiya M**, Chaturvedi N, Tewari L Khanuja SP .2007. An Alpha-1-antitrypsin genetic variant from India. *Indian J. Biochem Biophys*, 44(3): 176-8.